NIKHEF NATIONAL INSTITUTE FOR NUCLEAR PHYSICS AND HIGH-ENERGY PHYSICS

2002

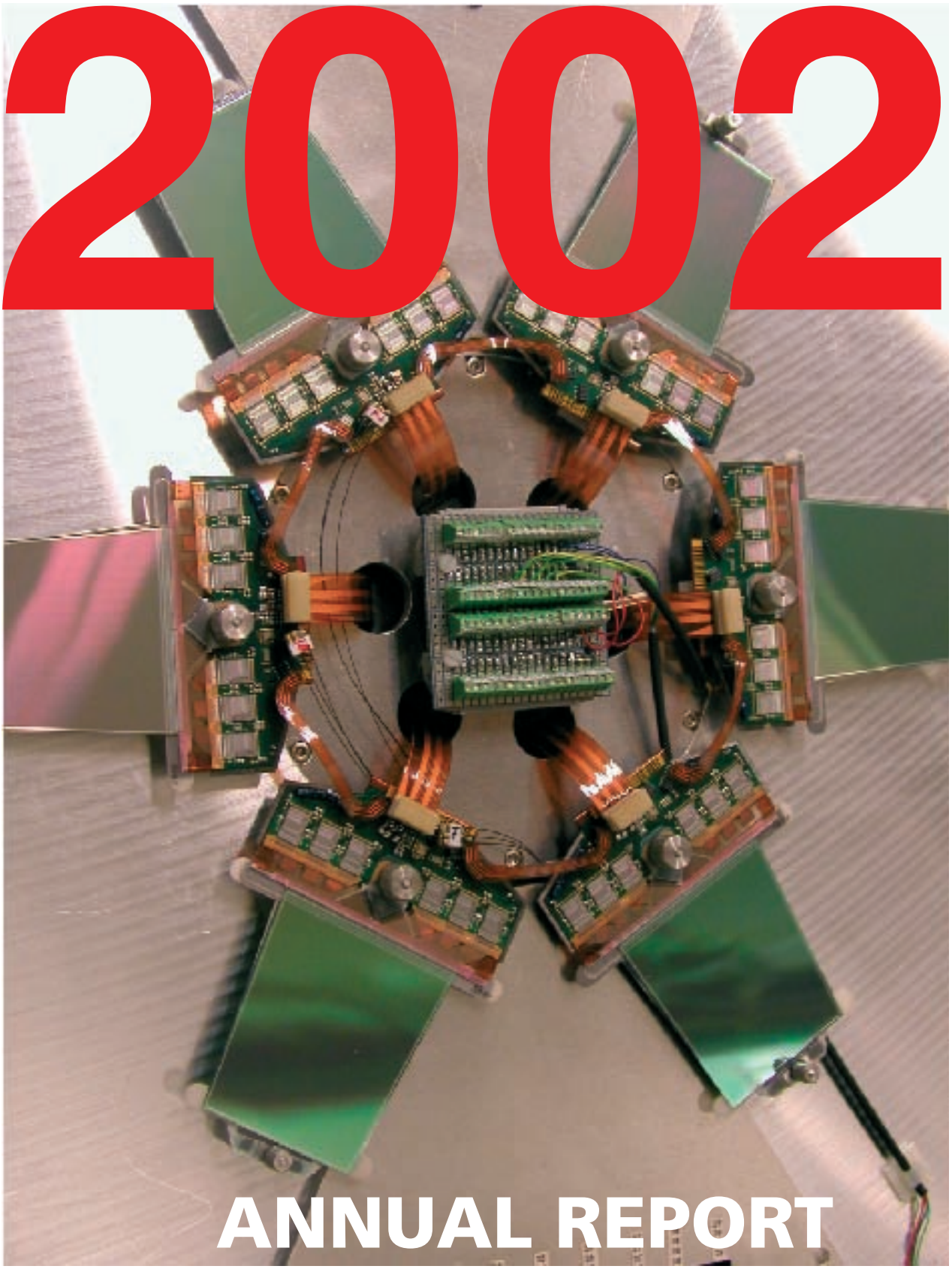

ANNUAL REPORT

NATIONAL INSTITUTE FOR NUCLEAR PHYSICS AND HIGH-ENERGY PHYSICS

ANNUAL REPORT

2002

Kruislaan 409, 1098 SJ Amsterdam
P.O. Box 41882, 1009 DB Amsterdam

Colofon

Publication edited for NIKHEF:

Address:	Postbus 41882, 1009 DB Amsterdam
	Kruislaan 409, 1098 SJ Amsterdam
Phone:	+31 20 592 2000
Fax:	+31 20 592 5155
E-mail:	directie@nikhef.nl

Editors:	Louk Lapikás & Marcel Vreeswijk
Layout & art-work:	Kees Huyser
Cover Photograph:	Atlas end-cap silicon modules mounted in the test box.
URL:	`http://www.nikhef.nl`

NIKHEF is the National Institute for Nuclear Physics and High-Energy Physics in the Netherlands, in which the Foundation for Fundamental Research on Matter (FOM), the Universiteit van Amsterdam (UvA), the Vrije Universiteit Amsterdam (VUA), the Katholieke Universiteit Nijmegen (KUN) and the Universiteit Utrecht (UU) collaborate. NIKHEF co-ordinates and supports all activities in experimental subatomic (high-energy) physics in the Netherlands.

NIKHEF participates in the preparation of experiments at the Large Hadron Collider at CERN, notably Atlas, LHCb and Alice. NIKHEF is actively involved in experiments in the USA (D0 at Fermilab, BaBar at SLAC and STAR at RHIC), in Germany at DESY (Zeus, Hermes and Hera-b) and at CERN (Delphi, L3 and the heavy-ion fixed-target programme). Furthermore astroparticle physics is part of NIKHEF's scientific programme, in particular through participation in the Antares project: a detector to be built in the Mediterranean. Detector R&D, design and construction of detectors and the data-analysis take place at the laboratory located in Sciencepark Amsterdam as well as at the participating universities. NIKHEF has a theory group with both its own research program and close contacts with the experimental groups.

Contents

A Preface

During the year 2002 steady progress was made towards the completion of detector systems for the three LHC experiments NIKHEF is involved in: Atlas, LHC-b and Alice. These systems are now either close to or well into the production phase. Although operation of the LHC is not foreseen before 2007 the size and complexity of the experimental set-ups require their installation and therefore the completion of the sub-systems well before this date. For example, the End Cap Toroids for Atlas, produced by Dutch industries with active involvement of NIKHEF, will be among the first items to be lowered into the Atlas experimental area. Similarly, the large muon chambers - more than half of them had been produced by the end of 2002 - will be among the first active detector elements to be installed. Clearly the LHC experiments dominate the activities in the Technical Departments, although also the Antares project is now going full steam ahead and requires considerable resources.

With detector production for the LHC experiments advancing well, other aspects of these projects are becoming more prominent. Test beam exposures of the novel detectors and system tests yield interesting results and publications. Furthermore the preparation of physics analyses of the future LHC data is becoming an increasingly important task of our staff physicists and PhD students. Most importantly a relatively modest but active involvement in D0, BaBar and STAR yields physics results that are of intrinsic interest but also relevant for the future LHC programme. Moreover, the creation of software and of a GRID infrastructure for data storage, retrieval and processing is in progress and is one of the big challenges of the coming years. Meeting this challenge will require new resources and will lead to many applications outside the field of high-energy physics.

For the LEP experiments Delphi and L3 data taking stopped at the end of 2000 when LEP was closed, but they still produce unique results within the framework of the Standard Model and the data are also scrutinized for signs of possible particles and interactions beyond this well-established framework. Observation of the Standard-Model Higgs boson is now excluded for a Higgs mass below 114.1 GeV at 95% confidence level (Delphi). A comprehensive overview of the most recent results in high energy physics was given at the 31^{st} International Conference on High-Energy Physics held in Amsterdam (July 25-31, 2002) in the organisation of which NIKHEF played a leading role. Also the ZEUS and Hermes experiments, both in the data-taking and analysis phase, were well represented at this conference. Both experiments have undergone detector upgrades with a large NIKHEF contribution and started data taking again after the luminosity upgrade of the HERA lepton-proton collider. Due to very unfavourable background conditions (ZEUS), further work on the HERA machine turned out to be necessary and the amount of data collected by both ZEUS and Hermes remained below expectations in 2002.

NIKHEF is a joint venture of FOM and four universities (UvA, VU, KUN, UU) and offers an excellent environment for training (under)graduates, to which also the NIKHEF Theory Department makes vital contributions. These activities are coordinated by the Research School (Onderzoekschool) Subatomic Physics and by the relevant institutes of the universities participating in NIKHEF. The institute also played an important role in setting up a Master programme Particle and Astroparticle Physics. These activities, very important for the dynamics of the institute, are carried by the whole staff and although not explicitly reported here, they are part of the mission.

Also in 2002 NIKHEF physicists have participated in discussions on the future of high energy physics beyond and in parallel to the LHC. At the moment there is very little room for unfolding activities in this direction but some small, interesting R&D projects aimed at developing detectors for a future e^+e^- Linear Collider are supported.

With the LHC experiments prominently at the top of our priority list, also for the coming years, with astroparticle physics as an interesting recent addition and with the need to start planning new projects a very long time ahead, life at NIKHEF will continue to be challenging and exciting for many years to come!

Jos Engelen

Excavating the vast underground cavern to house the ATLAS experiment at CERNs LHC collider. 100 m underground, it will be as high as a six-storey bulding.

B Experimental Programmes

1 The ATLAS Experiment

1.1 ATLAS experiment

In 2002 the construction of the detector systems for the ATLAS experiment has progressed extremely well: more than 50% of the muon spectrometer hardware exists; both end-cap toroid cryostats have been delivered to CERN and end-cap coil winding is progressing well; the first carbon fibre discs for the inner detector were delivered by industry to NIKHEF. The NIKHEF group made a major impact on the ATLAS test beam program at CERN with the delivery of the largest muon chambers together with all alignment and detector control mechanics, electronics and software. Finally, the ATLAS collaboration agreed upon a uniform framework for simulation, reconstruction and physics analysis: the ATHENA framework.

Muon spectrometer

NIKHEF carries many responsibilities within the muon spectrometer project: construction of 96 high-precision Barrel-Outer-Large-Monitored-Drift-Tube (BOL-MDT) chambers; construction of all barrel alignment components (RASNIKs) and associated software; construction of the detector control system (including the critical magnetic field probes with a relative precision of about 10^{-4}) and the construction of the high-end DAQ for the 1200 MDT chambers. Moreover Dutch industries are responsible for two of the three toroid systems which are at the heart of the ATLAS muon spectrometer. By the end of 2002 basically all of these tasks are either completed (e.g. alignment components) or in a steady production cycle (e.g. the toroids and the MDT chambers). As a consequence, the interest of the involved physicists is gradually moving towards the analysis of test beam data and the development of offline data reconstruction and data analysis software.

MDT chamber production

Manpower wise, NIKHEF's largest obligation vis-à-vis the ATLAS collaboration is the construction of the 96 large ($5 \times 2.2 \times 0.5$ m^3) MDT chambers. Over the course of 2002 the MDT chamber production process was reduced to a six-day cycle, the bare minimum since each chamber requires six overnight glue curing steps: one for each of the six tube layers comprising an MDT chamber. The critical improvement was the realization of a stand-alone set-up for the construction and calibration of the spacer structure of the MDT chambers. By the end of 2002 more than half of the individual MDT chambers were wired and tested and 37 chambers were constructed. The mechanical precision of seven MDT chambers was determined to be better than the required 20 μm r.m.s. using the CERN X-ray tomograph. The operational characteristics of MDT chambers were evaluated successfully in a large cosmic-ray test stand at NIKHEF as well as in the H8 test beam at CERN (see below).

A major set-back was encountered in October 2002 when it was discovered that the small brass gas pipes, used to connect each MDT to the gas distribution bar mounted on the MDT chamber spacer structure were defective. A change of base material, stainless steel instead of brass, cured the problem. Early 2003 the first good quality samples of stainless steel tubes became available.

Chamber construction is expected to reach completion in the summer of 2004, a few months ahead of schedule. In the fall of 2004 the BOL MDT chambers will be preassembled at CERN with their corresponding Resistive Plate Chambers, RPCs, in order to be ready for installation into the ATLAS underground cavern in 2005.

RASNIK alignment status

As reported in the 2001 NIKHEF annual report, the base components (image source, lens and image detectors) of the RASNIK MDT chamber alignment system have already been distributed to the various MDT construction sites. In 2002 the design of the on-chamber read-out multiplexers, coined RasMux, was completed and the order for the nearly 800 units was given to Dutch industries. This leaves two tasks to be completed: the calibration of the components of the important 96 projective alignment rays and the engineering design and procurement of the high- end data acquisition system. The latter comprises two more levels of multiplexing units (48 MasterMux units and 8 USA15Mux units) and 4-8 PCs equipped with commercial video frame grabbers. Prototype systems have already been delivered to various sites; the final system is only required to be available in 2005 in line with the installation of the MDT chambers into the ATLAS cavern.

Detector control system

The final specifications of the detector control system (DCS) for the ATLAS muon spectrometer were agreed upon in a meeting at NIKHEF early in 2002. The detector control system will:

- monitor the thermal environment with a precision of about 0.3°C using almost 20,000 thermal sensors mounted on the MDT chambers;
- monitor the magnetic field with a relative precision of 10^{-4} using about 1300 3D Hall sensors mounted on the MDT chambers;
- monitor the voltages and currents in each of the about 15,000 front-end read- out cards of thee MDT chambers;
- perform the initialization of the front-end electronics of the MDT chambers by means of about 1300 JTAG communication lines;
- monitor the integrity of the MDT chamber data during a run.

In 2002, the design of the basic CAN node motherboard taking care of all these tasks was completed and radiation tests were performed. The serial orders of the important electronic components have been placed. The temperature sensors were already delivered by NIKHEF in the earlier years. The 3D Hall sensor card design was finalized. Pre-series exist and NIKHEF started to work on the all-important calibration bench for the 1300 cards required. The starting point for this work was the prototype bench developed at CERN. The other requirements can be realized entirely in software since the CAN node is equipped with three connectors supporting various digital communication protocols as already foreseen at an earlier design phase.

The general-purpose software to monitor and control the ATLAS detector (the ELMB and the CAN node CPU developed jointly by CERN and NIKHEF) had to be modified as the hardware design was changed to yield a more radiation hard component. Also more features have been added to the software. In particular these changes allow the delivery of ELMBs with fully calibrated analog inputs. Furthermore a software framework has been implemented with support for communication on the basis of the CANopen standard. The framework provides developers with an environment in which dedicated software for the ELMB can be implemented. All these software developments are in the hands of a NIKHEF engineer. This work is not only relevant for the CAN nodes used in the ATLAS muon spectrometer but for all CAN nodes used in the ATLAS experiment.

The NIKHEF Detector Control System (DCS) work receives a lot of attention from other experimental collaborations. E.g. various institutes make use of the CAN nodes developed jointly by CERN and NIKHEF and the ELMB software entirely developed by NIKHEF. Moreover many experimental groups (e.g. CMS, LHCb, ALICE, MICE and NA48) plan to use the precision 3D Hall sensors from NIKHEF.

H8 test beam

A major collaborative effort in the summer of 2002 has been the evaluation of a projective tower of the ATLAS barrel muon spectrometer in the so-called H8 test beam at CERN. See Fig. 1.1 for an overview of the set-up. The set-up comprised two adjacent triplets (BIL-BML-BOL) of MDT chambers equipped with a complete set of RASNIK alignment rays (in-plane, axial and projective systems). These systems with the associated read-out hardware and analysis software were all delivered, installed and commissioned by NIKHEF. Furthermore the set-up made use of the CAN based detector control system developed by NIKHEF to monitor the thermal environment. Thermal deformations are the most important cause of relative chamber movements. The MDT readout electronics made use of prototype electronics procured by the American colleagues. After a period with run-in problems the read-out performed satisfactorily.

Apart from gaining operational experience with a projective tower of the ATLAS muon spectrometer, the aims of the 2002 H8 test beam were two-fold:

1. Verification of the efficiency and spatial resolution function of a single MDT using the near final read-out electronics and the state-of-the-art calibration and track reconstruction software;
2. Correlation of the chamber alignment as deduced from the alignment sensors with the alignment calculated using straight muon tracks.

The first goal (MDT operation) was to a large extent achieved with near 100% hit efficiencies for most MDTs. Regretfully a few dead channels and noisy channels were encountered in the smallest, BIL, MDT chambers. The cause of the dead channels is understood (slipped wires) and NIKHEF and the BIL production

Figure 1.1: *Overview photo of the H8 test beam set-up at CERN.*

Figure 1.2: *Lifting the two halves of one end-cap toroid cryostat across the recently built ski bridge in the French Jura mountain range near CERN.*

sites in Italy (Rome and Pavia) independently developed a repair method. The second goal (alignment) yielded impressive results showing a near perfect (order 5- 10 μm) agreement between *relative* MDT chamber movements and the results extracted from either the alignment data or the muon track data. However, such results were already achieved by a small group of mainly Dutch physicists in an earlier test of a prototype MDT chamber triplet (BIL-BML-BOL) in the former UA1 experimental cavern at CERN back in 1998 (see NIKHEF 1999 annual report). The main aim, however, the demonstration of *absolute* alignment measurements could not be achieved largely because of the unavailability of calibration data of the all important projective alignment systems. These systems will be calibrated at NIKHEF early 2003.

End-cap toroids

The end-cap toroids are an in kind contribution of NIKHEF to the ATLAS collaboration. Their initial design was made by the Rutherford Appleton Laboratory (RAL). Dutch Industry is responsible for its construction.

"Schelde-Exotech" in Vlissingen constructs the two enormous aluminum vacuum vessels. Each vacuum vessel resembles a 10.7 meter diameter and 5 m long 'battlemented' cylinder and weighs about 80 tons. The final machining of the vacuum vessels was sub-contracted to "Machinefabriek Amersfoort" in IJsselstein The second of the two vacuum vessels was delivered to and accepted by CERN in May 2002. Also this vessel was first fully assembled and vacuum tested at works prior to its transport in two halves to CERN. The transport was confronted with a newly built ski bridge and there was no detour possible. So the two half vessels of 40 tons each had to be lifted over the bridge, a spectacular operation that could be managed in less than a day (see Fig. 1.2). At CERN the vacuum vessels have been reassembled to perform geometrical measurement and vacuum testing. Both vessels met the specifications thereby completing successfully this part of our commitment to the ATLAS collaboration on schedule. Following these acceptance tests, both vessels were disassembled to install the thermal shields and the super-insulation to complete the cryostats for the cold masses.

"Brush-HMA" in Ridderkerk constructs the two cold masses. Each cold mass consists of eight superconducting coils of 4×4.5 m and eight keystone boxes. The keystone boxes are used as reinforcement of the whole structure and form a major part of the cold "buffer". The coils are indirectly cooled. The weight of a cold mass is 160 tons. Both cold masses were due to be delivered in the Fall of 2002. Largely because of changes at Brush-HMA, the delivery of the last cold mass is now foreseen for the end of 2004. Due to delays in the construction of the LHC accelerator, the ATLAS collaboration can cope with this delay. In the year 2002, a number of important qualification criteria were successfully completed: the cleaning of the large aluminum plates, the operation of the resin mixing system and a proper vacuum impregnation of the coils. Subsequently,

a full size dummy coil was impregnated and subjected to destructive testing mainly to verify the bonding quality of the resin. The results were fully satisfactory. Coil winding has matured to become a routine operation that is performed in two shifts. By the end of 2002 four coils were completely wound and the first coil was ready to be impregnated. The construction of the keystone boxes has been sub-contracted to "RDM" in Rotterdam. In 2002, four of the 16 keystone boxes were welded and final machining has started. The manufacture of the cooling circuits has been sub- contracted to "Cryovat" in Nijkerk. In particular, the welding of the aluminum pipes is very critical. There are hundreds of welds and leaks are not allowed, as this would spoil the insulation vacuum of the toroid cryostats. The welds will therefore be subjected to thermal shocks, pressure and vacuum tests and 10% of the welds will be X-rayed. The procedures for the manufacturing and testing have been agreed and a number of qualification tests were performed but welding qualification is still ongoing.

Semi conductor (silicon) tracker

The carbon-fibre discs which will hold the silicon strip modules made major progress in 2002. The conflicting requirements of high stability with very low-mass coupled with tight geometrical tolerances lead to a search for high-quality companies to carry out the work. Companies were visited in Germany, France, Britain and the USA where finally the contract was placed. The first two discs were delivered at the end of the year. Whilst top quality in almost all respects, one disc was insufficiently flat; the company is working hard to improve on this difficult requirement.

Meanwhile preparation of discs for mounting services and modules has progressed. The tooling and methods for machining all holes needed in the discs have been successfully made and tested. The many types of inserts and pads on a disc for attaching the services to have also been developed and tested, with Torlon® selected as the lightest material suitable for our high precision needs. At the end of the year, a prototype disc was machined and fully equipped with about 300 inserts and pads. This has been sent to RAL for services development.

Major progress has also been made in the end-cap silicon modules. The electronics circuit board (known as the hybrid) had suffered a major set-back in 2001 with the discovery of problems with the K4 prototype. A rush program produced the K5 hybrid as well as a very different module design (KB) which adopted the hybrid from SCT Barrel modules. Both performed very well and in spring 2002 the decision was made to proceed with K5. Several assembly sites produced module prototypes with K5 hybrids, including 5 at NIKHEF. Fig. 1.3 shows NIKHEF silicon modules in a special test box. These performed very well, with low noise and none of the feed-back that dogged the K4 hybrid. The mechanical precision remains excellent, better than 2 μm. Three of the NIKHEF modules are used in the CERN system test; one has been irradiated to check it can survive 10 years in the harsh radiation environment at ATLAS; and one has been equipped with thermocouples and is used for cooling studies. A search for companies to carry out the various stages necessary to make hybrids has been made, with the order expected to be placed in early spring 2003; module production can begin soon after.

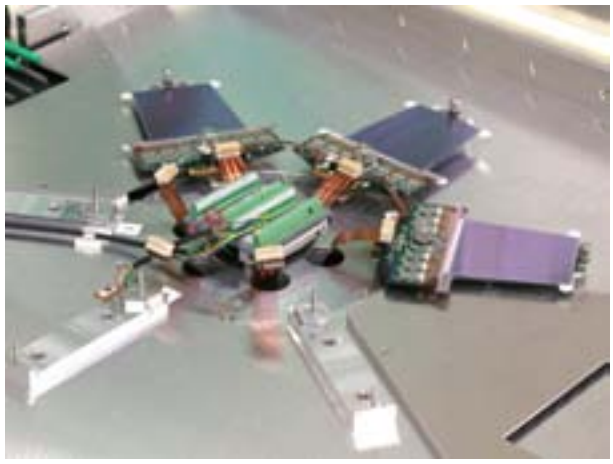

Figure 1.3: *End-cap silicon modules mounted in the light tight box for electronic performance evaluation.*

Looking ahead to 2003, NIKHEF's major task will be to mount almost 1000 modules with all their services onto discs, and then assemble the discs into an end-cap. Considerable thought has gone into the tooling for this, and now detailed design is beginning. The assembly environment is very important, needing clean conditions with temperature and humidity control. The equipment required has been specified and will be installed in Spring 2003.

Trigger, Data-Acquisition & Detector Control

The submission date of the ATLAS trigger, DAQ and DCS Technical Design Report (TDR), originally December 2002, was delayed until the summer of 2003,

due to the anticipated late availability of software needed for trigger studies. The submission date of this report is an important milestone for the project.

In the beginning of the year a workshop on the further development of the ROS (Read-Out System) took place in the French Jura. The outcome has been the start of a common project for developing Read-Out Buffer hardware, in which the University of Mannheim, University of London (Royal Holloway) and NIKHEF are participating. A PCI board able to receive and buffer two 160 MByte/s data streams and with a Gigabit Ethernet network interface has been designed and is expected to be available for testing early in 2003. The board allows exploration of two different options for data collection: via the PCI-bus or directly via the network connection. The design builds upon earlier designs for ROBin hardware, for the contribution from NIKHEF in particular elements of the design of the CRUSH board have been used. Also a new project for development of the software for the ROS was started, NIKHEF contributes to the error handling.

The performance requirements for the trigger and DAQ system are derived from the "paper model". In this model up-to-date knowledge about relevant quantities (e.g. event fragment sizes, trigger rates, acceptance factors for the various steps in the second-level trigger, algorithm execution times) is used to compute message frequencies, data volumes and the minimum amount of CPU power needed. Maintenance of and extraction of results from the spreadsheet used for this purpose proved to be problematic and time-consuming. For this reason the spreadsheet has been replaced by a command line program written in C++, which is driven by files specifying parameters as well as the type and format of the results to be output. The output is in the form of ASCII text. By running the program from a script results for different inputs can be easily generated in a form, which makes direct comparison of the results possible. This has proven to be a major improvement with respect to the earlier spreadsheet.

During 2002 work towards the production version of the MROD, the Read-Out Driver for the muon chambers, continued with production of additional MROD-1 boards, software development, testing and modification of the MROD-In. After testing the MROD-Out motherboard and the two MROD-In daughter boards, which were available at the end of 2001, 4 additional mother- and 7 additional daughter boards have been produced. Problems with the mounting of the ball-grid array packages of the processors were found and solved. Software has been developed and used for testing all functions of the hardware and for testing the performance with respect to throughput. It has been demonstrated that there are no problems with respect to functionality, and, for simple tests, with the throughput. More work is needed, however, to ascertain that the more complicated software needed in the final system will not cause the throughput to be insufficient. Tests with the TTC system (distributes first-level trigger accepts) were successful, although it was found that the module interfacing to the TTC system needs further development (not by NIKHEF). For using the MROD-1 in conjunction with the cosmic ray test stand a module (the "CSMUX") has been developed in Nijmegen. It allows sending data from the TDCs on the chambers to the MROD-In. Data-acquisition using the CSMUX and the MROD-1 has been demonstrated. Together with the group of the University of Michigan supplying the CSM (on- chamber electronics sending TDC data to the MROD - the TDCs used in 2002 in the cosmic ray test stand differ from the TDCs to be used in ATLAS) it has been decided in the fall to include more error information in the data output by the CSM. This made reconfiguration of the FPGAs of the MROD-Ins necessary. The changes required have been implemented and have been tested with success, using the MROD-Out as data generator. Also it was decided to make use of the GOL chip, a radiation-hard transmitter developed by CERN, for the link between CSM and MROD-In. A test board with the GOL chip has been designed and produced. Testing with this board and a modified HOLA (High-speed Optical Link for ATLAS) S-link destination card as receiver produced satisfactory results.

1.2 Software and physics analysis

In 2001, the ATLAS software based on the object oriented coding language C++ was put to test successfully in the "Data Challenge Zero" project. In 2002 the "Data Challenge One" project was started. This includes the simulation and reconstruction of about 50 million events, amounting to about 30 TB of data. For a fraction of these events the effects of "pile-up", due to the occurrence of multiple soft hadronic interactions within a single proton-proton bunch crossing, were included in the simulation[1]. An important ingredient of the ATLAS software is the event or persistency model

[1] The ATLAS collaboration decided to use the simulation of pile-up data as a test case of the GRID technology: The pile-up data was therefore generated using GRID software which submitted the jobs to processors in 16 different locations all over the world. NIKHEF was one of these locations. See the NIKHEF GRID section for more details.

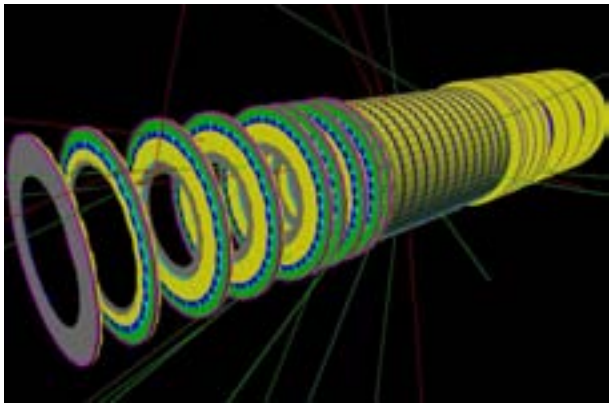

Figure 1.4: *Simulation of the Semi Conductor Tracker (SCT) with electrons passing through the detection layers.*

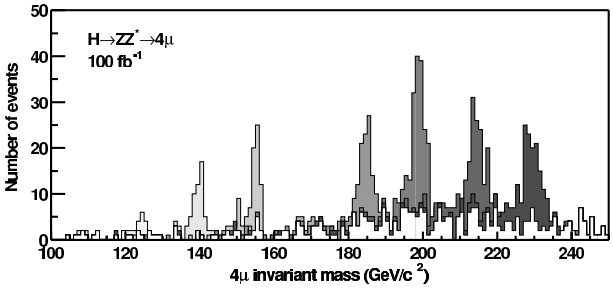

Figure 1.5: *Expected signal for a Higgs particle. Shown are the results for different Higgs mass hypotheses.*

i.e. the method used to archive the information of each event. The ATLAS collaboration decided to use CERN's ROOT software package to achieve this both for the real data i.e. the raw data coming from the ATLAS data acquisition system as well as for the simulated data obtained from the GEANT3 or GEANT4 software packages.

An important ingredient of the ATLAS software is the bookkeeping method used to keep track of what the more than 100 million different sensitive detector volumes of the ATLAS detector record for each proton-proton interaction. The NIKHEF group developed the detector description software for the Semi Conductor Tracker (SCT). This software is not only used in the simulation and reconstruction software but also in the event display graphics software. As an example, Fig. 1.4 shows the SCT geometry, with electrons passing through the SCT detector material.

In preparation of data taking with the ATLAS detector several analyses on simulated events have been performed and a number of analyses is still ongoing. The Physics Technical Design Report is used as benchmark to compare with the results of new event generation-, simulation- and reconstruction-programs and analysis techniques.

At NIKHEF the gold-plated ATLAS discovery channel, the Standard Model Higgs decay into four leptons (electrons or muons), was studied. The excellent combined precision of the central tracker and the muon spectrometer is used to optimize the significance of the Higgs observation. Figure 1.5 shows the reconstructed four-muon invariant mass for Higgs particles masses between 110 and 230 GeV.

We also studied the Higgs decay into two photons: $H \rightarrow \gamma\gamma$. This channel is particularly important in case the Higgs particle has a mass close to the lower bound from LEP (114.5 GeV). In about 20% of the $H \rightarrow \gamma\gamma$ decays one or both of the photons convert to an e^+e^- pair due to the non-negligible amount of material in the SCT. We have developed photon conversion reconstruction software to recover these events. With the use of this software ATLAS can improve both the statistical significance and the mass resolution of the $H \rightarrow \gamma\gamma$ analysis.

NIKHEF is also involved in a series of physics analyses utilizing the fast simulation (based on parametric descriptions of the detector response as opposed to a complete GEANT simulation). For example, effort is put in the question whether the Higgs particle, once found at ATLAS, is a scalar or a *pseudo*-scalar particle. Finding a pseudo-scalar Higgs would be a real possibility in the Minimal Supersymmetric Standard Model and thereby a definite sign of new physics. Another area of research are studies of the heavy bottom and top quarks. These are partly motivated by our work on the D0 experiment at FERMILAB where the t-quark was originally discovered and where the b-quark production cross section was found to be significantly higher than the Standard Model prediction. For the LHC we worked on Monte Carlo predictions for the total B_c production cross section including the octet model. Possible experimental signals for octet model contributions to B_c P-wave production are investigated. In the near future, these Monte Carlo simulations can be compared to data from the D0 experiment at FERMILAB. Finally, reconstruction of single top production via gluon-boson fusion in ATLAS is studied at NIKHEF as well. The

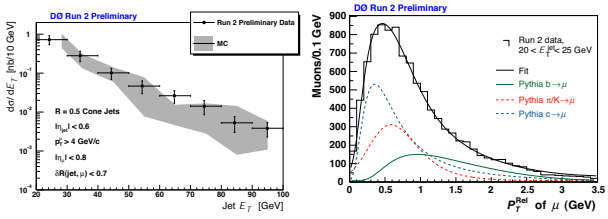

Figure 1.6: *Cross section for the production of muons associated with jets as a function of jet E_T, and the distribution of the p_T of the muon relative to the jet axis for various contributing components.*

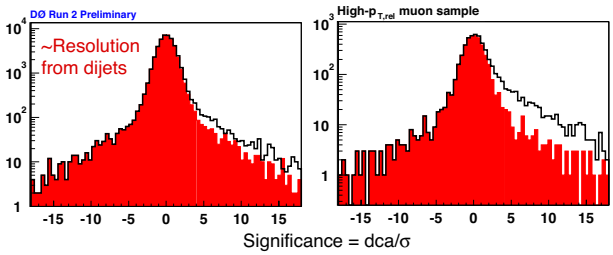

Figure 1.7: *DCA significance for tracks in a general QCD sample and a sample with muons with high p_T relative to the jet axis.*

ATLAS group is working together with the theory department and our D0 colleagues to develop a Next to Leading Order single-top Monte Carlo program to assess the prospects of observing single top production at the LHC.

1.3 D0 experiment

The Tevatron Run IIa is aimed at collecting an integrated luminosity of at least 2 fb^{-1}. During 2002, the performance of the Tevatron at FermiLab has gradually improved and surpassed the Run I performance. However, typical instantaneous luminosities at the end of the year still lingered a factor 2 to 5 below the Run II design goal. During 2002, DØ collected data corresponding to an integrated luminosity of 70 pb^{-1} for physics analysis, equivalent to some 200 million recorded events.

Early 2002 the instrumentation of the read out of the fibre tracker and the pre-shower detectors was finished, thereby completing the detector. The data acquisition system was substantially improved in 2002. A large part of the trigger is commissioned, and further evolution is foreseen for 2003. DØ has moved from commissioning of the detector to a mode of stable data taking.

NIKHEF detector hardware status

The radiation monitoring system consists of silicon diode sensors mounted on the DØ Silicon Microvertex Tracker, and beam loss monitors. The system has been running stably in 2002, and its calibration is almost finished. The increase in bias current with integrated luminosity has been shown to be in good agreement with predictions.

The Run IIb upgrade of the silicon tracker requires a new radiation monitor, which will again be the responsibility of NIKHEF-Nijmegen. The readout will remain unchanged, while a start has been made with the redesign of the sensors and front-end electronics.

An important addition to the trigger system is a Silicon Track Trigger (STT) at Level 2, which will help triggering on displaced vertices. The firmware coding of the electronics boards re-distributing the track information obtained at trigger Level 1 over the independent sectors of the STT has been largely finalized.

The Hall probe magnetic field sensor system has been running smoothly in 2002, and a long-term stability study has been performed. The sensors (an early spin-off of the NIKHEF R&D for the ATLAS experiment) show that the 2 T solenoidal field is stable to better than 10^{-4}. (This incidentally demonstrates that the precision aimed for by the ATLAS experiment can be achieved using this technology.)

The forward proton detectors, for which NIKHEF has designed and made positioning components, are now generally operational during data taking, and their commissioning is in progress.

Computing

At NIKHEF, a 50-node dual processor farm produces Monte Carlo events for DØ making NIKHEF the second biggest production center. In 2002, some 11 million fully simulated events were requested and produced. Data transfer to and from the DØ data management system SAM is automatic. The NIKHEF-Nijmegen group has set up a computer farm and a 2 TByte disk server for data analysis. The NIKHEF group plays an important role in pursuing full-scale data analysis outside FermiLab. In this context, a web server has been set-up in Nijmegen to allow for a homogeneous interface to all of DØś meetings and to facilitate posting of relevant documentation.

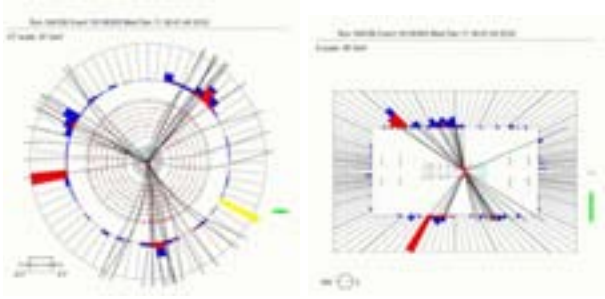

Figure 1.8: *Event candidate for $t\bar{t} \rightarrow e\nu jjjj$.*

Software and physics analysis

NIKHEF PhD students and staff are involved in the development of software for *b*-quark tagging and muon and tau lepton reconstruction.

The production of *b*-quarks can be recognized by secondary vertex reconstruction, impact parameter tagging, and soft lepton tagging ($b \rightarrow c\ell\nu$). A NIKHEF PhD-student has measured the cross section for the production of muons associated with jets in the first Run II data, as shown in Fig. 1.6. Such muons can originate from *b* or *c* quark decay, or π or *K* decay in light-quark QCD events. These components can be disentangled by studying the p_T of the muon relative to the jet axis, which is larger for the more massive *b*-quarks. A fit to the data for jets with 20 GeV $< E_T <$ 25 GeV is shown in Fig. 1.6.

Algorithms have been developed for impact parameter tagging, where signed impact parameters are used to calculate probabilities for tracks to originate from the primary vertex. As an example, the signed distance of closest approach (dca) significance is shown in Fig. 1.7 for tracks in a general QCD sample and a sample enhanced in *b*-quarks by demanding a muon with high p_T relative to the jet axis. These algorithms are used to measure the *b*-quark production cross section, with the objective of a double-tag measurement.

A further analysis focuses on an exclusive *b*-decay mode, namely $B_d \rightarrow J/\psi K^0_S$. The J/ψ production cross section has been measured in the muon decay mode, and extensive studies in 2002 have focussed on the reconstruction of charged pions from K^0_S decay.

A *b*-tagging algorithm based on secondary vertex probabilities is being developed for the study of top-quark-pair production, and their hadronic decay into (at least) six jets. One PhD-student has finalized a NLO calculation of the single top quark production cross section, and now focuses on the measurement of $t\bar{t}$ production and decay into electron, neutrino, and four jets. A candidate event is shown in Fig. 1.8.

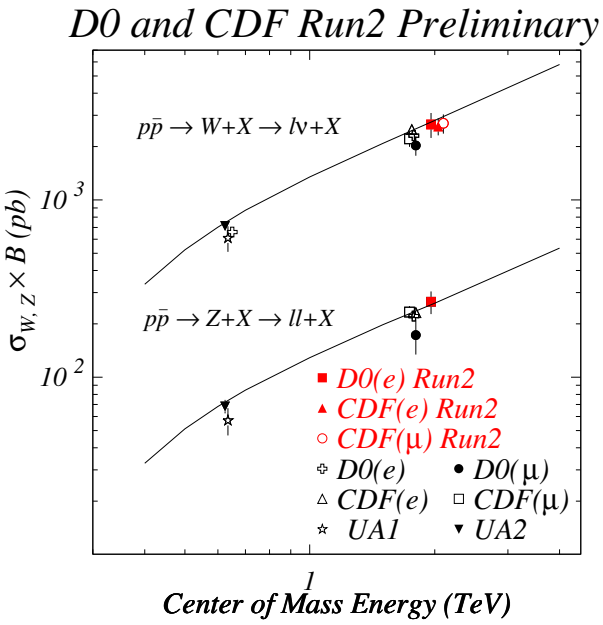

Figure 1.9: *W and Z boson production cross section in $p\bar{p}$ collisions, times the branching ratio into one lepton species. The curves represent the Standard Model predictions.*

Further focus is placed on the identification of τ leptons using tracking and calorimetry. During 2002, much effort has been spent on understanding the calorimeter response. The first signals of $Z \rightarrow \tau^+\tau^-$ decays (where one tau decays hadronically and the other decays to a muon) have now been observed. The electron and muon decay modes of W and Z bosons have been used for a first measurement of W and Z production cross sections in $p\bar{p}$ collisions at $\sqrt{s} = 1.96$ TeV, as shown in Fig. 1.9. The results are consistent with the Standard Model predictions, also shown in Fig. 1.9.

2 B Physics

2.1 Introduction

The B physics group of NIKHEF participates in the LHCb experiment at CERN and the HERA-B experiment at DESY. The HERA-B detector has been essentially completed in the course of 2002 and an extensive commissioning and physics run commenced in the second half of the year. However, due to the limited performance of both the experiment and the HERA accelerator, HERA-B is not expected to be capable of contributing in a significant manner to our understanding of $\mathcal{CP}$ violation in the B system. At the end of 2002, NIKHEF joined the BaBar experiment at the Stanford Linear Accelerator Center in Palo Alto, U.S.A. Recently, BaBar and its competitor experiment Belle in Japan demonstrated unambiguously that $\mathcal{CP}$ violation in B meson decays does indeed occur. Although various accurate measurements can be made by both experiments, these experiments cannot measure all relevant parameters with sufficient precision to pinpoint the origin of $\mathcal{CP}$ violation. That task will fall to the LHCb experiment at the LHC collider of CERN, which is planned to come into operation in April 2007. The development of the detector components for LHCb is generally proceeding on schedule. The same is true for software development and the study of data-analysis methods.

2.2 Status of HERA-B

The long shutdown of HERA, which did not deliver beam before summer 2002, has been used to recheck all systems, to improve them where necessary, and to prepare for data taking as soon as the beam would come on.

The subsystem that underwent the most intensive overhaul was the Outer Tracker. All large chambers have been strengthened in order to prevent bending leading to broken wires. In addition, on all HV distribution boards the capacitors that suffered from radiation damage have been exchanged. The system works now with high reliability and low failure rate; the efficiency obtained is as high as 98%.

The Outer Tracker chambers in the magnet have been taken out of the active region. This resulted in much less multiple scattering, in less background, and in less photon conversion and electron bremsstrahlung.

Installation and commissioning of the Inner Tracker was completed by October 2002. However, this system remains sensitive to unstable beam conditions. In fact, due to (not understood) spikes in the (electron ?) beam of HERA, it trips frequently.

The Muon detector has been improved and runs currently at track efficiencies of about 70% .

The most crucial single subsystem of HERA-B, the first-level trigger (FLT), which was not really commissioned in the year 2000, has been thoroughly investigated. The optical links work now reliably due to improved tuning possibilities of the DAC settings on the link boards, and the performance of the FLT is now such that it is routinely used for data taking. The efficiency is about 30%.

The intermittent periods of proton beam since July 2002 have been used for commissioning, alignment studies, and final tuning of the detector. Since October 30, 2002, HERA-B is routinely used for data taking. Trigger conditions are either a 2-lepton track (either electron or muon pairs) for J/ψ triggering, or an 'interaction trigger' for minimum bias events. A logging rate in excess of 1 kHz of minimum bias events is routine. J/ψ triggering occurs at an event-logging rate of about 200 Hz, and results in more than 1,000 $J/\psi \to \ell^+\ell^-$ events per hour.

During the about 450 hours of data taking, about 250 million minimum-bias events and 150 million di-lepton trigger events (containing about 300,000 $J/\psi \to \ell^+\ell^-$) have been logged on tape, demonstrating the high performance of the data-acquisition and multi-level trigger systems, as well as the stability of the detector under normal beam conditions.

Until now, the physics program redefined in the year 2000/2001 has by far not been achieved, exclusively due to the beam-time allocation to the HERA-B experiment.

Analysis of the data is in progress. Here, only a few preliminary results can be indicated.

Minimum bias

The data allow to reconstruct all hyperons up to, and including, Ω^- and $\bar{\Omega}^+$, of which about 110 events have been found in about 25% of the total data set. Similarly, about 130 D^0 and 90 D^+ events have been found in about 40% of the data set, which indicates the possibilities offered by the present data.

The search for Λ_c has been started.

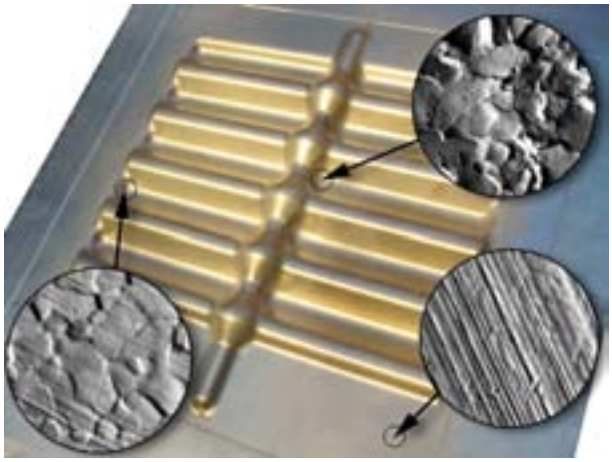

Figure 2.1: *Sample of a* 0.25 *mm thick encapsulated aluminum foil produced with the superplastic deformation process. At regions with a strong deformation the crystal reorientation and growth caused tiny vacuum leaks.*

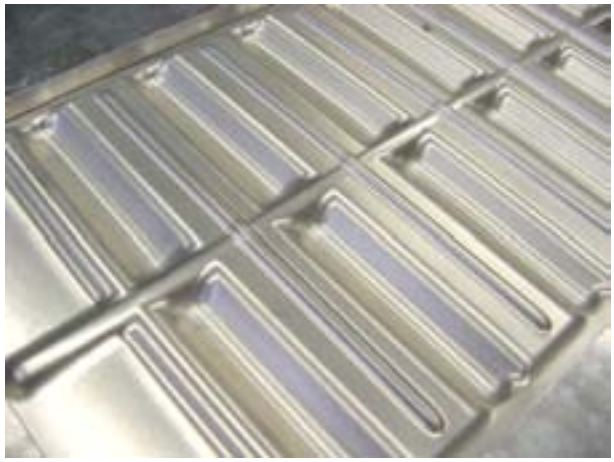

Figure 2.2: *Full-size* 0.3 *mm thick encapsulated aluminum foil produced with the hot metal gas forming technique.*

J/ψ triggered data

The present sample contains about 300,000 J/ψ events, about 10% of the expected data sample.

First results on nuclear suppression of J/ψ production at negative values of Feynman's x seem to show, against all expectations, a *rise* of α (*i.e.* an enhancement rather than suppression). Thus, the hope to discriminate with the new HERA-B data between the available models seems to have vanished, for the simple reason that all of them predict values for α of less than one, whereas we find a considerable rise of α above one, implying that all available models seem to be ruled out.

Moreover the present data set includes several 10,000 χ_c events, and thus has significantly increased the previously available amount of data. These χ_c events are identified by the decay $\chi_c \rightarrow J/\psi\gamma$. Whereas with γ detection in the ECAL high efficiency can be obtained, it is not possible in this way to resolve the χ_{c_1} and χ_{c_2} states. However, making use of conversion in the detector material in front of the magnet, it is possible to detect the γ through the e^+e^- pair, which leads to higher resolution at the price of less efficiency.

About 0.1% of all J/ψ events is produced through the decay of B mesons, giving us a realistic chance of reconstructing exclusive B decays. By now, clear evidence for a detached J/ψ peak (indicative of B meson production) has been established.

2.3 Vertex detector of LHCb at CERN

NIKHEF is responsible for the mechanical design of the LHCb vertex detector. Critical components in the design are both the thin aluminum foil that separates the silicon sensors from the LHC proton beams, and the large bellows that allows to retract and insert the silicon detectors during filling and stable operation of LHC. In addition, in the past year significant attention was paid to the vacuum control system of the vertex detector.

The mechanical design of the vertex detector has been further optimized. The construction of the RF foil has given several problems, but after intensive R&D studies a solution has been found that produces vacuum tight foils. Previous attempts with superplastic deformation did not give the expected results. Especially at the strongest deformed places, crystal growth produced a rough crystal structure as shown in Fig. 2.1, which resulted in tiny vacuum leaks.

With hot-metal-gas-forming we succeeded to obtain good foils. In this process the material is heated, after which gradually the pressure is increased. Both the formation temperature and the duration of the pressing turned out to be very sensitive parameters. Optimal results are obtained for 4 hours formation at 350 °C. Fig. 2.2 shows a full-size foil produced with this technique.

The foil is made from 0.3 mm thick AlMg3, an Al-Mg alloy with 3% Mg. The profile has been measured at a 3D measuring machine, and the deviations from the

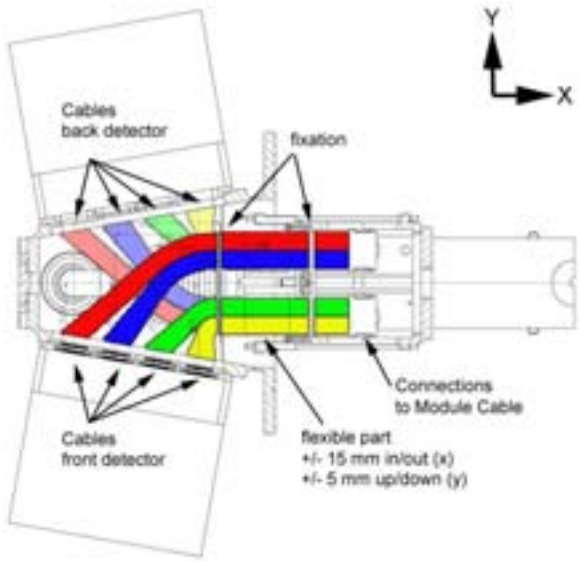

Figure 2.3: *Suggested routing of the kapton cables inside the vacuum vessel.*

design shape where within 0.2 mm.

The deformation of the RF vacuum box due to small (up to 5 mbar) pressure variations between the primary and secondary vacuum during venting and evacuation, has to be seen in relation to the position of the silicon detectors. The actual deformation can of course only be determined if a complete RF box is available. But based on the deformation of just a complete foil, combined with finite-element calculations for both a foil and a complete box, a safety gap of 1.2 mm has been deduced.

Brazing of the rectangular bellow was not successful yet. Some uncontrollable effects resulted in small vacuum leaks. Therefore, preference is given to welding of the bellows. First results are very promising, although the process is very time-consuming.

For the cables inside the vacuum system, kapton flat cable is chosen because of the radiation hardness and flexibility. It consists of three 17 μm copper layers, separated by kapton. The middle copper layer contains 100 μm broad lines. The layout of the cabling is shown in Fig. 2.3.

Outgassing properties of these kapton cables has been determined; no problems are foreseen for application in the secondary vacuum system.

For the gravity valve, measurements have been performed to determine the response during venting and evacuation. Results are shown in Fig. 2.4. Only one vacuum is pumped or vented, the other one follows because of gas flow through the gravity valve. The results indicate that the valve acts as expected. It opens at differential pressures of a few mbar. Leak rate during normal operation and response of the gravity valve to leaks needs to be determined.

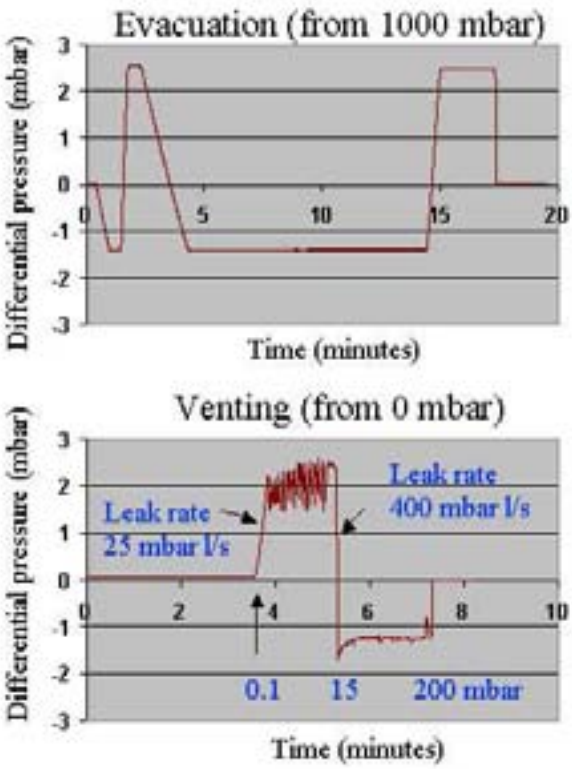

Figure 2.4: *Response of the gravity valve. The maximum pressure difference is limited to 2 mbar.*

It is possible to evacuate and vent the system with a maximum pressure difference of 2 mbar. In the operational mode the pressure in the primary vacuum system is 10^{-8} mbar.

To test the system in a stage where not all hardware components are available, testing will be performed with a printed circuit board, equipped with Field Programmable Gate Arrays (FPGA). This testing device is a mock-up for 130 valves, vacuum meters and pumps.

During injection the detector halves have to move apart in order to accommodate the undamped beams. During the measurement stage the detectors have to be moved

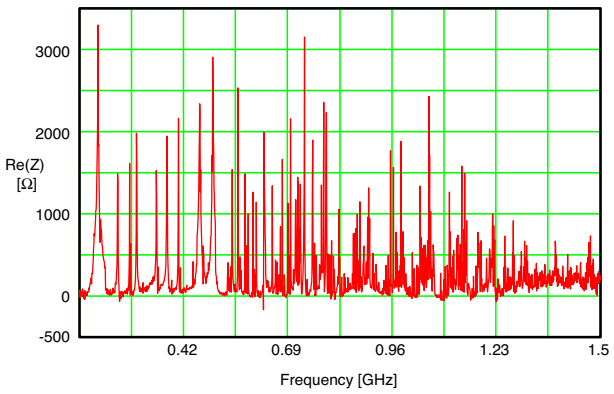

Figure 2.5: *The real part of the longitudinal impedance for the vacuum vessel with the two detector boxes without wake-field suppressors.*

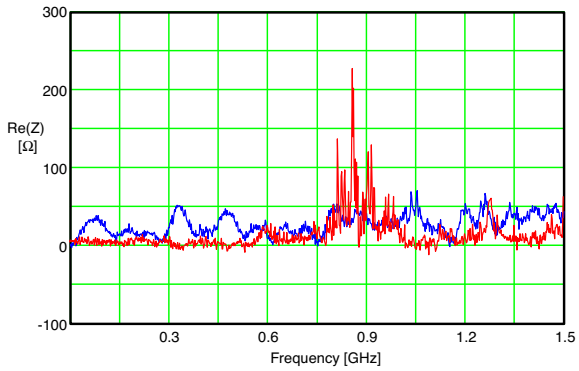

Figure 2.7: *The RF response of the vacuum vessel with the wake-field suppressor closed (blue curve) and open(red curve).*

in again. A prototype is being constructed to test the motion control system. It consists of a stepping motor and an encoder/resolver.

The RF properties of the system have been measured in a one-to-one scale model of the Vertex Locator (VELO). With just the RF boxes in place the vacuum vessel will show a large number of resonances, as shown in Fig.2.5.

Several types of wake-field suppressor have been tried; the latest design has the best properties combined with a minimum amount of material. The situation with the wake-field suppressor in place for the completely closed (measurement) and opened (injection) mode is shown in Fig. 2.6 and Fig. 2.8.

The resonances are almost completely eliminated for the closed wake-field suppressor, but also for the situation where the RF boxes are 60 mm opened the resonances are strongly reduced (see Fig.2.7).

An Engineering Design Review with representatives from the LHC machine groups has taken place at CERN on December 16 and 17. The present design has been approved, and the production stage has started.

Figure 2.6: *The inside of the vacuum vessel with the two detector halves and the wake-field suppressor in the closed position.*

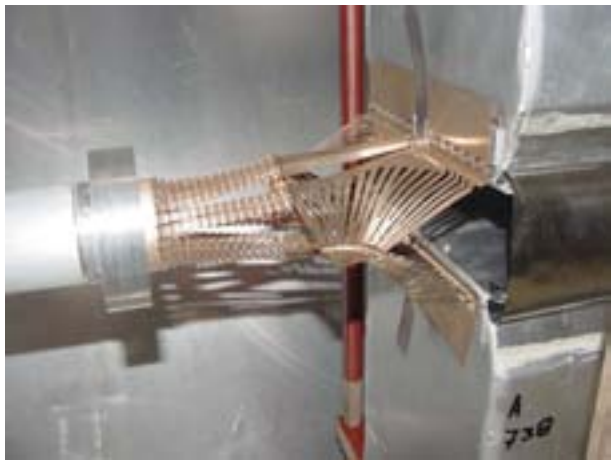

Figure 2.8: *The inside of the vacuum vessel with the two detector halves and the wake-field suppressor in the opened position.*

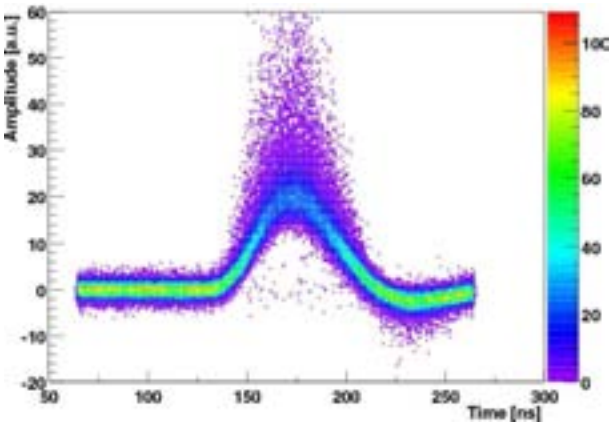

Figure 2.9: *Typical pulse shape of a Beetle 1.1 chip as measured at the X7 test beam of CERN on a hybrid with 16 chips.*

2.4 Development of a radiation hard front-end chip for the vertex detector of LHCb

The development of a radiation hard front-end chip in 0.25 μm CMOS technology for the vertex detector of LHCb is continuing. In a collaboration between the ASIC-lab in Heidelberg, Oxford University and NIKHEF various submissions have been prepared and subsequently tested. Test chips containing a variety of improved front-end designs based on NMOS or PMOS input pre-amplifiers and a modified PMOS feedback transistor were extensively tested in Heidelberg, Zürich and at NIKHEF. Based on these lab measurements a new front-end design was selected and implemented in the new 128 channel 40 MHz full-size chip *Beetle* 1.2, which is presently under investigation. Furthermore a prototype VELO hybrid was designed, produced and equipped with 16 *Beetle* 1.1 chips that were bonded to a 300 μm thick PR02 r-measuring silicon strip detector. After commissioning the setup and its control and DAQ systems at NIKHEF, the system has been used for performance tests in the X7 test beam at CERN. Data were collected in stand-alone mode and in coincidence with a tracker delivering x-y information. High statistics data, covering all regions of the detector, were collected for a variety of bias settings. A typical pulse shape is shown in Fig. 2.9, in which the noise dominated baseline and the Landau dominated peak region are clearly visible.

Channel dependent pulse-shape characteristics, like rise time and spillover after 25 ns, have been determined. Bias settings resulting in pulse shapes that comply with

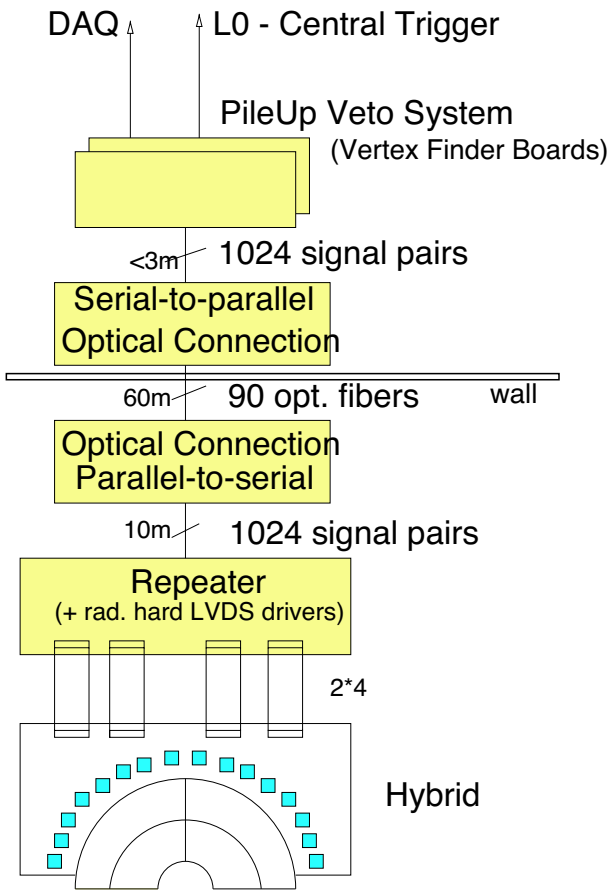

Figure 2.10: *Overview of the Pile-Up VETO system.*

LHC*b* requirements were found. Signal to noise ratios, $(S/N)_{cluster}$, ranging from 14.3 till 19.5 were extracted for detector regions with a small and large capacitance, respectively. The *Beetle* was one of the two candidate front-end chips for the LHC*b* vertex detector. In a review the *Beetle* has been selected as the front-end chip that is ultimately going to be used in the experiment.

2.5 Pile-Up Veto System

A large fraction of the crossings at LHCb will contain multiple interactions. They will be rejected by the Pile-Up Veto System (Fig. 2.10) at the first trigger level. In the *Beetle* chip the signals of silicon strip detectors are amplified and compared with an individual threshold before being sent further to the processing system. A first prototype Hybrid with 16 *Beetle* chips (Fig. 2.11) has been designed at NIKHEF, a second one including the binary discriminator outputs for the the Pile-Up system is in development. The data will be sent over

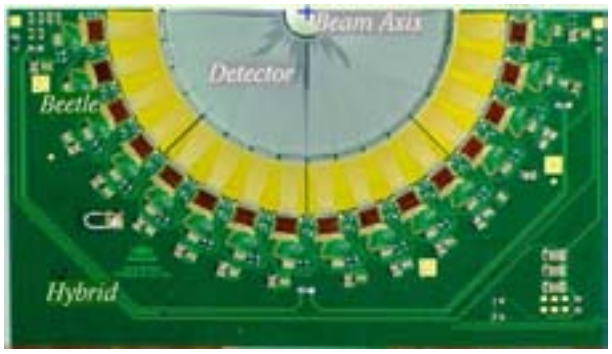

Figure 2.11: *Prototype hybrid as produced by NIKHEF with a Si-detector mounted. The detector strips are circular arcs, the pitch increases with the distance to the beam axis.*

Optical Ribbons (a technique common to other LHCb trigger projects) to the processing system. This year an important step has been to design and produce a prototype Vertex Finder Board, a key element in that system. In this module the histogramming of vertices and the finding of the vertex is performed (Fig. 2.12). The performance of the system and the adjustment of parameters is simulated with Monte-Carlo data. The system, as part of the overall LHCb trigger system, will be reviewed in 2003.

2.6 Grid Computing for LHCb

The LHC experiments require massive computing power. For LHCb, over a million SI95-equivalent CPU's are needed in 2007 and data storage is in the order of 1 Pb (a million Gb) per year. The LHC strategy to meet these requirements is to perform computing via an international datagrid, and NIKHEF is actively involved in the development of the necessary architecture and tools via the European Data Grid (EDG) project (see elsewhere in this report).

For LHCb specifically, we employed 2 small farms containing each a server and 10 dual pentium-III worker nodes. One farm was used as a general grid testbed to develop EDG software, and was accessible for all EDG users; the other farm was reserved for LHCb-use exclusively in the so-called LHCb data challenges. These data production runs are performed to test the robustness of the distributed system under mass production conditions and require a stable running environment. For the LHCb experiment, the chosen data challenge test case was the distributed production of Monte-Carlo data, which is the most CPU-intensive aspect of LHCb

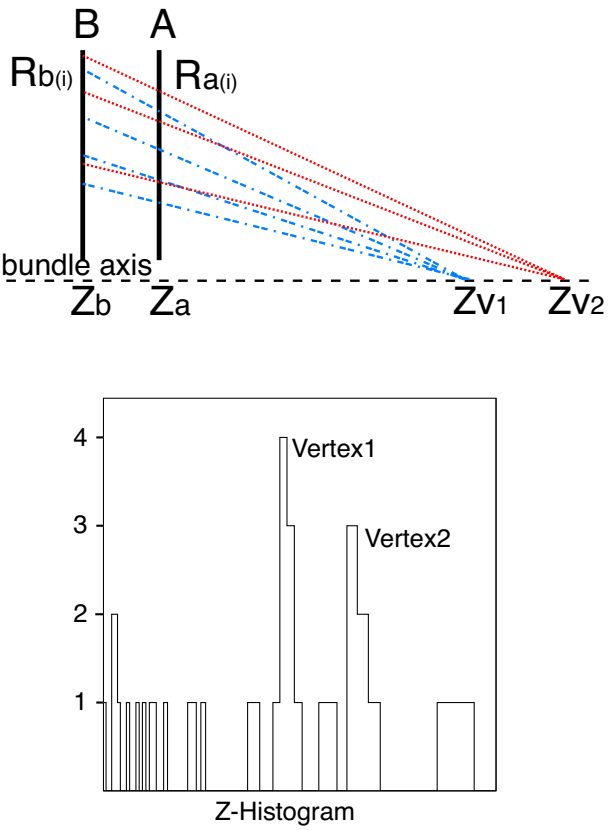

Figure 2.12: *Basic principle of detecting multiple vertices in a crossing. The readout hits of Si-detector planes A and B (at z=-23 and z=-30 cm from the nominal interaction point) are combined in a coincidence matrix. All combinations are projected onto a z-histogram. The peaks indicated correspond to the two interaction vertices in this particular Monte-Carlo event.*

computing. The produced data were used for the trigger and LHCb-light technical design reports. The farm has been operated efficiently throughout the 2002 data challenge. Most supervisionary interactions were required for solving problems that occurred during the data transfer from the farm to CERN and the storage at CERN. We aim to implement the usage of the EDG storage element located at SARA for data storage in 2003.

2.7 Outer Tracker

With the approval of the Technical Design Report (TDR), the focus of the project shifted from the R&D to the preparation of the detector production. All

designs presented in the TDR were translated into detailed technical solutions that can be implemented in a production scheme. Several parallel activities were carried out throughout 2002 in preparation for the launch of the mass production of the detector modules:

- A detailed internal schedule was agreed upon among the groups participating to the Outer Tracker (OT) construction and a detailed list of project milestones was provided to LHCC to monitor the project developments.
- A pre-requisite for the launch of production is the availability of all production and quality-control tools: the design of these tools was therefore finalized and their construction was either initiated in the cooperating institutes or commissioned to industry.
- The design guidelines presented in the TDR were implemented in actual engineering design and technical drawings: these will be officially reviewed by an external panel in an Engineering Design Review (EDR) in June 2003.
- The market was surveyed to identify producers of the various mechanics and electronics parts necessary for detector modules production. The process to draft and seal contracts was started.

In addition to this, considerable progress was made in the design of the OT Front-End Electronics, which is entirely NIKHEF responsibility.

Production Facilities and Tooling

The construction of an assembly facility, including a large clean-room, was completed. Here the mass production of more than two thirds of the longest ($\sim$5 m) detector modules (about 130) will take place.

Among the module assembly tools, a central role is played by the Straw Templates. These are essentially alignment jigs where all 64 straws forming a half-module are positioned to be then glued to their supporting panel. The high intrinsic resolution of the drift-cells (about 200 μm) requires very tight mechanical tolerances (of the order of $\pm$50 μm) in the straw-alignment pattern. The Straw Template also plays a crucial role in defining the detector planarity; this results in the request of a jig planarity tolerance within $\pm$100 μm, by no means a trivial requirement for an object about 40 cm wide and 5 m long. We identified a suitable producer in the High Tech Aerospace unit of the Philips Enabling Technologies Group. After some trial and error, the right quality of aluminum in combination with a stress-free machining procedure were found; a first down-scaled prototype, shown in Fig. 2.13, with a length of about 1 m, was produced by Philips and tested at NIKHEF and found to meet our specifications.

Figure 2.13: *Straw Template during machining at the High Tech Aerospace unit of the Philips Enabling Technologies Group.*

Engineering Design

NIKHEF has been the leading group in the engineering design of the detector modules and the Engineering Department of NIKHEF is responsible for the completion of all technical drawings to be reviewed in the June 2003 project EDR. In correspondence with the design and production of a down-scaled version of the Straw Template tool, we designed also a down-scaled version (about 1 m) of a long detector module, comprising all the design solutions and details of the full-size modules. A complete set of technical drawings (assembly, sub-parts, construction-aiding etc.) has been produced. Such a 1 m Module will be produced before the EDR in order to provide factual evidence for the adequacy of our design.

Production of Detector Elements

The central elements for the production of the detector modules are the straw tubes. In collaboration with market-leading producer LAMINA Dielectrics Ltd., we converged on a design consisting of two windings of the following materials (from the straw inside to the

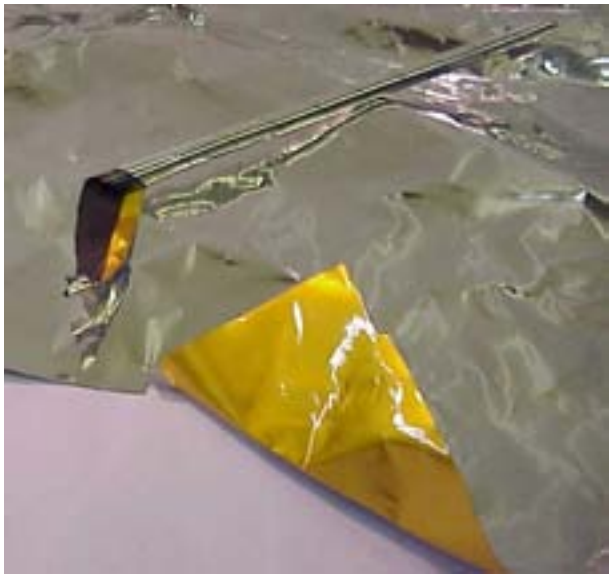

Figure 2.14: *View of straw prototype produced by LAMINA Dielectrics Ltd., exhibiting the two windings, lying on top of a foil of the laminate of Kapton and Aluminum used for the inner winding.*

outside):

- 40 μm Kapton XC (XC-160);
- a laminated foil, with a total thickness of about 40 μm, consisting of 25 μm Kapton XC (XC-100) and 12 μm aluminum.

Pre-series straw tubes have already been produced by LAMINA (see Fig. 2.14), which was then awarded the production contract.

Other key elements for the production of detector modules are the sandwich panels, used to support the straw tubes and to define the gas box. Our strict mechanical requirements, combined with the request for a minimum material budget, render the production of these panels as standard industrial laminates difficult and expensive. In the R&D phase, the Cracow Institute, availing of its substantial experience in producing carbon-fiber composite structures, has produced in a low temperature process test panels that have demonstrated excellent performance. A cooperation agreement has thus been sealed between NIKHEF and INP Cracow for the production of these basic elements. First full-scales prototypes have been delivered to NIKHEF, where their geometrical and mechanical properties were measured

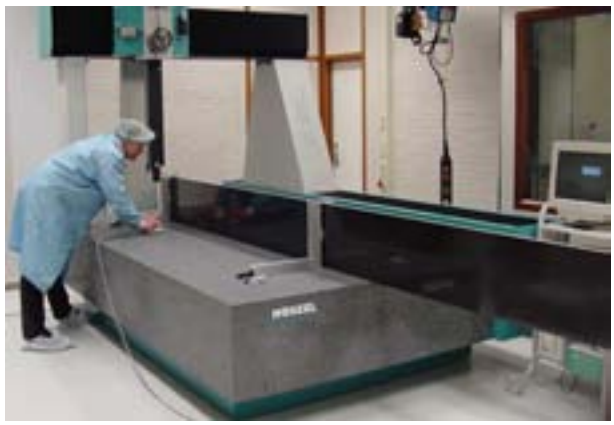

Figure 2.15: *5 m long carbon-reinforced sandwich panels produced by INP Cracow surveyed at NIKHEF.*

(see Fig. 2.15) and found meeting the technical specifications.

At the end of each straw tube, wire-support elements and gas distribution blocks are necessary. These two functionalities have been combined into single "blocks". Additionally, due to their length, wires have to be supported at intermediate positions by so called "wire locators". All these elements will be produced with injection molding, which can attain the tight required tolerances (about $\pm 20\,\mu$m in the relative position between the anode wire and the cathode straw tube) for such a large number of pieces (about 400,000) at an affordable price. After contact with different producers, we selected Philips Centre for Industrial Technnology (Philips CFT). The engineering design of the pieces was finalized in collaboration with Philips CFT, a four-fold mould constructed, and first prototypes, shown in Fig. 4.2 in Chapter D4, produced.

Front-End Electronics

Several activities were carried out in order to finalize the design of the Front-End Electronics:

- The global layout was finalized, with the block diagram of all FE support-boards (Wire-support Feed-through board, HV board, ASDBLR board, OTIS board, AUX board) and their interfaces.
- The detailed layout of the Wire-support Feed-through board and of the HV board was completed and a pre-series of about 30 boards produced.
- Detailed cooling studies were initiated, in simulated as well as in real FE Electronics models.

Figure 2.16: *Mock-up module of the FE Electronics, showing (left) the full assembly and (right) the detail of the wire-support feed-through board, with the ground spring and the wire connectors.*

- In cooperation with the mechanical engineering design, considerable progress was made in the definition of the cabling and cooling services to the detector modules. A first design of the detector service box (24 in total, two per each quarter station, providing interface to the slow and fast control, and to the low and high voltage systems) was also realized.
- An order to produce 28 wafers of ASDBLR preamplifier and discriminator was placed in cooperation with the ATLAS TRT detector at the DMILL producer ATMEL, France.

In particular, the geometry of the detector modules was considered in close combination with the mechanics of the Front-End Electronics. For this purpose, a complete mock-up module of the Front-End Electronics, shown in Fig. 2.16, was produced.

2.8 Track Reconstruction and Physics: LHCb reoptimization

Reduction of Material

As described in the Technical Proposal (TP) the LHCb tracking system consisted of a Vertex Locator (VELO) of 25 Si stations and a main tracking detector of 9 Inner Tracker and Outer Tracker stations. As the detailed designs of the sub-detectors matured, their material budget increased, in particular for the tracking stations. The material up to RICH-2 corresponded to 40% of X_0 (10% of λ_I) at the time of the TP, and had increased to 60% of X_0 (20% of λ_I) at the time of the Technical Design Report of the Outer Tracker, where X_0 (λ_I) is the radiation (interaction) length. Detector material with a small radiation length deteriorates the detection capability of electrons, positrons and photons, increases the multiple scattering and increases occupancies in the tracking stations. With decreased nuclear interaction length, more kaons and pions interact before reaching the last station of the tracking system. The number of reconstructed B mesons therefore decreases, even if the efficiency of the tracking algorithm is maintained high for those tracks that traverse the full spectrometer. For this reason, the detector has been reoptimized to reduce the material budget to the level of the original proposal.

The material budget of the VELO and the RICH-1 detector has been reduced by minor modifications and improvements in their design. For the VELO the thickness of the silicon sensors has been reduced from 300 to 220 μm, and the number of stations from 25 to 21.

Compared to the original proposal the material of the RICH-1 mirror has been changed from glass to carbon-composite material and the mirror supports have been moved outside the acceptance.

For the main tracking stations, it was found to be very difficult to reduce material below a level of 3% of X_0 (1.2% of λ_I) per station. A reduction in the number of tracking stations was therefore considered. In the original design it was observed that hit occupancies of the tracking stations inside the magnet region were high due to low momentum particles (from secondary interactions) trapped in the magnetic field. In the case of electrons the stations in the magnetic field caused emission of bremsstrahlung photons, which could not be recovered with the calorimeter system.

These problems have been avoided by removing the tracking stations inside the magnet. The number of tracking stations behind the magnet has been reduced

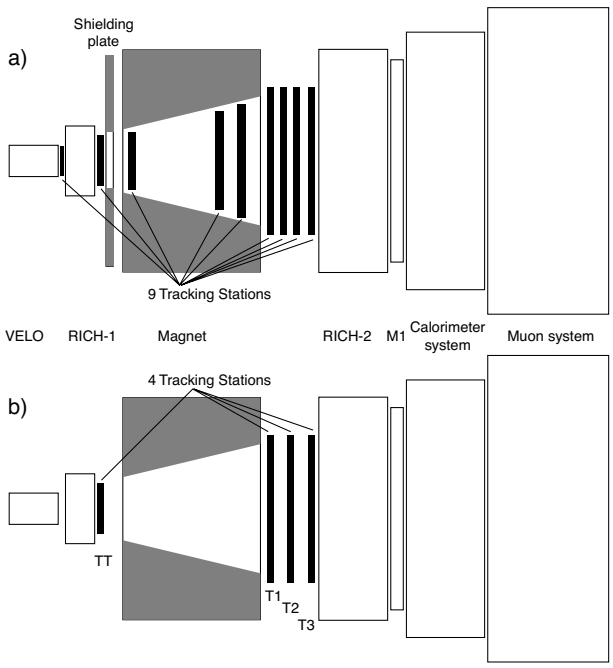

Figure 2.17: *A schematic view of the LHCb detector: (a) before the reoptimization and (b) after the reoptimization.*

from four to three (T1, T2, and T3), which are now of identical construction. Since each station has eight measurement layers for the straw Outer Tracker part and four layers for the Silicon Inner Tracker part, three stations are found to be sufficient.

The pattern recognition program has been adapted to this layout, and now relies mainly on matching the tracks found in the VELO to the hits in the stations T1-T3. An additional station, the Trigger Tracker (TT), is placed in front of the magnet just behind RICH-1. By matching the track segments found in the stations T1-T3 to the hits in TT, also pions from K_s^0 particles decaying outside the VELO volume but upstream of TT can be reconstructed.

Figure 2.17a gives a schematic overview of the original LHCb layout and 2.17b of the reoptimized layout. After this reoptimization, the material budget in front of RICH-2 is back to the level of 40% of X_0 and 12% of λ_I.

Track Reconstruction

In the original setup tracks were reconstructed in the upstream direction. Track seeds were searched in the stations behind the magnet and were traced back across

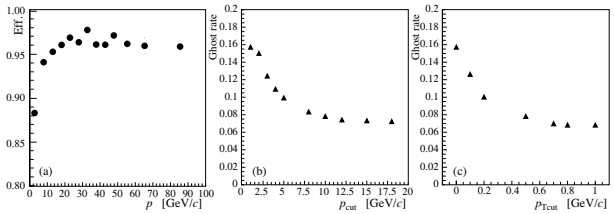

Figure 2.18: *Left: Track reconstruction efficiency as function of track momentum, Right: Fraction of reconstructed ghost tracks with a reconstructed momentum larger then a cut-off value p_{cut}.*

the magnet toward the vertex detector. In the LHCb light setup this upstream track following method is replaced by methods that link track segments in the vertex region directly to hits in the downstream detector. It turns out that this can be done without additional loss in efficiency for *long tracks*; tracks that traverse the whole spectrometer. The resulting reconstruction efficiency and the ghost rate is plotted as function of the track particle momentum in Fig. 2.18. For tracks origination from a B decay the average efficiency is found to be 96%.

The average momentum resolution of the reconstructed tracks is the same in both detector layouts ($< \delta p/p >= 0.37\%$). It turns out that the reduction in multiple scattering approximately cancels the reduced number of measurement planes.

B Decay Reconstruction

The precision of the reconstruction is verified by studying the invariant mass resolution of reconstructed B mesons and the time resolution of the observed B decays. A good invariant mass resolution is crucial for a background free selection of signal events, while excellent decay time resolution is required to resolve the high oscillation frequency of the B_s mesons. The resolutions obtained are very similar to those of the TP. When similar performance can be achieved, a tracking system based on fewer tracking stations is advantageous. It contains less material, causing less multiple scattering and generating a smaller number of secondary particles due to photon conversions. Fewer particles are lost due to interactions with the material. The system is in addition simpler to maintain and operate, and the reduced event size simplifies the design of the higher level trigger and data acquisition.

To further establish the validity of the reoptimized

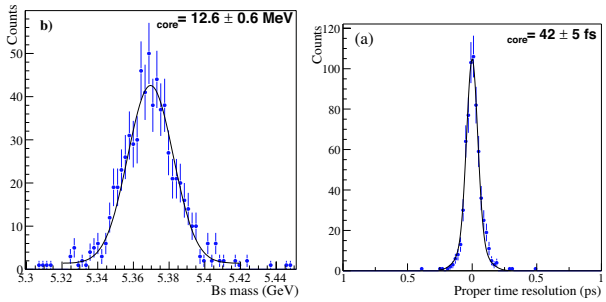

Figure 2.19: *Left: mass resolution, right: decay time resolution*

LHCb set-up 25k events of eight specific B decay modes are simulated in a realistic LHC luminosity environment. In addition 10M general B decay events are simulated to test background suppression in the individual decay selections. The selection procedures in each of the signal decays have been tuned to give maximal efficiency but no background contamination from the 10M sample.

The total signal selection efficiencies as obtained in these preliminary studies are given in the first column of table 2.1. The total efficiency is given by various factors. For the $B \to \pi\pi$ decay mode for example, it is a product of 13% geometrical acceptance, 96% track reconstruction efficiency per track, 22% efficiency for the off-line selection, 61% for the Level-0 and 51% for the level-2 trigger efficiencies. The second column of the table gives estimates for untagged event yields expected in 2 fb^{-1} of data, corresponding to a 'nominal' year of of 10^7 s at an average luminosity of 2×10^{32} cm^{-2} s^{-1}. For comparison the event yields of the TP are also given.

Channel (c.c included)	efficiency	yield	TP
$B^0 \to \pi^+\pi^-$	0.78%	27k	11k
$B^0 \to K^+\pi^-$	0.85%	115k	38k
$B_s^0 \to K^+K^-$	0.94%	35k	-
$B_s^0 \to D_s^-\pi^+$	0.26%	72k	86k
$B_s^0 \to D_s^\mp K^\pm$	0.34%	8k	6k
$B_s^0 \to J/\psi(\mu^+\mu^-)\phi$	1.66%	109k	81k
$B_s^0 \to J/\psi(e^+e-)\phi$	0.29%	19k	32k
$B^0 \to K^{*0}\gamma$	0.09%	20k	22k

Table 2.1: *Estimates for the total efficiencies and the annual yields of benchmark B-hadron decays for the reoptimized LHCb detector. For comparison the yields of the Technical Proposal are given in the last column.*

Since the TP, many conditions and assumptions have changed. The most significant changes are that the current performance is based on a more realistic description of the LHC collisions, a more realistic detector description, and a new object oriented reconstruction software. In addition, events with multiple interactions were ignored at the time of the TP, whereas pile-up is now treated in a proper way.

The physics performance study also shows that the reoptimized LHCb detector will be able to reconstruct similar statistics of B meson decays of interest as in the TP and hence maintains its physics potential.

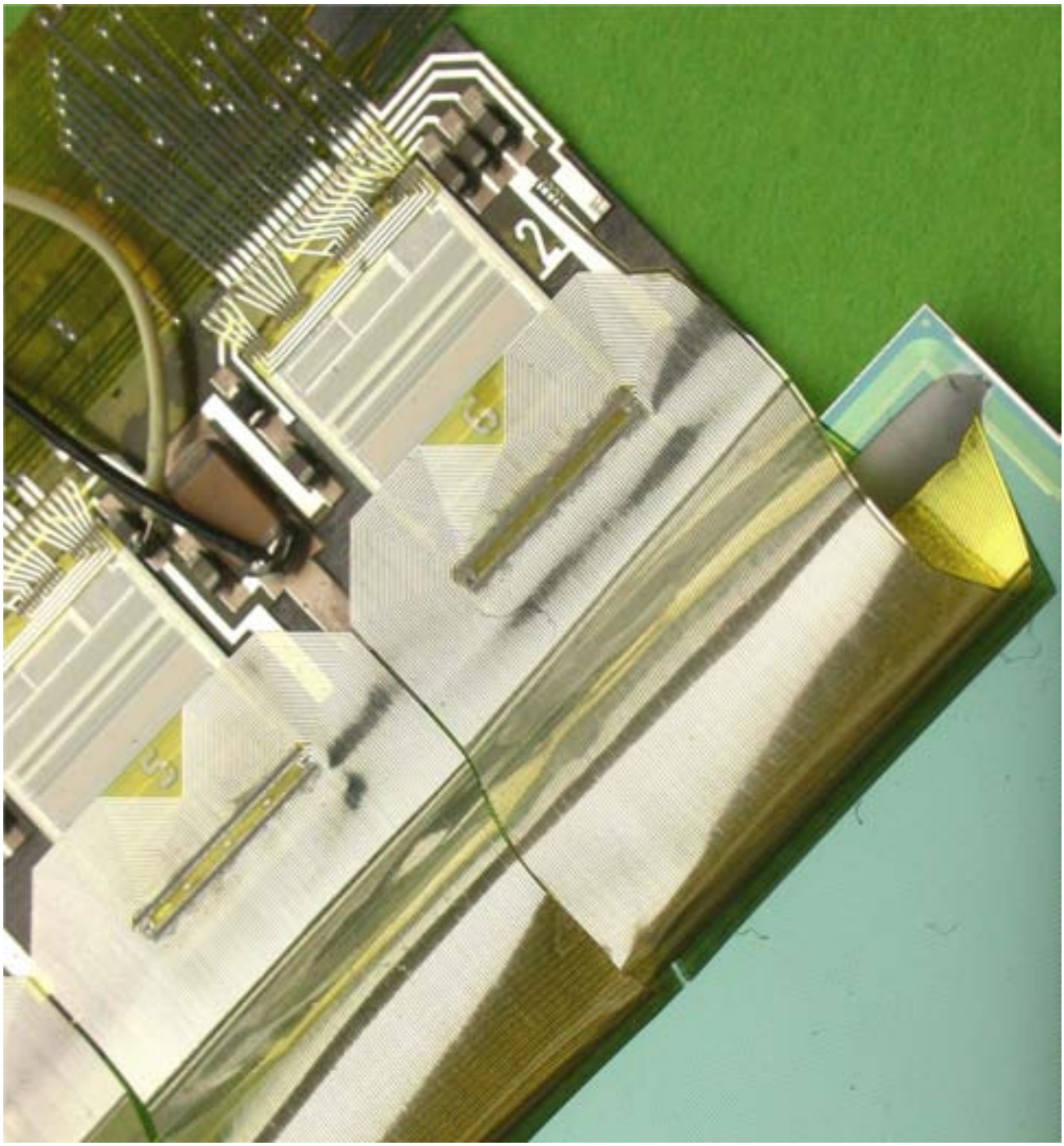

A module for the Alice ladder.

3 Heavy Ion Physics

3.1 Introduction

The heavy-ion group at NIKHEF participates in the NA57 and NA49 experiments at the CERN SPS. Both experiments have completed data taking

In 2002 NIKHEF has joined the STAR collaboration. STAR allows the study of heavy-ion collisions at energies up to $\sqrt{s}$=200 GeV/nucleon. The NIKHEF group is interested in the study of particle spectra and the results of the upcoming pA run.

In addition, NIKHEF contributes strongly to the preparation of the ALICE experiment. The NIKHEF group concentrates on the design and construction of the ALICE silicon microstrip tracker.

3.2 The NA57 experiment

The NA57 experiment has been designed to study the production of strange baryons and anti-baryons in p-Be and Pb-Pb collisions at the CERN SPS. It intends to extend the scope of its predecessor, the WA97 experiment, which observed an enhanced production of strange particles in Pb-Pb collisions with respect to p-A collisions at 158 GeV/nucleon beam energy.

The NA57 experimental set-up features a high granularity, allowing a detailed study of the strange baryon production at mid-rapidity. One such study, done by NIKHEF, is the determination of the polarization of the Λ and $\bar{\Lambda}$ produced at small rapidities.

Polarized Λ production

A significant transverse polarization of Λ particles produced with unpolarized proton beams and even in heavy ion collisions has been observed. In these experiments the polarization is measured with respect to the direction perpendicular to the event plane. The event plane is defined as the plane spanned by the direction of the incoming beam and the direction of the produced Λ.

This polarized Λ production is largely unexplained because QCD predicts no polarization if the incoming particles are not polarized. However, several semi-classical models attempt to describe the experimental results. These models describe the polarization of the Λ as a function of its Feynman x_F and transverse momentum p_t. The models differ in their predictions for both large x_F and for small x_F. The model proposed by DeGrand and Mietinen[2] tries to explain the observed polarization by assuming that and s-quark from the sea is accelerated by the attractive force generated by a ud quark pair from the projectile. In this case the velocity vector of the s-quark is not parallel to the change in its momentum and the spin vector precesses until it aligns perpendicular to the acceleration (Thomas precession). The s-quark determines the polarization of the produced Λ. The Berlin model[3], assumes a correlation between the transverse momentum of valence quarks in the nucleon and their spin orientations. The Troshin-Tyurin model[4] describes polarization as a result of multiple scattering of constituent quarks from the projectile by the mean field of the nucleons which overlap during the collision. Here, strange quarks are produced during the collision.

Understanding of this effect is of importance to the search for the quark-gluon plasma because a quark-gluon plasma has no memory of the original beam direction and therefore cannot produce polarized particles. The available data comes mainly from pp and pA collisions, but recently the first results from heavy-ion collisions have become available.

Λ production in NA57

The NA57 experiment has collected a large number of events for both pA and AA collisions at a center-of-mass energy per nucleon of $\sqrt{s}$=19 GeV/nucleon. The large number of events allows selection of a basically background free sample of Λ particles. The relatively small size of the NA57 detector limits the detection of decaying particles to those where both tracks remain inside the fiducial volume of the detector. This is only the case when the tracks bent toward each other (cowboy events). When the tracks diverge (sailor events) only short sections of the tracks are measured and the momentum cannot be determined accurately. Therefore the distribution of measured decay angles is distorted. Detailed simulations were needed to correct for this. When only counting the number of Λ particles produced a simple weighting procedure, where the acceptance for Λ particles is determined by Monte Carlo methods, had been sufficient. However, when looking at the internal decay angles of the Λ this is no longer adequate. A sophisticated correction method, based on the deconvolution method developed by Blobel[1], was implemented. This method does not only correct for acceptance, but also considers the effects of the measurement resolution.

Because the NA57 experiment has collected a very large number of events, the statistical error on the result is quite small and in fact accuracy of the result is dom-

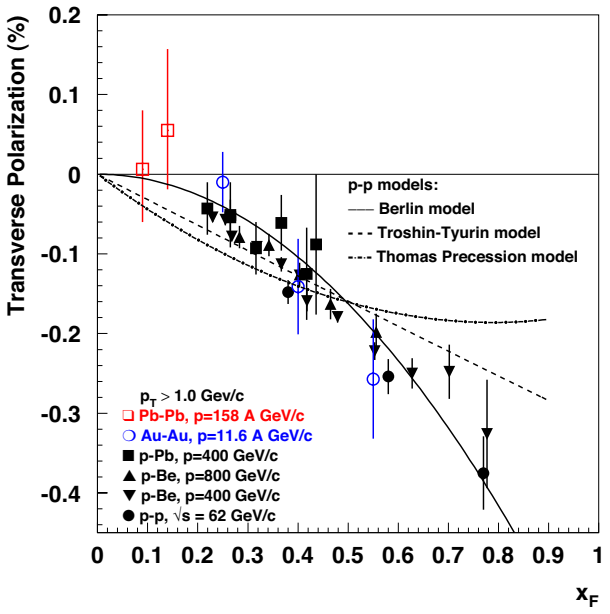

Figure 3.1: *Transverse polarization of Λ particles produced in pp, pA and AA collisions. The NA57 results are indicated by the open squares. The error bars for the NA57 results include statistical and systematic errors. For comparison the predictions of three semi-classical models are shown.*

inated by systematic errors. Therefore the systematic errors were also studied in detail. For this purpose the polarization of the K^0particles was determined with the same method and for the same dataset. The analysis was done separately for the two orientations of the magnetic field that NA57 uses. Since it is known that the K^0 are not polarized the results could be interpreted as an estimate of the systematic error resulting from the limited accuracy of the Monte Carlo description of the detector. Indeed it was shown that the systematic errors are slightly larger than the statistical errors. In order to exclude additional systematic effects due to the slightly different acceptance for Λ compared to K^0 a detailed study of the stability of the results as a function of the experimental selection cuts was also done.

Fig. 3.1 shows the results of the transverse polarization measurement of the NA57 experiment, compared to results from other experiments and compared to three semi-classical models. The available data from pA collisions at high x_F seems to prefer the Berlin model. The analysis of the NA57 data shows that the polarization at small x_F is small as expected from the available models. However, the systematic errors in this result are too large to allow rejection of any of the available models. A more detailed investigation in the asymmetries in the detector set-up could reduce the systematic error.

3.3 The NA49 experiment

The NA49 detector [5] at the CERN SPS is a large acceptance fixed-target magnetic spectrometer designed to study hadronic reactions ranging from elementary proton-proton (p-p) via proton-nucleus (p-A) to heavy ion (A-A) interactions. A set of large Time Projection Chambers provides momentum measurement and particle identification through dE/dx. About a 1000 charged tracks are routinely reconstructed in a central 158 GeV/nucleon Pb-Pb event. At central rapidity the particle identification is improved by a measurement of the time-of-flight. The centrality of A-A collisions is determined from the energy deposition of spectator nucleons in a downstream calorimeter.

Within the large and diverse physics program of NA49, NIKHEF has taken part in the analysis of the energy dependence of particle production in central Pb-Pb collisions at 40, 80 and 158 GeV/nucleon beam energy [6]. In 2002 the energy scan was completed by taking data at 20 and 30 GeV/nucleon; preliminary results at 30 GeV/nucleon have recently become available [7].

In the year 2000 a large sample of 3 million Pb-Pb events was taken at 158 GeV/nucleon to measure rare particle production like the Ω and to search for open charm in heavy ion collisions. The search for open charm production has been carried out at NIKHEF and preliminary results are presented in [8].

Fig. 3.2 shows a compilation of transverse mass spectra measured by NA49 in central Pb-Pb collisions at 158 GeV/nucleon. These spectra reflect the state of the expanding system in the latest stage of the evolution where (elastic) collisions between the produced hadrons are so rare that they cannot change their momentum distributions anymore. This freeze-out can, in a hydro-dynamical picture, be described in terms of a kinetic freeze-out temperature $T_{\rm k}$ and a transverse flow velocity $\beta_{\rm T}$ (blast-wave parameterization). All available NA49 data measured at 40, 80 and 158 GeV/nucleon, except for the pion and deuteron data, were fitted to the blast-wave parameterization and gave results similar to those shown in Fig. 3.2 for 158 GeV/nucleon [8]. The pion spectra at low m_T are not expected to be described by the blast-wave parametrization because they are dominated by resonances. The deuteron spectra are not expected to be described because they are pro-

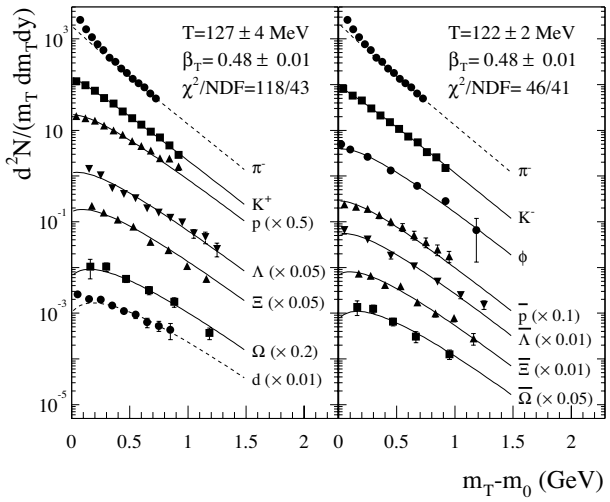

Figure 3.2: *Transverse mass spectra measured by NA49 in central 158 GeV/nucleon Pb-Pb collisions. The solid curves show the result of blast-wave fits to the data. The dashed curves show the corresponding predictions for the pion and deuteron data (see text).*

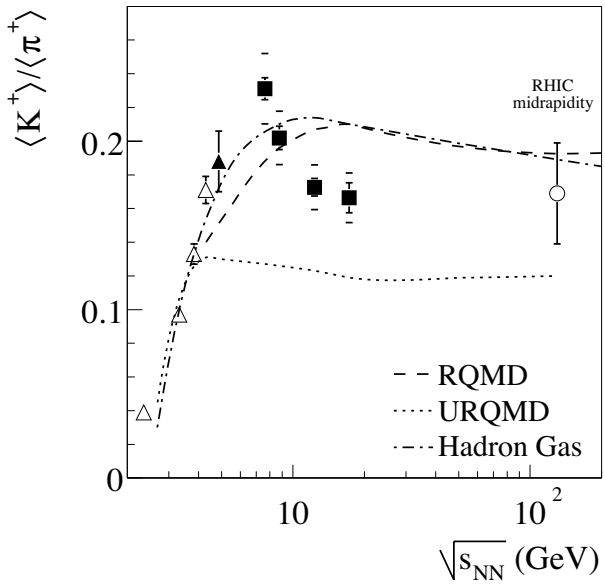

Figure 3.3: *The energy dependence of the K^+/π^+ ratio measured in central Pb-Pb collisions at the AGS (triangles), by NA49 (squares) and at RHIC (Au-Au collisions). The curves show predictions from a statistical hadron-gas model and from the dynamical string models RQMD and URQMD.*

duced by a coalescence mechanism. These blast-wave fits have attracted considerable attention because they indicate that, contrary to expectations, heavier particles like the Ξ and the Ω fully participate in the flow and decouple together with the rest of the hadron fluid.

The measurements of particle yields and ratios probe an earlier stage of the expanding system when the 'chemical' composition is frozen out. Statistical hadron-gas models have been very successful in describing the relative particle abundances measured in A-A collisions at energies ranging from the AGS up to RHIC in terms of a baryonic chemical potential $\mu_{\rm B}$ (which is a measure of the net baryon density) and a chemical freeze-out temperature $T_{\rm f}$ [9, 10]. It turns out that $\mu_{\rm B}$ decreases with energy while $T_{\rm f}$, at SPS and RHIC energies, increases to a value close the critical temperature $T_c \approx 160$ MeV where, according to lattice QCD calculations, a transition to the quark-gluon plasma should occur. Interpolation of the chemical potentials and freeze-out temperatures measured at the various energies yields a prediction of the energy dependence of particle ratios.

Fig. 3.3 shows the energy dependence of the K^+/π^+ ratio of full phase-space yields measured by NA49 at 40, 80 and 158 GeV/nucleon [6], together with the preliminary result at 30 GeV/nucleon [7]. This ratio increases steeply at AGS energies, then turns over and decreases at the SPS followed by a plateau between the highest SPS energy and RHIC. Also plotted are the predictions from a statistical hadron-gas model [11] and from the dynamical string models RQMD [12] and URQMD [13]. Whereas both the hadron-gas model and RQMD qualitatively capture the trend it is seen that, in their present version, these models fail to describe the strong decrease of the ratio measured by NA49.

In contrast to these models, the Statistical Model of the Early Stage (SMES) [14] assumes a phase transition to the quark-gluon plasma at SPS energies. Fig. 3.4 shows the ratio of total strangeness to pion production yields (E_s) versus the Fermi measure of the collision energy ($F \propto s^{1/4}$). Also shown is the SMES prediction. The anomalous energy behavior predicted by this model, which well describes the data, is caused by the assumed phase transition and is essentially due to the larger number of degrees of freedom which become available in a quark-gluon plasma, compared to a gas of confined hadrons. The analysis of the NA49 data at the lowest energy of 20 GeV/nucleon is presently in progress.

All available (about 4 million) central Pb-Pb events at 158 GeV/nucleon were used in an invariant mass anal-

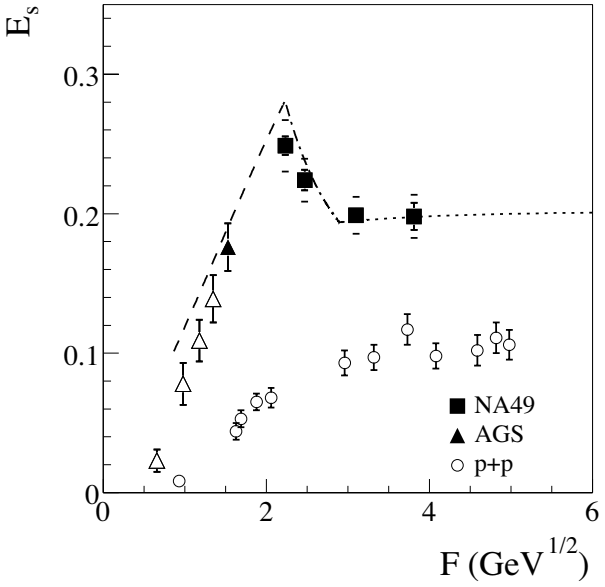

Figure 3.4: *The ratio of strangeness to pion yields (E_s) versus the Fermi energy measure (F) compared to the prediction of the SMES model.*

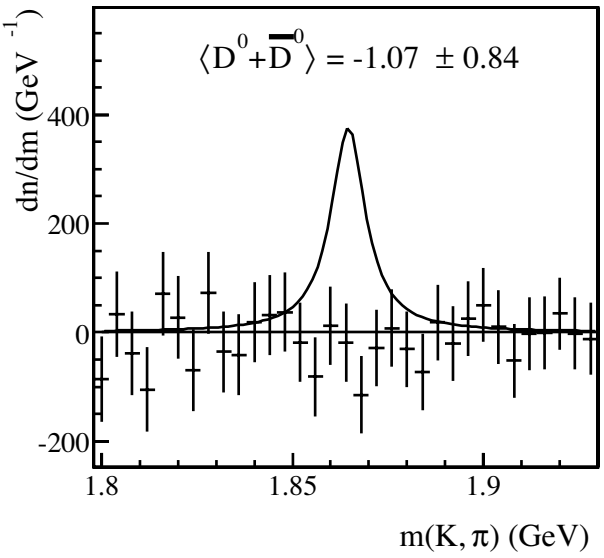

Figure 3.5: *Background subtracted invariant mass spectrum of K π pairs in 158 GeV/nucleoncentral Pb-Pb collisions. The curve shows the expected signal of thermal charm production in a quark-gluon plasma.*

ysis to measure open charm. The invariant mass was calculated for all pairs of pion and kaon candidates to detect the decays $D^0 \rightarrow K^-\pi^+$ and $\bar{D}^0 \rightarrow K^+\pi^-$. In Fig. 3.5 is shown the invariant mass spectrum of D^0 and $\bar{D}^0$ candidates after subtraction of the large combinatorial background. Clearly no signal is observed. This result excludes thermal production of charm quarks in a hot quark-gluon plasma (see upper curve in Fig. 3.5) as expected by the SMES [15]. In the context of this model, this could mean either that no quark-gluon plasma is formed or that, in contrast to strangeness, the charm equilibration time is longer than the life time of the plasma.

3.4 The STAR Experiment

The Solenoidal Tracker at RHIC (STAR) is one of the two large detector systems constructed at the Relativistic Heavy-Ion Collider (RHIC) at the Brookhaven National Laboratory.

RHIC became operational in June 2000. The first year it delivered collisions between gold nuclei at center of mass energies of $\sqrt{s_{NN}} = 130$ GeV. In 2001/2002 collisions between gold nuclei at the top energy of $\sqrt{s_{NN}} = 200$ GeV became available together with the first polarized proton proton collisions at the same center of mass energy. The ongoing 2003 run will provide 16 weeks of deuterium gold collisions again at $\sqrt{s_{NN}} = 200$ GeV as well as 8 weeks of polarized proton proton collisions.

NIKHEF was involved in STAR in 2002 and officially became a STAR member in the end of 2002.

STAR is designed primarily for measurements of hadron production over a large solid angle, featuring detector systems for high precision tracking, momentum analysis, and particle identification. The large acceptance of STAR makes it particularly well suited for event-by-event characterization of heavy-ion collisions and for the detection of hadron jets.

The layout of the STAR experiment is shown in Fig. 3.6. The year 2001 configuration consisted of the following systems. A room temperature solenoidal magnet with a maximum magnetic field of 0.5 T providing a uniform magnetic field for charged particle momentum analysis. A Silicon Vertex Tracker (SVT) consisting of 216 silicon drift detectors (13 million pixels) arranged in three cylindrical layers at a distance of approximately 7, 11 and 15 cm from the beam axis. The SVT covers a pseudo-rapidity range of $|\eta| \leq 1$ with complete azimuthal coverage. A large Time Projection Chamber (TPC) for charged particle tracking and identification. The TPC starts at a radial distance of 50 cm from the

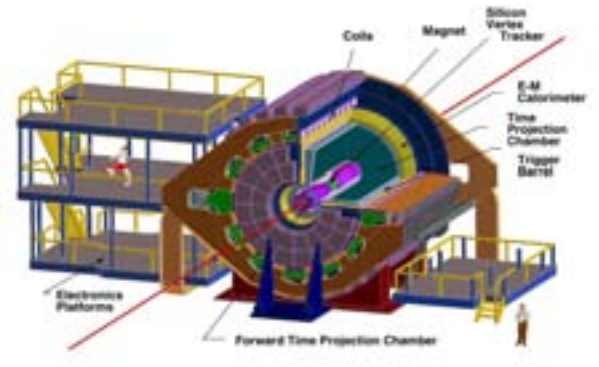

Figure 3.6: *Perspective of the STAR detector, with a cut-away for viewing inner detector systems.*

beam axis and extends to 200 cm. The TPC is 4 meters long and covers a pseudo-rapidity range $|\eta| \leq 1.8$ with complete azimuthal symmetry. It provides 136,608 channels of front-end electronics, each read-out in 512 time bins. In the forward region tracking is done using a radial drift TPC (FTPC) which covers the pseudo-rapidity range $2.5 \leq |\eta| \leq 4$, also with full azimuthal coverage and symmetry. To extend particle identification in STAR to larger momentum two small solid angle detectors are used. The Ring Imaging Cherenkov detector (RICH) covers $|\eta| \leq 0.2$ and $\Delta\phi = 0.11\pi$ and a Time-Of-Flight (TOF) patch covers $-1 \leq \eta \leq 0$ with $\Delta\phi = 0.04\pi$. It is proposed in the long range plan that the TOF system will be extended to match the TPC coverage thus allowing event-by-event characterization of identified particles in the intermediate p_t-range. It is also foreseen that an additional vertex detector will be installed based on CMOS technology around the beam pipe which will allow characterization of the open charm production. 50% of the full-barrel electromagnetic calorimeter (EMC) has been installed for 2002. The remaining EMC and an end-cap electromagnetic calorimeter (EEMC) will be installed over the next two years. This will give an eventual coverage of $-1 \leq \eta \leq 2$ and $\Delta\phi = 2\pi$. It will allow for measurement of the transverse energy of events, and provide a trigger and measure high transverse momentum photons, electrons, and electromagnetically decaying hadrons. The EMC modules include shower-maximum detectors to distinguish high-momentum single photons resulting from π^0 and η decays. The EMC will also provide prompt charged particle signals essential to discriminate against pile-up tracks in the TPC, prevalent at pp collision luminosities ($\approx 10^{32}\text{cm}^{-2}\text{s}^{-1}$).

3.5 The ALICE experiment

The Large Hadron Collider (LHC) at CERN, now under construction, will provide nuclear collisions at a center-of-mass energy 30 times higher than the present Relativistic Heavy Ion Collider (RHIC) at Brookhaven. It is expected that the energy density in the collisions of lead-ions is high enough to treat the generated quark-gluon plasma as an ideal gas.

The ALICE experiment, an experiment dedicated to the study of the quark-gluon plasma at the LHC, is developing rapidly. The ALICE detector is designed as a general purpose detector to cover all relevant observables for detection and characterization of the quark-gluon plasma. The dutch participation in the ALICE experiment concentrates on the development and production of the Silicon Strip Detector system (SSD). This system is part of the ALICE tracking system, which consists of a large TPC and six layers of silicon detectors. The SSD forms the two outer layers of the silicon detector system. The tracking system will be playing an essential role in all physics analysis of the ALICE project.

The ALICE detection modules use silicon strip sensors coupled to custom designed chips (HAL25). The modules are optimized for a low material budget and low power consumption. Therefore the front-end electronics is cooled using water flowing through metal tubes with a wall thickness of only 40μm. The corrosion resistance of these tubes was investigated together with industry.

An important event in 2002 was the realization of the first silicon strip module for the SSD, using prototype chips and a preproduction sensor, in a coordinated effort of all involved laboratories. NIKHEF played a crucial role in providing the test facilities.

A thermal model for the heat exchange between the SSD ladders and the surroundings was made and checked against measurements with a simplified prototype (see [16]). With it, the optimum temperature of the cooling water, i.e resulting in no net heat exchange, was estimated. This number is important for the design of the inner tracking system (ITS) cooling.

The end-cap modules take care of buffering of the front-end signals, the power regulation and the front-end control. In addition the end-cap modules isolate the front-end electronics, operating at the bias voltage of the sensor, from the readout electronics operating at ground potential. The end-cap modules are located just outside the active volume of the ALICE inner track-

ing system. Two chips (ALABUF and ALCAPONE) were designed in the same IBM 0.25 μm technology as the HAL25 front-end chip. During 2002 these designs were optimized for power consumption. Test set-ups for these chips were realized and successfully interfaced to the HAL25 chip, using prototype chips. Yield problems with this IBM production process still exist notwithstanding extensive effort by the designer teams.

The production of the carbon fibre frames in St. Petersburg is completed. In addition to the 80 frames needed, another 20 of lesser quality are available for prototyping and production development. The mechanical properties of these frames will be determined using equipment designed and built by NIKHEF. The carbon fibre frame properties, like rigidities in all axes, are needed to predict the sagging of the detector ladders: once mounted inside the ITS this sag cannot be measured.

The overall design of the ITS has required a lot of manpower. A substantial amount of manpower was spent to define the interfaces between the SSD and the ITS, both for the cabling and cooling and the mechanics.

References

[1] V. Blobel, Unfolding methods in high energy physics experiments, Proc. of the 1984 CERN school of computing, CERN 85-09, 88(1985).

[2] T.A. DeGrand and H.I. Mietinen, models for Polarization Asymmetry in Inclusive Hadron production. Phys. Rev. D 24, 2419(1981).

[3] C. Boros and L. Zuo-Tang, Hyperon Polarization and Single Spin left-Right Asymmetry in Inclusive Production Processes at High Energies, Phys. Rev. Lett. 79,3608(1997).

[4] S.M. Troshin and N.E. Tyurin, Hyperon Polarization in the Constituent Quark Model, Phys. Rev. D 55, 1265(1997).

[5] NA49 Collab., S. Afanasiev et al., Nucl. Instr. Meth. **A430** (1999) 210.

[6] NA49 Collab., S. Afanasiev et al., Phys. Rev. **C66** (2002) 054902.

[7] NA49 Collab., V. Friese, presented at Strangeness in Quark Matter 2003, Atlantic Beach, North Carolina, USA.

[8] NA49 Collab., M. van Leeuwen, nucl-ex/0208014, presented at Quark Matter 2002, Nantes, France.

[9] P. Braun-Munziger et al., Phys. Lett. **B465** (1999) 15, Phys. Lett. **B518** (2001) 41.

[10] F. Becattini et al., Phys. Rev. **C64** (2001) 024901, J. Phys. **G28** (2002) 1553.

[11] P. Braun-Munziger et al., Nucl. Phys. **A697** (2002) 902.

[12] H. Sorge et al., Nucl. Phys. **A498** (1989) 567c, Phys. Rev. **C52** (1995) 3291.

[13] UrQMD Collab., S. Bass et al., Prog. Part. Nucl. Phys. **41** (1998) 255.

[14] M. Gaździcki and M. Gorenstein, Acta Phys. Polon. **B30** (1999) 2705.

[15] M. Gaździcki and C. Markert, Acta Phys. Polon. **B31** (2000) 965.

[16] J. Manschot, Cooling of the ALICE Silicon Strip Detector ladders: measurements, modeling and predictions, NIKHEF report RA-M21, 18 November 2002.

4 ANTARES

4.1 Introduction

The Antares project aims to build an underwater neutrino telescope. The neutrino detection is based on the detection of Čerenkov light associated with muons originating from charged current neutrino scattering in or near the active volume of the detector.

In the year 2002, the Antares collaboration completed the phase of prototyping with the deployment of the first detector line at the foreseen site in the Mediterranean sea (at a depth of 2500 m and 40 km off the coast near Toulon, France). In Figure 4.2, the various steps towards the completion of this line are shown. The first line consists of a so-called sector, comprising 15 photo-multiplier tubes (PMTs), arranged as triplets covering 5 floors with a spacing of 12 m. The final detector will consists of 12 lines each supporting five such sectors.

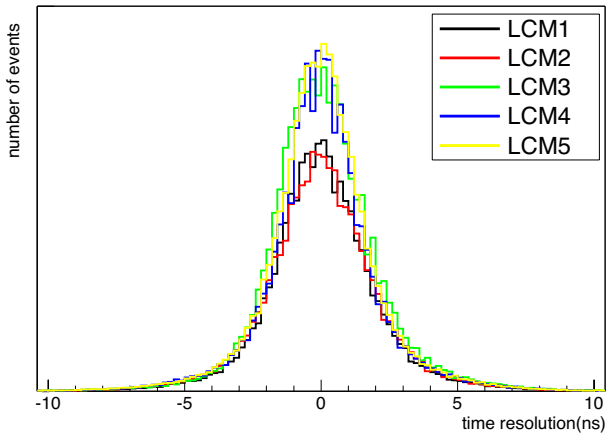

Figure 4.1: *Measured time resolution of the detector. Every Local Control Module (LCM) corresponds to a floor with three photo-multiplier tubes.*

4.2 NIKHEF contributions

For the construction of the first detector, NIKHEF has developed the following products:

- Optical–fiber data communication
- On–shore data filtering and data archiving
- Cooling system
- String power system
- Run Control and Graphical User Interface

NIKHEF has proposed a novel data-acquisition concept based on the idea to send all data to shore. For this purpose, a high-bandwidth connection between the detector and the shore is needed and a data-processing system that can filter the data in real-time. Therefore, an optical–fiber network has been developed based on the Dense Wavelength Division Multiplexing technology. With this technique up to 8 channels of standard Gb Ethernet can be transmitted through a single pair of fibers. In addition, an on-shore data-processing system has been developed that consists of a farm of standard PCs. These computers run a fast algorithm that is able to filter the physics signals from the background at the foreseen maximum data rate. The off-shore electronics are housed in pressure resistant (250 bar) titanium cylinders. Reliable operation of the off-shore electronics is achieved by a passive cooling system, designed at NIKHEF, that transports the heat produced by the electronics to the sea water surrounding the cylinder. The electrical power needed for the off-shore electronics has been partially developed in the Netherlands under the responsibility of NIKHEF. The NIKHEF contribution consists of the string power module, which provides power to a complete detector line (1 kW), and the power boxes, which supply low voltages needed for the various electronics components.

4.3 Test results

The angular resolution of the detector depends crucially on the accuracy in the determination of the arrival time of the Čerenkov light and the position accuracy of locating the PMTs. Therefore, the time accuracy of the prototype detector has been measured prior to deployment in the laboratory using a pulsed laser. The obtained resolution for the various PMTs is shown in Figure 4.1. The average time resolution is about 1 ns. Combined with the (measured) position accuracy of 20 cm, the expected angular resolution is 0.2 degree.

4.4 Outlook

It is planned that the first detector will be connected to the main junction box early 2003. This will allow us to start the operation of the detector and take the first data. It is expected that mass production for the complete detector will start by the end of 2003.

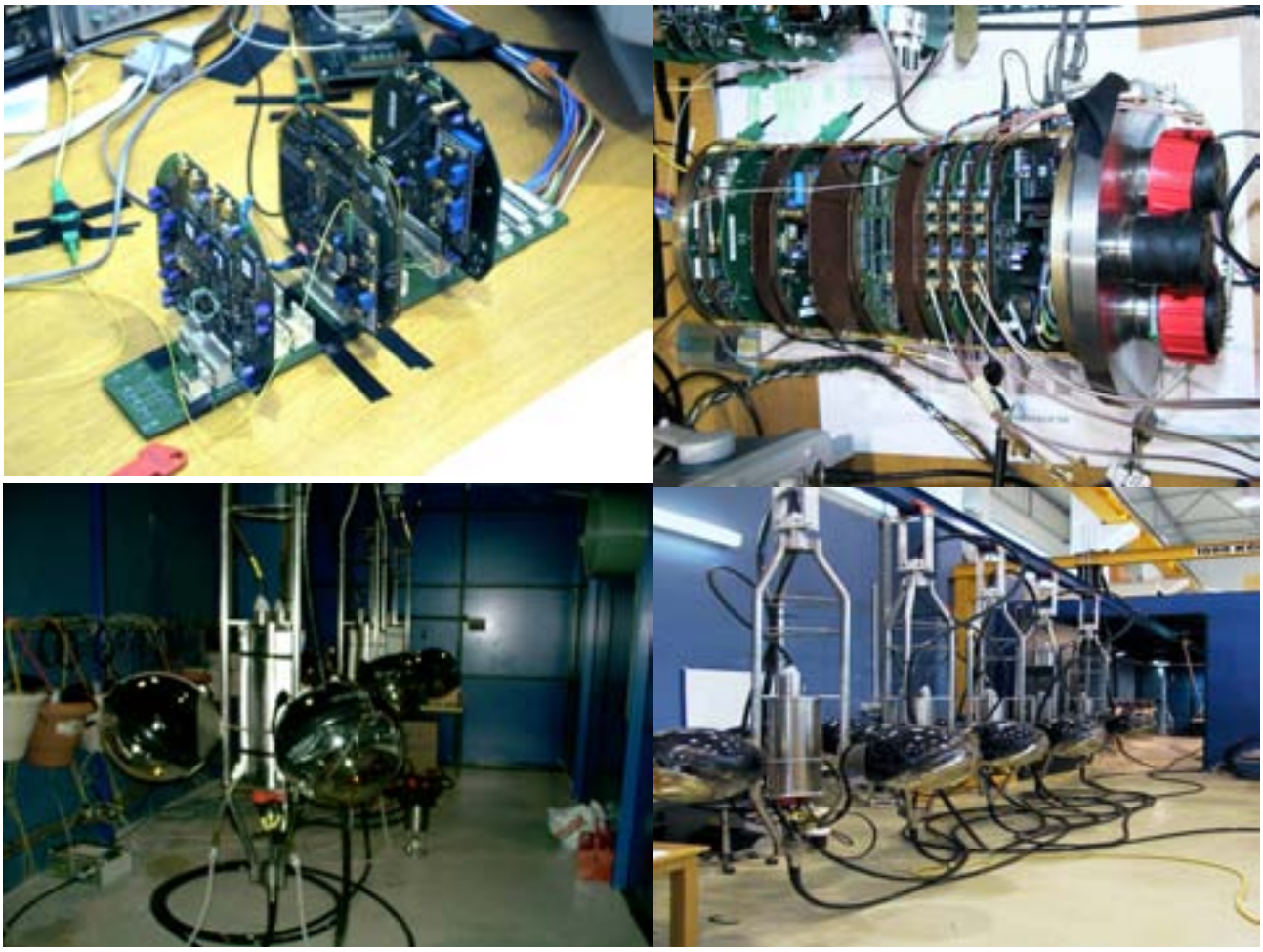

Figure 4.2: *Progress in 2002 of the first detector. From left top clockwise: electronics for the readout, complete readout system (with a crate designed and built at NIKHEF), first three floors and first complete sector line.*

5 ZEUS

5.1 Introduction

This year was the first year of data taking after the HERA luminosity upgrade. Almost immediately it became clear that the more intense beams produced by the accelerator after the upgrade caused unacceptable background conditions in both the ZEUS and H1 interaction regions. In particular the backgrounds produced a significant increase in the current drawn by the ZEUS central tracking detector. Under the foreseen running conditions these currents were so large that they precluded the use of the tracking detector. Therefore most of this year's data taking was devoted to understanding the nature and then the cause of the background. The background can be separated into three distinct categories:

- Synchrotron radiation photons produced by the positron beam as it is deflected in the magnets of the accelerator (the position and magnetic field-strengths of these magnets had been modified during the upgrade),
- background, mainly consisting of electrons and positrons, caused by interactions of the positron beam with the gas remaining inside the HERA beampipe and also with the beampipe itself,
- interactions of the proton beam with the rest-gas and the collimator structures inside the beampipe.

Below, we discuss our studies concerning the background and present some results on data analysis.

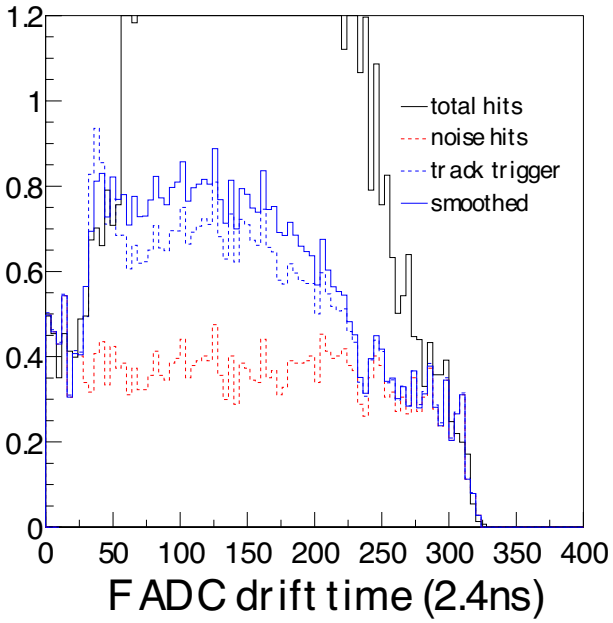

Figure 5.1: *The arrival time of pulses in the CTD due to background radiation. The red line is the regular noise level, the blue line indicates the charged particle background and the black line is the total spectrum including synchrotron radiation. Note that the synchrotron radiation arrives late with respect to the tracks.*

5.2 Investigation of the backgrounds

The complexity of the backgrounds can be understood when one realizes that the synchrotron radiation from the positron beam can cause significant outgassing as it strikes material inside the beampipe, which increases the pressure inside the pipe, which in turn increases the other backgrounds. The investigation provided detailed information on the backgrounds and has entailed a large amount of simulation and measurements to fully understand the nature of the backgrounds. As an example, it has been shown that the major contribution from synchrotron radiation stems from photons being reflected back into the detector from an absorber placed at about 11 m downstream of the detector in the positron beam. Fig. 5.1 shows the arrival time of the pulses generated by the synchrotron radiation in the central tracker. Clearly an increase is observed at a time which is 60 ns late with respect to the beamcrossing. This means that the photons have traveled about 20 m before impinging on the tracking detector, which points the finger to reflection from the above mentioned absorber.

The investigation into the backgrounds have led to a number of modifications to the accelerator being proposed, which according to detailed simulations, will significantly reduce the backgrounds. These modifications will be made in the beginning of next year, and entail a redesign of the system of masks, collimators and absorbers installed inside the accelerator's beampipe. This mainly attacks the problem of synchrotron radiation.

Midway through this year a decision was taken to attempt, in addition to continuing the investigation of the backgrounds, to achieve a number of specified goals. Two milestones were achieved by the accelerator. Firstly the accelerator group has proved that the foreseen luminosity can be reached. There is, apart

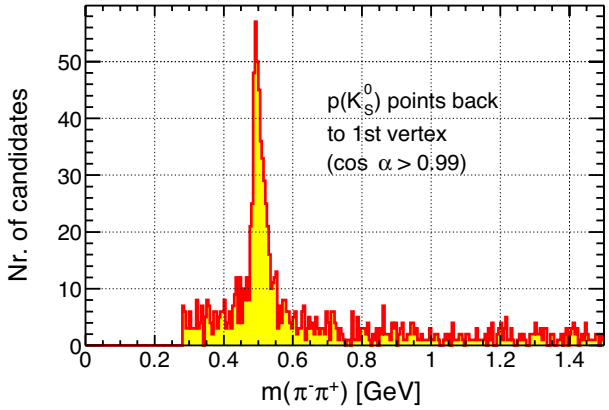

Figure 5.2: *The invariant mass spectrum of $\pi^+\pi^-$ from tracks wit a separated vertex.*

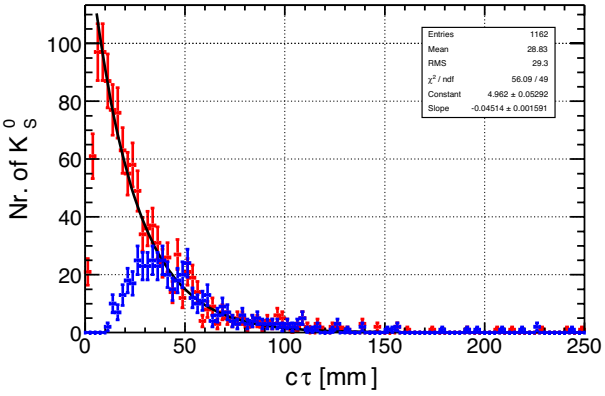

Figure 5.3: *The lifetime distribution for K^0 particles reconstructed with the microvertex (red) and with central tracker information only(blue).*

from the background, no technical reason why the accelerator could not run at the design values of currents and luminosity. Secondly it has been shown that the positron beams can be longitudinally polarized to a value close to the 50% design value. This polarization was indeed retained while collisions with the proton beams were taking place. These two achievements show that the post-upgrade physics program of HERA can be performed, when the backgrounds are brought under control.

5.3 Some data

In the latter part of the year the a decision was taken to allow a period of stable running, at necessarily reduced beam intensities, in order to allow the experiments to perform first commissioning measurements with a number of newly installed detector components. In this running period, which lasted through the first months of 2003, ZEUS collected a total of 1.5 pb^{-1} of integrated luminosity. In order to achieve the highest possible currents with the poor background conditions, the high voltage of the central tracking chamber was reduced to 95% of its nominal value. The currents drawn by the chamber were thereby reduced by approximately 50%, but it necessarily led to a reduced efficiency (-5%) for track reconstruction.

For the microvertex detector, which had been installed a year earlier in 2001, the analysis of this small amount of data proved very useful as it was possible to reconstruct the first particles with a separated vertex using the microvertex detector. Fig. 5.2 shows the reconstructed mass spectrum of two charged pions. To produce this figure the tracks were selected by the requirement that they were consistent with emanating from one point in space, but that position was inconsistent with the primary vertex position, which was reconstructed from other tracks in the event. From the distance of the vertex to the primary vertex and the momentum of the particles the lifetime of the K^0 could be reconstructed. Fig. 5.3 shows the distribution of the lifetimes measured in this way. The figure also shows the distribution obtained when no use is made of the microvertex. The difference is convincing. The microvertex detector allows the reconstruction of separated vertices to much smaller distances from the primary vertex. Eventually the microvertex detector is to be used to reconstruct

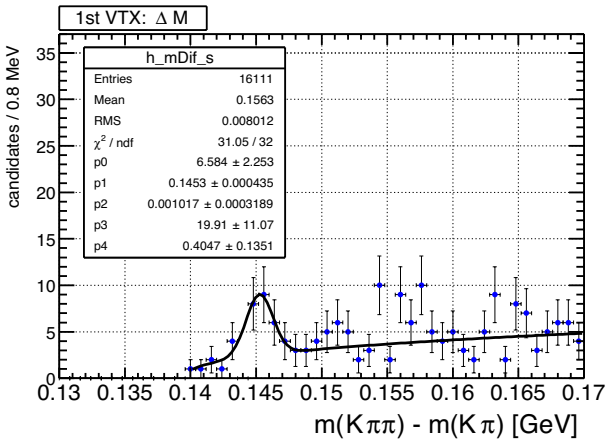

Figure 5.4: *The mass difference $\Delta M = M(K^{\pm}\pi^{\mp}\pi^{\mp}) - M(K^{\pm}\pi^{\mp})$.*

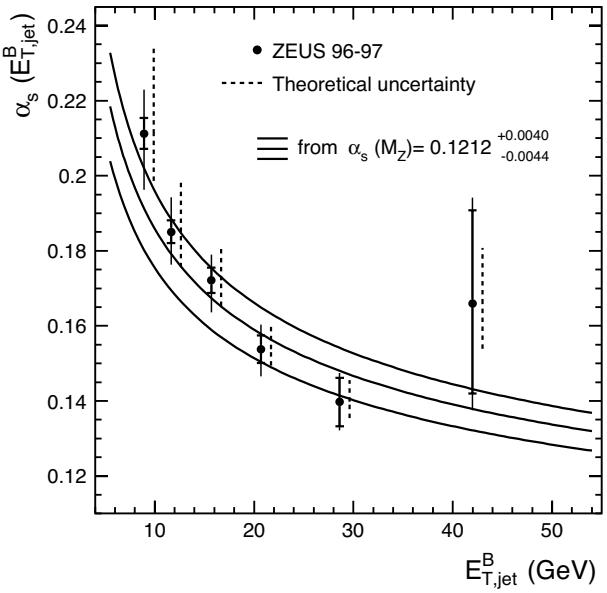

Figure 5.6: *The value of α_s extracted from jet-rates in DIS as a function of Q^2*

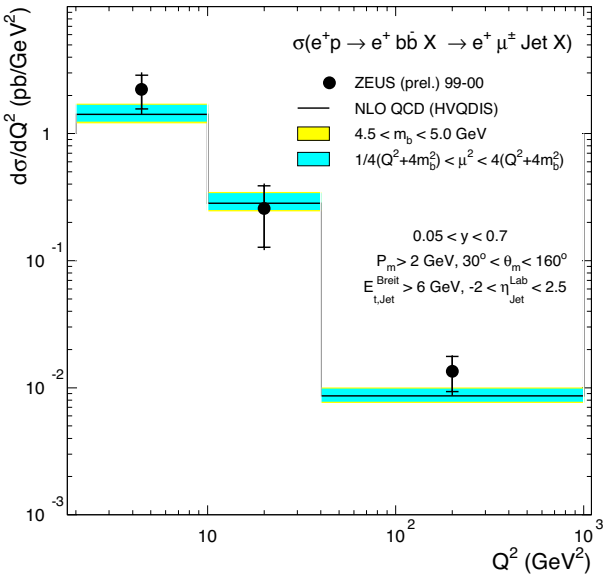

Figure 5.7: *Comparison of visible cross section of the semi-leptonic b-quark decay muons with the NLO QCD calculation*

particles which contain either a charm or bottom quark. The lifetimes of these particles is significantly shorter than that of the K^0 and these particles are also much less prevalent. Nevertheless in this small amount of data a search was performed for one of the more common ones, the D^*. Fig. 5.4 shows that most probably a handful of these particles have been detected.

Because of the higher levels of radiation during the running of the HERA accelerator the vertex detector has received a larger radiation dose than foreseen. The radiation dose has been continuously monitored during the year and at present, a year and a half after HERA startup, we estimate that the integrated dose is close to 100 krad. The estimated dose was of the order of 20 krad/year. Because the detector had been designed to withstand a total dose of the order of 200 krad no problems have yet occurred and with the reduced backgrounds reliable operation should be possible to the end of HERA data taking. The frontend electronics has in fact been shown, during irradiation tests, to be able to withstand up to 500 krad without serious implications for data taking.

5.4 Physics results

With the absence of new data the analysis effort has concentrated on the data taken between 1996 and 2000. The analysis backlog has in fact successfully been removed. Many results were shown at large international conferences such as DIS02, held in Krakow in April, where presentations were given by two of the NIKHEF ZEUS members, and ICHEP02 in Amsterdam. Of the many topics we mention a few highlights. The QCD analysis of the structure-function data, which allowed an unprecedented precision on the extraction of the densities of quarks and gluons in the proton. Fig. 5.5 shows the extracted quark and gluon distributions with their respective errors. The value of the strong coupling constant α_s has been extracted from data on inclusive jet rates in deep inelastic scattering. Fig. 5.6 shows the value of α_s as a function of Q^2 showing the clear variation of the coupling as a function of Q^2. Last but not least the production of b-quarks has been studied in deep inelastic scattering. The production cross sections are in agreement with NLO QCD calculations as is clearly seen in Fig. 5.7. We look forward to increase the precision of this measurement in the coming years using the micro vertex detector.

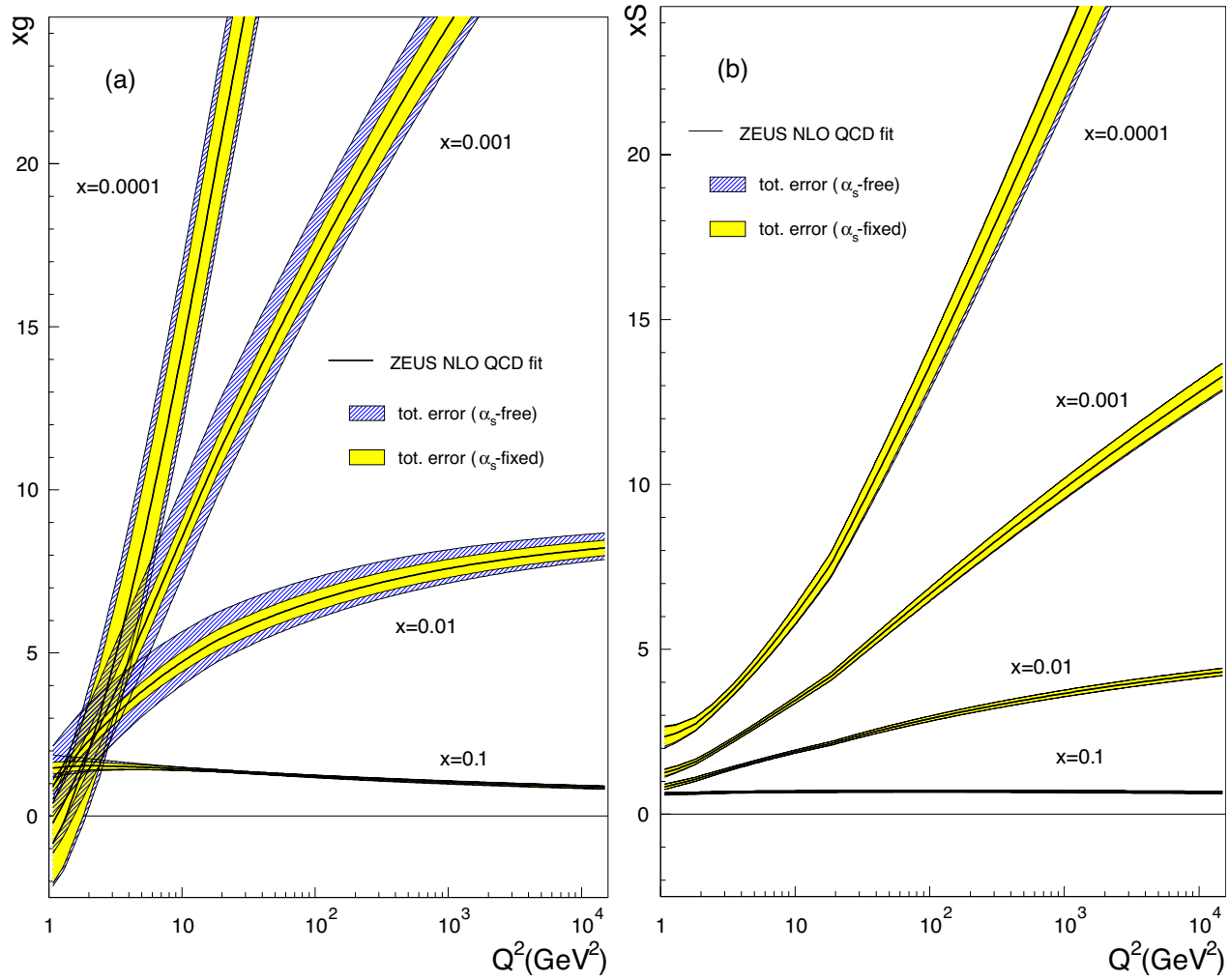

Figure 5.5: *(a) The scaling violations of the gluon density extracted from a NLO QCD fit to the ZEUS F_2 data.(b)The same for the quark densities.*

6 HERMES

6.1 Introduction

The primary objective of the HERMES experiment at DESY (Hamburg) is the study of the origin of the proton spin. By scattering polarized high-energy electrons (or positrons) off polarized targets, the amount of spin carried by the various quark types can be measured. More recently, the role of gluons and possibly even the orbital angular momentum of the quarks is being investigated.

In the year 2002 the HERMES experiment started to collect data again, following the extended shut-down period of the HERA collider. During this period changes were made to HERA such as to increase the luminosity of the collider experiments, while simultaneously the luminosity available for the (fixed-target) HERMES experiment was unaffected. As the commissioning of the upgraded HERA storage ring was delayed, data taking only started after the summer (see section 6.2).

In parallel to the measurements, the large amount of data collected during HERMES Run I (1995 - 2000) was further analyzed. Among the new results that were obtained from this analysis, the structure function $b_1(x)$ is one of the most prominent. This observable exists only for spin-1 targets and is commonly referred to as the tensor-polarization dependent structure function. It can only be determined on a tensor-polarized deuterium target as available at HERMES in the year 2000, and is sensitive to the tensor polarization of the sea quarks in the deuteron. As a non-zero value was found for $b_1(x)$, these data provide first evidence for a deformation of the sea-quark distributions in the deuteron.

A second important result that was obtained in the year 2002 is the decomposition of the quark spin-distribution functions in *five* separate flavors. These data show that the sea quarks are essentially unpolarized. The spin-flavor decomposition results are the subject of one of the four PhD theses that were written in our group this year. A selection of results described in these PhD theses is presented in section 6.3. Two of the PhD theses were already successfully defended in the last months of 2002, while the other two will be defended in the first months of 2003.

In 2002 the Lambda Wheels, a new wheel-shaped array of silicon detectors mainly developed at NIKHEF, were finally installed at HERMES. Despite several difficulties the new instrument was successfully commissioned in the second part of the year (see section 6.4). In order to protect the Lambda Wheels against excessive radiation caused by the loss of the electron (or positron) beam in the vicinity of the HERMES experiment, a Beam-Loss-Monitor system was developed. This system, which was already installed in 2001, operated successfully during the entire year.

The NIKHEF group in HERMES also shares the responsibility for the operation of the longitudinal polarimeter. Following the many changes of HERA related to the collider luminosity upgrade, it had to be demonstrated again that it was possible to create polarized lepton beams in the storage ring. During a dedicated test run it was shown that polarized positron beams can still be produced by HERA and that the longitudinal polarimeter was fully operational again (see section 6.5).

Given the improved performance of HERA near the end of 2002, it is hoped that data taking can be resumed under improved conditions in 2003. With all the new instrumentation now operational, this should result in first data on the transverse spin distribution of the quarks in the nucleon.

6.2 Data taking

In the year 2002 data on deep-inelastic scattering of positrons from a transversely polarized hydrogen target have been collected. These data are used to measure the transverse spin distribution function $h_1(x)$, which to date is the only experimentally unknown leading-order structure function of the proton. Since gluons do not contribute to this structure function, a measurement of $h_1(x)$ makes it possible to study the role of quarks in the spin structure of the proton more directly. In fact, it is predicted that due to the absence of the gluon contribution the Q^2 evolution of $h_1(x)$ is much weaker than that of the other leading-order structure functions. Moreover, the first moment of $h_1(x)$ (also known as the tensor charge of the proton) is predicted to be much larger than the first moment of the longitudinal structure function $g_1(x)$. These are unverified QCD predictions that will now be addressed by the new HERMES data.

The amount of data accumulated in 2002 is illustrated in Fig. 6.1. With a similar amount of data added in 2003 it will be possible to make first estimates of the size of the structure function $h_1(x)$.

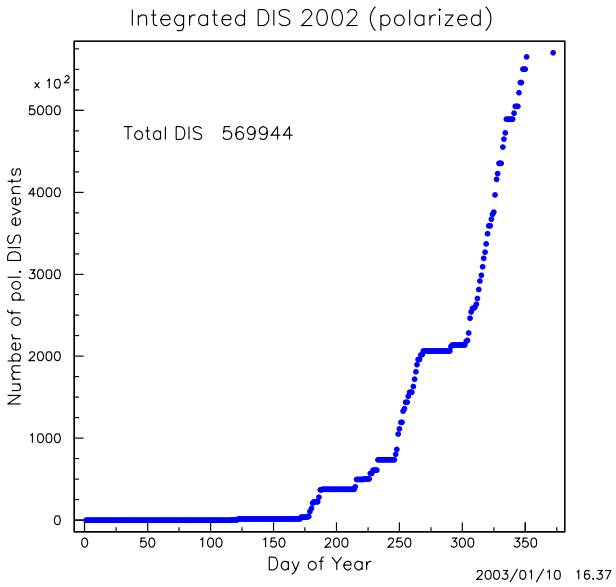

Figure 6.1: *Integrated number of deep-inelastic scattering events collected by the HERMES experiment at DESY in the year 2002. Due to delayed commissioning of the HERA collider data taking only started after the summer.*

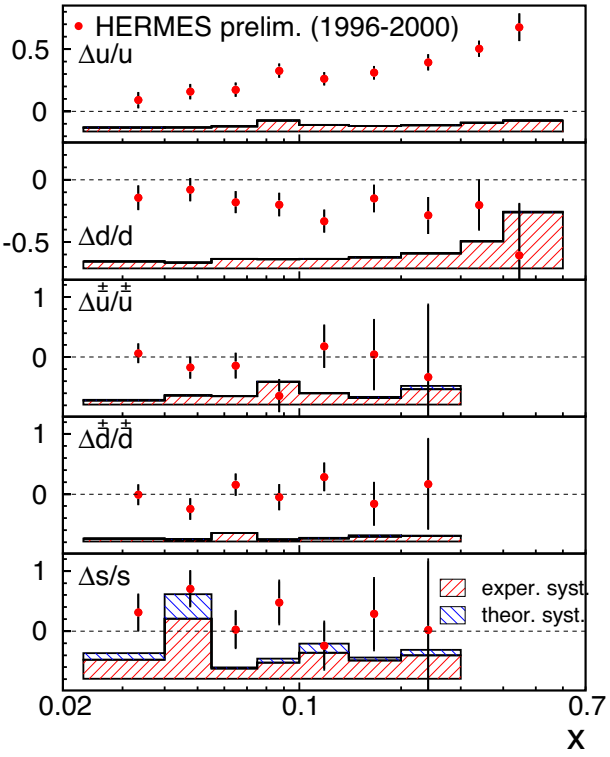

Figure 6.2: *Flavor-separated quark-helicity distributions as a function of the Bjorken scaling variable x. The band in the bottom part of each plot represents the systematic uncertainty of the data.*

6.3 Physics analysis

Many physics results have been obtained by the HERMES collaboration in the year 2002. In the following subsections the emphasis is on those results that formed (part of) the subject of the four PhD theses that were written in our group in 2002.

Flavor decomposition of the nucleon spin

In semi-inclusive deep-inelastic scattering experiments both a hadron, i.e. a pion, a kaon or a proton, and the scattered electron are detected. The probability to observe a specific hadron depends on the flavor of the struck quark and the type of target (proton or deuteron) used. These probabilities are measured in experiments in which neither the beam nor the target is polarized. The results of these measurements are parameterized in Monte-Carlo programs describing this hadronization process. By performing semi-inclusive deep inelastic scattering experiments on polarized targets and using polarized electron beams, it is possible to extract information on the polarization of individual quark flavors by making use of the aforementioned tagging probabilities. The polarization of u-quarks in the proton, for instance, can be derived from measurements of the asymmetry of the normalized number of events with respect to the relative spin orientation of beam and target in which both a scattered lepton and a produced π^- particle are observed.

At HERMES, such spin-dependent deep-inelastic scattering data have been collected since 1996 on polarized proton and deuteron targets. Making use of Monte-Carlo techniques to account for the various tagging probabilities, it has been possible to derive the polarization of u, d, $\bar{u}$, $\bar{d}$ and s quarks from the data. The results are displayed in Fig. 6.2 as a function of the Bjorken scaling variable x. It is observed that u and d quarks are oppositely polarized, whereas the sea quarks ($\bar{u}$, $\bar{d}$ and s) carry hardly any spin. In particular the small (and if anything positive) polarization of the s-quarks has raised considerable interest, as previously it has often been suggested that the s quarks would be negatively polarized in the proton.

Higher-twist effects in deep-inelastic scattering

In HERMES Run I a large amount of unpolarized deep-

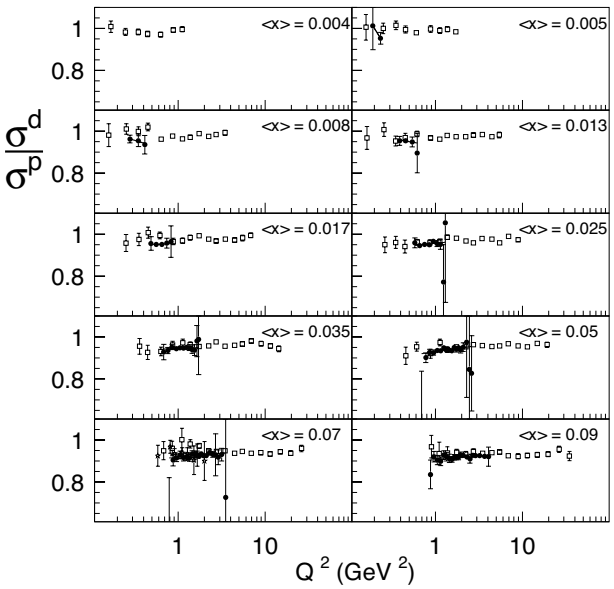

Figure 6.3: *Ratio of deep-inelastic lepton scattering cross sections on the deuteron and the proton as a function of the value of the squared four-momentum transfer Q^2. Each panel corresponds to a different x-bin. The HERMES (NMC) data are represented by the closed (open) symbols.*

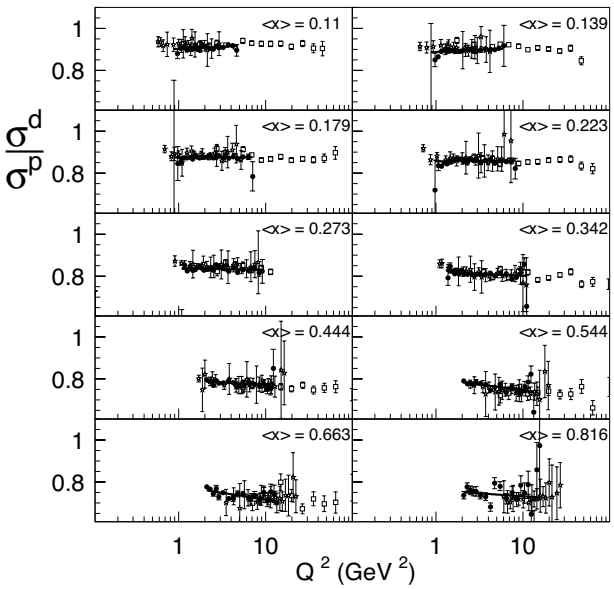

Figure 6.4: *Ratio of deep-inelastic lepton scattering cross sections on the deuteron and the proton as a function of the value of the squared four-momentum transfer Q^2. Each panel corresponds to a different x-bin. The HERMES (NMC) data are represented by the closed (open) symbols.*

inelastic scattering data has been accumulated on proton and deuteron targets. By comparing these data to similar data obtained by the NMC experiment at CERN (at much higher incident energies) one can investigate possible differences between the two data sets. At low values of x, deviations can be caused by a possible increase of the longitudinal (or non spin-flip) component of the deep-inelastic scattering cross section on the deuteron as compared to that on the proton. Such an increase on the deuteron might represent partonic correlations that are not the same for the proton and the deuteron. At larger values of x the structure functions themselves may receive additional Q^2 dependent contributions. In either case, such effects – if observed – may indicate the presence of partonic correlations that are not contained in the standard leading-order deep-inelastic scattering framework. They are commonly referred to as higher-twist effects.

The results of such a comparison are shown in Fig. 6.3 (for the low x data) and Fig. 6.4 (for the high x data). No significant deviation between the NMC and HERMES data has been observed. Consequently, the interpretation of deep-inelastic scattering data obtained at HERMES does not suffer from (complicating) higher-twist effects.

The same data have also been used to evaluate the Gottfried Sum Rule (GSR), which relates the difference between the deep-inelastic scattering structure functions $F_2(x)$ for the proton and the neutron to an asymmetry between $\bar{u}$ and $\bar{d}$ sea-quark distributions. The results are shown in Fig. 6.5. The value of the GSR integral (given by $\int_{x_{min}}^{1} dx\ (F_2^p - F_2^n)/x$) is displayed as a function of its lower integration boundary (x_{min}). Surprisingly, the data are within statistics similar to the data obtained by NMC at a significantly higher average Q^2 value. These data thus demonstrate the Q^2 independence of the $\bar{u}$-$\bar{d}$ differences in the proton.

Photoproduction of Λ_C baryons

The production of charmed baryons or mesons in interactions between longitudinally polarized electrons and longitudinally polarized nucleons provides information on the contribution of gluons to the nucleon spin if the production process is dominated by photon-gluon fusion. Such processes are particularly interesting, as the gluon polarization is expected to be large in view of

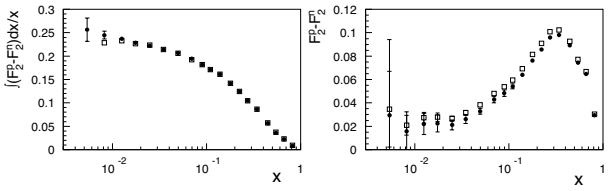

Figure 6.5: *Left: value of the Gottfried Sum Rule integral as a function of the (chosen) lower limit (in x) of the integral. Right: value of the integrand times x as a function of x. Both the HERMES data (closed symbols) and the NMC data (open symbols) are shown.*

the relatively small fraction of the nucleon spin that is carried by the quarks.

Using the data collected in 1998, 1999 and 2000, the decay $\Lambda_C^+ \rightarrow \Lambda^0 + \pi^+$ was investigated. The analysis was performed in two steps. First, the invariant mass of the Λ^0 hyperon was extracted from the four-momenta of the pions and the protons in an event. In the second step, the invariant mass spectrum of the Λ_C^+ baryon was evaluated from the four-momenta of the Λ^0 hyperon and the π^+ meson. The background has been suppressed by requiring that the propagation directions of the Λ^0 hyperon as determined either from the difference between the Λ^0 and Λ_C^+ vertex points, or from the vector sum of the decay particles, are highly co-linear. Moreover, the momentum of the Λ^0 hyperon perpendicular to the beam direction was required to be high: 0.6 GeV $\leq P_{T,\Lambda^0} \leq$ 0.8 GeV. Despite the small cross section and small branching ratio for this decay, a clear signature for the production of a Λ_C^+ baryon has been observed at its known invariant mass of 2.3 GeV.

To determine the cross section for Λ_C^+ photoproduction, the probability $P_{\Lambda_C^+}$ that a produced Λ_C^+ particle was identified in the HERMES detector, has been evaluated using events generated with the Monte-Carlo program AROMA. The result is shown in Fig. 6.6. The Λ_C^+ photoproduction cross section near threshold is seen to be larger than the *D*-meson cross section by about an order of magnitude.

The intensity of the Λ_C^+ peak is, however, too small to extract a double-spin asymmetry. As an alternative, such an asymmetry has been determined for partially reconstructed Λ_C^+ baryons. By considering the domain in the $\Lambda^0\pi^+$ invariant mass-spectrum between 1.45 and 2.32 GeV, the statistics has been increased. Monte-Carlo calculations performed with the codes AROMA

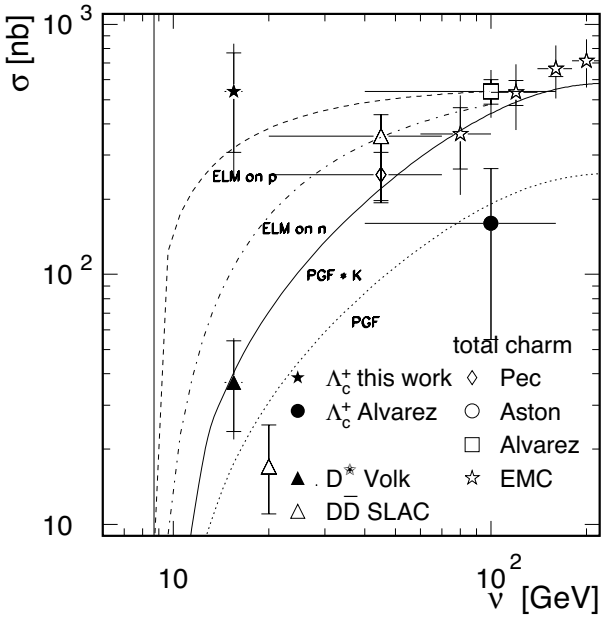

Figure 6.6: *Cross section for quasi-real photoproduction of charmed hadrons. The open symbols at higher energies correspond to the total charm photoproduction cross section. The closed non-triangular symbols correspond to Λ_C^+ photoproduction, while the two triangular symbols correspond to two measurements of the D-meson photoproduction cross section. The lower two curves correspond to leading-order photon-gluon fusion calculations, while the upper two curves correspond to the results of calculations using the Effective Lagrangian Approach.*

and PYTHIA indicate that a sizeable fraction of the yield in this region can be attributed to Λ_C^+ production. The relative contribution of Λ_C^+ events and non-charmed background to the events was also studied with these Monte-Carlo programs. These simulations indicate significant photon-gluon fusion contributions for events with a tranverse momentum p_{T,Λ^0} of the Λ^0 hyperon with respect the Λ_C^+ propagation direction larger than 0.6 GeV, and a transverse momentum p_{T,Λ_C^+} of the partially reconstructed Λ_C^+ with respect to the beam-axis larger than 1.2 GeV. The double-spin asymmetry extracted from these partially reconstructed Λ_C^+ baryons is positive and suggests that the gluons are positively polarized.

Nuclear effects

In deep-inelastic scattering nuclear targets can be used

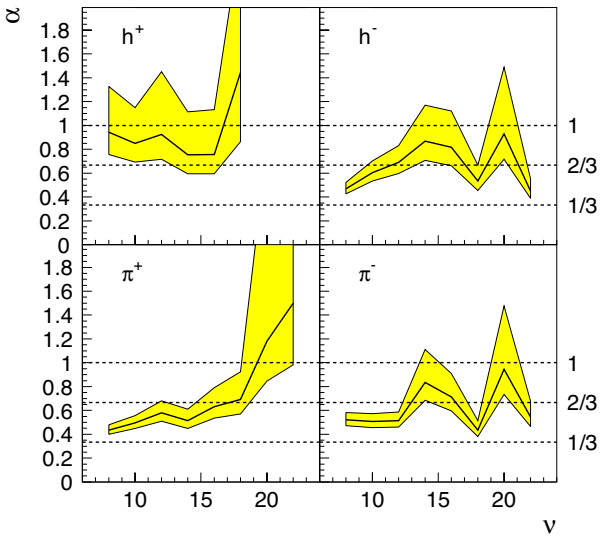

Figure 6.7: *Value of the exponent α describing the the A-dependence of the hadron attenuation as determined from data collected on nitrogen and krypton targets. The data are displayed as a function of the energy transfer ν for positive and negative hadrons (top two panels) and positive and negative pions (bottom two panels). The uncertainty on the exponent is represented by the error band.*

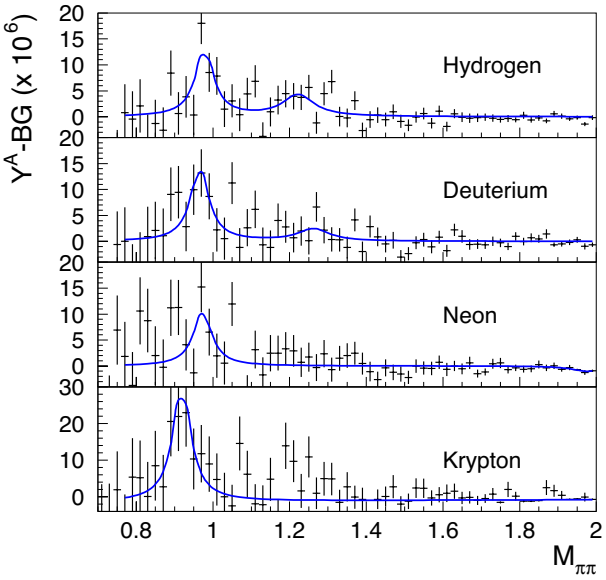

Figure 6.8: *Two-pion invariant mass spectrum for semi-inclusive deep inelastic scattering from four different nuclear targets. The background (which is mainly due to the prominent ρ^0 peak) has been subtracted using a Monte-Carlo simulation. In each of the spectra evidence is found for the production of the $f_0(980)$ scalar meson.*

as a filter at the femtometer scale to selectively study certain processes. This concept has been used in two studies based on data obtained with the HERMES experiment. The results of both studies are described below.

When describing the propagation of quarks in nuclear matter it has been predicted that the energy loss would scale with the square of the distance traversed due to large interference effects between the coherently propagating quarks and the emitted gluons. This QCD effect is known as the Landau-Pomeranchuk-Migdal (LPM) effect. The predicted quadratic dependence on distance is in contrast to the usual linear dependence of the energy loss of a hadron propagating in nuclear matter. By comparing the attenuation of hadrons produced in deep-inelastic scattering on nuclear targets of various sizes a distinction can be made between these two mechanisms. Actually, this corresponds to a study of the dependence of hadron attenuation on the nuclear mass number A. If the LPM effect is dominant a quadratic dependence, corresponding to $A^{2/3}$ is expected, otherwise the standard $A^{1/3}$ dependence will be observed.

In Fig. 6.7 the results of such a study are displayed. By comparing the attenuation for hadrons or identified pions (of either sign) in ^{14}N and ^{84}Kr and assuming an A^{α} dependence, the value of the exponent α has been determined for a range of energy transfer values. The data for negative hadrons and pions of either sign clearly favor the $A^{2/3}$ dependence expected from the LPM effect. The exponent for positive hadrons seems to be even larger than 2/3, which may be caused by large proton-rescattering contributions that enhance the positive hadron yield.

A second example of nuclear filtering concerns the production of the $f_0(980)$ scalar meson in deep-inelastic scattering. The structure of this object has been the subject of a long-standing debate. It has been argued that the $f_0(980)$ scalar meson could be either a $K\bar{K}$ molecule, a $q\bar{q}q\bar{q}$ hybrid or a normal $^3P_0$ meson. By electro-producing an $f_0(980)$ meson on various nuclear targets, a significant attenuation is expected on heavy targets if the $f_0(980)$ has a significant size, i.e. comparable to that of a hadron.

This idea has been applied to the HERMES data when

it was realized that – unexpectedly – $f_0(980)$ electroproduction could be observed (see Fig. 6.8). Although the margins of uncertainty are still large, the more or less equally strong excitation of the $f_0(980)$ scalar meson in each of the four targets investigated already suggest that it is less likely that the $f_0(980)$ has a $K\bar{K}$ molecular structure.

The JLab experiment

In addition to the studies of the A-dependence of deep-inelastic scattering based on the HERMES data, an additional experiment was carried out at JLab in order to increase the kinematical range (and statistical precision) of such studies. The experiment measured the cross section of inclusive electron-nucleon and electron-nucleus scattering at low values of x (0.007-0.55) and Q^2 (0.03-2.8 GeV/c^2). The data will be used to determine the ratio of DIS cross sections σ^A/σ^D, and to perform Rosenbluth separations to extract the ratio $R = \sigma_L/\sigma_T$ of the longitudinal to transverse photo-absorption cross sections.

The experiment was carried out in hall C of JLab (Newport News, Virginia) using 2.301, 3.419 and 5.648 GeV electron beams of about 25 μA, and the High-Momentum Spectrometer for the detection of the scattered electrons. Data were taken at various scattering angles between 10 and 60 degrees on the targets LH_2, LD_2, C, Al, Cu and Au.

Several steps in the analysis have been finalized. Tracking, Čerenkov and Calorimeter efficiencies have been determined. The charge-symmetric background has been determined for all targets from the measured cross section with a detected positron. Pion rejection was implemented in the hardware trigger, and the further remaining pion background was determined by using the particle-identification information from the Čerenkov and Calorimeter detectors. Corrections for density changes due to boiling of the cryo targets were applied.

During the data analysis a rate dependence was found. The effect was especially noticeable in case of high rate runs; at the highest rate of 400 kHz about 4% of the selected tracks were wrong. By improving the track-selection algorithm this value could be reduced to less than 0.2 %. As the radiative corrections and radiative tail subtraction from the measured cross sections are very important for these data, a comparison between different prescriptions for such corrections is presently being made.

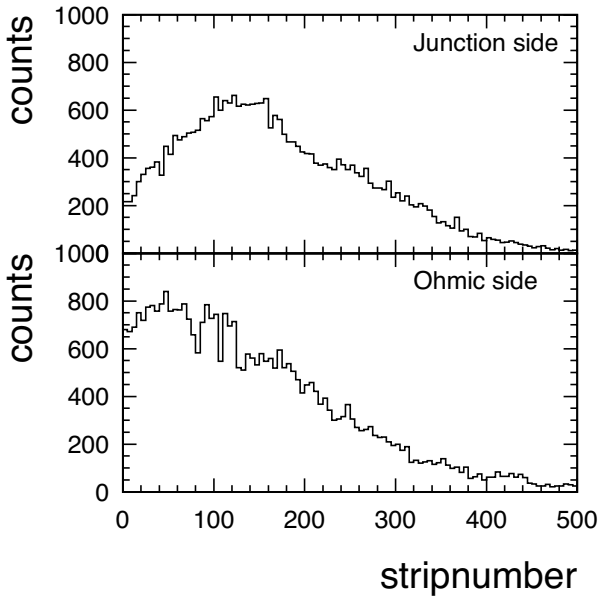

Figure 6.9: *Response of individual strips of a single Lambda Wheel module ("strip map"). The downward slope to higher strip numbers is caused by a reduction in strip length.*

6.4 The Lambda Wheel project

In the spring of 2002 the Lambda Wheels were reinstalled, after an absence of about one year, in the expectation of more favorable beam conditions at HERA in the year to come. Their operation during the rest of the year was hampered by the much too high fringe field of the transverse-target magnet. However, during the short periods when this magnet was switched off, the Lambda-Wheel electronics was tuned and by the end of the year the Lambda-Wheel data were included in the normal data stream. Fig. 6.9 shows the strip map for a single module obtained in the first run. The hit pattern of events recorded in the same Lambda-Wheel module (displayed in Fig. 6.10) is seen to reflect the geometrical shape of the module.

The Beam Loss Monitor (BLM) saw its first complete year of operation. For the greater part of 2002 it was also connected to the dump kicker of the HERA lepton storage ring. No beam dumps were triggered by the system this year. The output of the BLM was used to estimate the accumulated radiation dose in the front region of the HERMES detector. Fig. 6.11 shows the results of the chambers closest to the beam pipe, located at approximately 6 cm from the beam. The dose

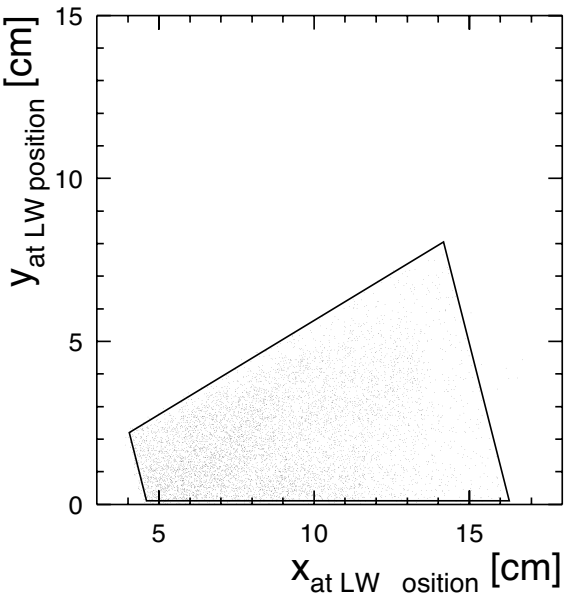

Figure 6.10: *Position of hits recorded in a single Lambda-Wheel module. The threshold used for this plot is set at half of the signal produced by a minimum ionizing particle (i.e. 0.5 MIP).*

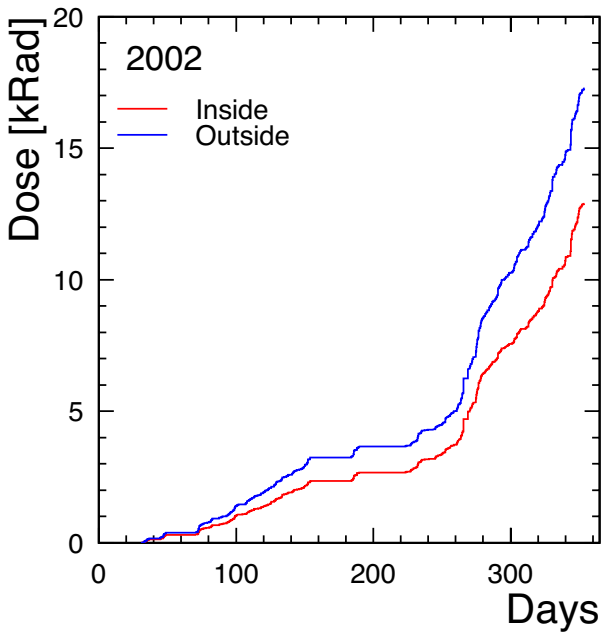

Figure 6.11: *Accumulated dose recorded with two of the six ionization counters of the HERMES Beam Loss Monitor. The dose is seen to increase in the course of the year due to the increased positron beam currents injected in HERA. The red (blue) curve represents the results of a chamber located on the inside (outside) of the ring.*

falls off rapidly with distance to the beam. The length characterizing this decrease amounts to 6.5 cm on the inside curvature of HERA, while the decrease is slightly less at the outside of HERA corresponding to a characteristic length of 8.5 cm. The total accumulated dose in 2002 did not exceed 20 kRad.

6.5 Longitudinal Polarimeter

The longitudinal polarimeter (LPOL) at HERA exploits the asymmetry in the Compton cross section by scattering circularly polarized photons off longitudinally polarized electrons. The interaction point is located 39 m downstream of the center of the HERMES target. The backscattered photons are detected in a calorimeter that measures the total energy of the photons. Due to their very large boost almost all photons are scattered into a very small cone around 180° in the laboratory frame and travel along the electron beam. In order to separate the photons from the electron beam a dipole magnet is used to bend the electrons by 0.54 mrad. This is enough to extract the photons from the beam line 16 m downstream of this bend.

Two calorimeters are available to measure the backscattered photons. The first is a crystal calorimeter made from four independent crystal detectors which allow the simultaneous determination of the energy and position of the scattered photon on the face of the detector. The second, sampling calorimeter is not segmented and needs an independent detector to measure the position of the Compton photons. For this purpose a scintillation fiber detector is located in front of the sampling calorimeter that has a position resolution of better than 1 mm. A new scintillation fiber detector for horizontal and vertical beam positioning has been built as a replacement. Also a new case to hold the detector has been built with much better shielding against low energy synchrotron radiation to protect the fibers against radiation damage.

After the upgrade of HERA the LPOL was used to monitor the first attempts to build up polarization in the reconfigured HERA lepton storage ring. At the same time these attempts could be used to test the performance of LPOL after porting the data acquisition system and all analysis software to a new Linux-based operating system. Figure 6.12 shows the polarization of the positron beam in the HERA machine as measured by the LPOL.

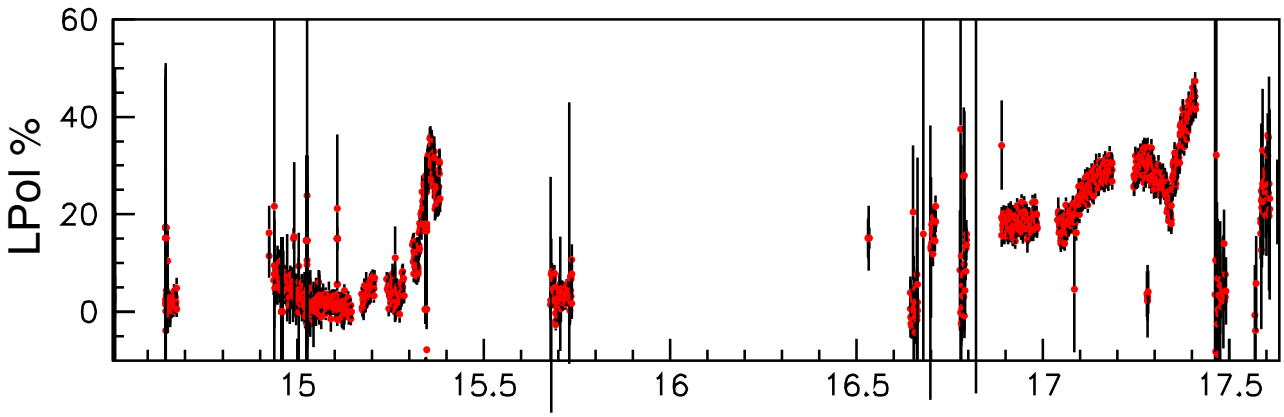

Figure 6.12: *First evidence of polarization of the positron beam stored in HERA after the upgrade of 2001. The data have been recorded with the longitudinal polarimeter during two periods in October 2002. On the horizontal axis the day number in October is displayed.*

The maximum polarization measured during these first polarization-tuning efforts was around 40%.

6.6 Outlook

In the year 2003 data taking with the transversely polarized target will continue. It is expected that sufficient data will be collected to carry out a first determination of the transverse structure function $h_1(x)$. The anticipated margins of uncertainty will depend strongly on the availability of high-intensity HERA lepton beams during the entire year.

A small modification of the local electronic read-out of each Lambda-Wheel module is foreseen for the spring of 2003. This modification will make it possible to operate the new silicon detectors in the high fringe fields of the transversely polarized target. Thereafter, data taking in the extended acceptance opened by the Lambda Wheels will get started.

7 DELPHI

7.1 Detector exhibit

The DELPHI detector stopped data taking at the end of the year 2000. The barrel part of the DELPHI detector is being prepared as a permanent exposition for CERN visitors. In December it was moved to its final position in pit 8, compatible with the spatial arrangement of the LHCb counting houses. It is foreseen to make the detector exhibit available to the public from summer 2003 onwards.

7.2 Reprocessing

No real data reprocessing took place this year, most of the analyses being based on the last data processing finished in 2001. Although the bulk of the Monte Carlo event generation was made in 2001, a further 170 million events were generated and reconstructed in 2002. These samples were mainly used for the study of systematics in the high precision measurements.

7.3 Selected research topics

A total of 8 papers were published or accepted for publication in refereed journals in 2002 and an additional 3 papers were submitted for publication. Out of these, 3 papers were still based on LEP1 data. In addition, 28 papers are in preparation and many other analyses are still underway, which should lead to another 30 publications in the next two years.

Sixty papers were submitted to the ICHEP Conference in Amsterdam, of which 19 were exclusively based on LEP1 data.

The NIKHEF group contributed to B physics, W physics, measurement of the ZZ cross section and to the Higgs search. One PhD thesis was finished, discussing the measurement of Z boson pair production and the search for the Higgs boson. Three topics, with contributions from the NIKHEF group, will be discussed here.

Search for the Higgs boson

The final result on the search for the Standard Model (SM) Higgs boson has been sent to the journal. The latest calibration and alignment of the detector during the full LEP2 data taking and new Monte Carlo simulation (both for the 4-fermion and the 2-fermion physics) have been used. The analyses have an improved sensitivity with respect to previous DELPHI Higgs searches and were extended to low Higgs masses, down to 12 GeV/c^2. The SM Higgs mass was excluded to be lighter

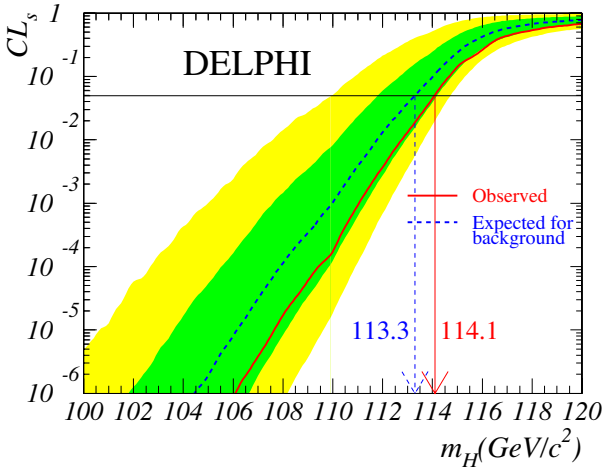

Figure 7.1: CL_s, *the pseudo confidence level for the signal hypothesis as function of the Higgs mass,* m_H. *Curves are the observed (full) and expected median (dashed) confidences from experiments with only background channels while the bands correspond to the 68.3% and 95.0% confidence intervals for the hypothesis of only background processes. The intersections of the curves with the horizontal line at 5% define the expected and observed 95% CL lower limits on* m_H.

(at 95% CL) than 114.1 GeV/c^2, while an exclusion limit at 113.3 GeV/c^2 was expected. The pseudo confidence level for the signal hypothesis as function of the Higgs boson mass, m_H, is shown in Figure 7.1. Typically, for a Higgs mass of 110 GeV/c^2 one would expect to observe a 4 standard deviation signal, which would be hard to miss. Lower limits on the masses of neutral Higgses in the minimal supersymmetric model have also been set.

W production cross section and branching ratios

The analysis of the W pair production cross section for the full data set has been finalised. The total luminosity corresponds to about 670 pb^{-1}. Hadronic and leptonic decays of the W have been selected. The measured cross section as a function of the centre of mass energy ranging from 161 to 209 GeV is shown in Figure 7.2. The hadronic and leptonic W branching ratios are shown in Figure 7.3. All results are in excellent agreement with the Standard Model predictions.

From the W decay branching ratios one can, using the experimental knowledge of the sum $|V_{ud}|^2 + |V_{us}|^2 +$

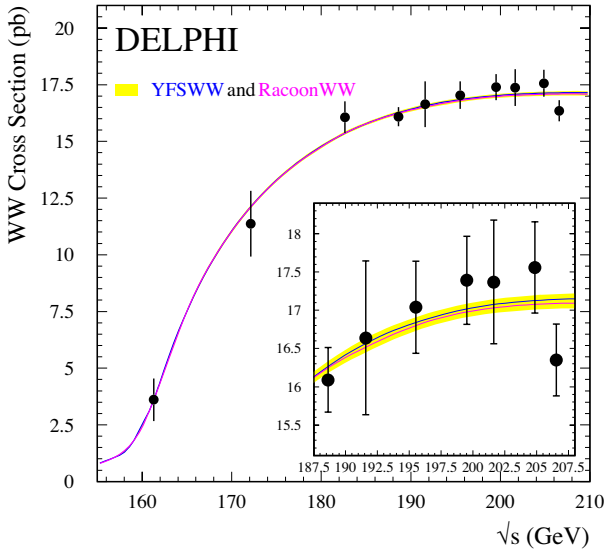

Figure 7.2: *Measurements of the W^+W^- cross section compared with the Standard Model prediction. The shaded area represents the uncertainty on the theoretical calculations.*

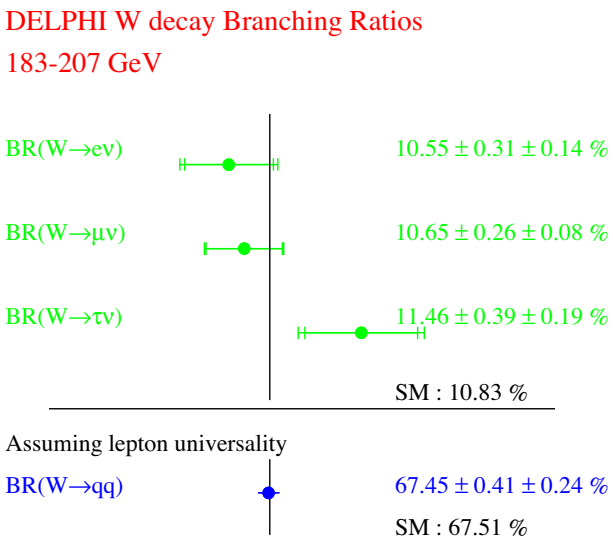

Figure 7.3: *Measurements of the W branching ratios in comparison with the Standard Model expectations.*

$|V_{ub}|^2 + |V_{cd}|^2 + V_{cb}|^2$, derive a rather precise value of the CKM matrix element $|V_{cs}|$ of $0.973 \pm 0.019(stat) \pm 0.012(syst)$.

Trilinear Gauge Boson Couplings

An important topic is the study of Trilinear Gauge boson Couplings (TGC), i.e. the coupling of three bosons. Different processes are sensitive to the WWZ or $WW\gamma$ couplings: the production of a W^+W^- pair (in particular the production cross section discussed above) and e.g. the production of a single W in the reaction $e^+e^- \rightarrow We\nu$.

Here only the results based on the analysis of the single W process will be discussed. The main processes with a WWZ or $WW\gamma$ vertex leading to a $We\nu$ final state are shown in Figure 7.4.

The data are used to determine Δg_1^Z, the difference of the WWZ coupling strength and the Standard Model value, $\Delta\kappa_\gamma$, the difference of the value of the dipole coupling and the Standard Model value, and $\Delta\lambda_\gamma$, the difference for the $WW\gamma$ quadrupole parameter. In the Standard Model g_1^Z and κ_γ are equal to 1 and λ_γ is 0.

In the analysis an effective Lagrangian for the interaction of two W bosons and a photon or Z is used imposing CP conservation and SU(2) × U(1) invariance. This leads to the following relation of the $WW\gamma$ and WWZ parameters $\Delta\kappa_Z = \Delta g_1^Z - s_w^2/c_w^2\Delta\kappa_\gamma$ and $\lambda_Z = \lambda_\gamma$, where s_w and c_w denote respectively the sine and cosine of the electroweak mixing angle.

The data set taken from 1998 to 2000 for energies ranging from 189 GeV to 207 GeV was analysed, corresponding to a total integrated luminosity of 570 pb^{-1}. Three different final states were selected: the W decayed leptonically either to an electron and a neutrino (1), or to a muon and a neutrino (2), or hadronically to a quark pair (3). In total 23 events with an electron, 31 events with a muon and 207 hadronic events were selected. The corresponding efficiencies (signal purities in brackets) were respectively 37% (57%), 50% (69%) and 20% (30%). The single W cross sections for the different final states were determined using a likelihood fit and the results are shown in Figure 7.5. The results

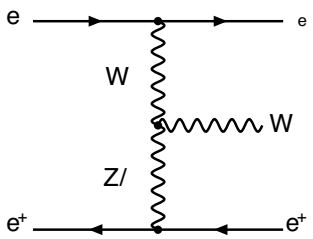

Figure 7.4: *Feynman diagrams leading to a single W in the final state.*

coupling	68% CL
$\Delta\kappa_\gamma$	$-0.13^{+0.12}_{-0.14}$(stat) $\pm$ 0.05(syst)
$\Delta\lambda_\gamma$	$-0.02^{+0.26}_{-0.25}$(stat) $\pm$ 0.01(syst)
Δg_1^Z	$+0.25^{+0.34}_{-0.66}$(stat) $\pm$ 0.05(syst)

Table 7.1: *Single W results for the centre-of-mass energies $\sqrt{s}$ = 189 - 206.7 GeV for the TGC parameters $\Delta\kappa_\gamma$, $\Delta\lambda_\gamma$ and Δg_1^Z with the 68% CL errors.*

are compatible with the Standard Model expectation.

For the extraction of the couplings, the production cross sections for the three final states were combined. To improve - slightly - the sensitivity to the couplings, the forward-backward asymmetry in the leptonic channels was also used. From the data the TGC parameters Δg_1^Z,$\Delta\kappa_\gamma$ and $\Delta\lambda_\gamma$ were fitted. The results are summarised in Table 7.1. The single W channel is in particular sensitive to the parameter $\Delta\kappa_\gamma$.

The results for the trilinear gauge couplings are compatible with the Standard Model expectation. Determinations of the TGC parameters using other observables, such as the cross section and the W production angle in W pair production, confirm this conclusion.

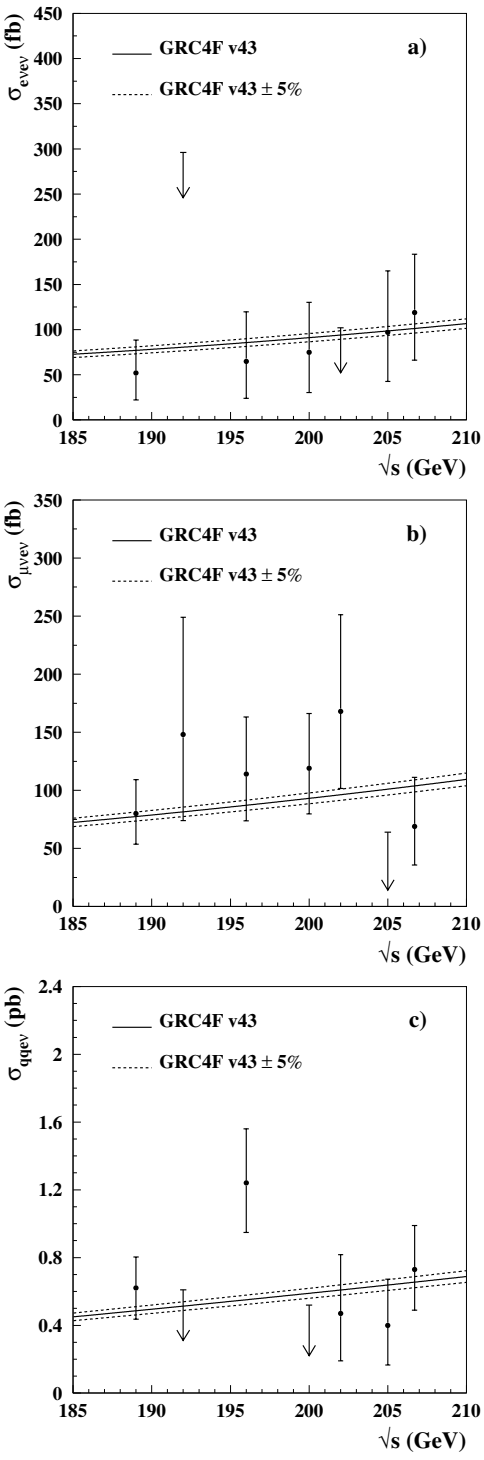

Figure 7.5: *The single W cross section as a function of the energy for the final states (a) $e\nu e\nu$ (b) $\mu\nu e\nu$ (c) $q\bar{q}e\nu$. The dots correspond to the measurements, the arrows to the 95% CL upper limits and the solid line to the Standard Model expectation. The bands reflect the uncertainty on the predictions.*

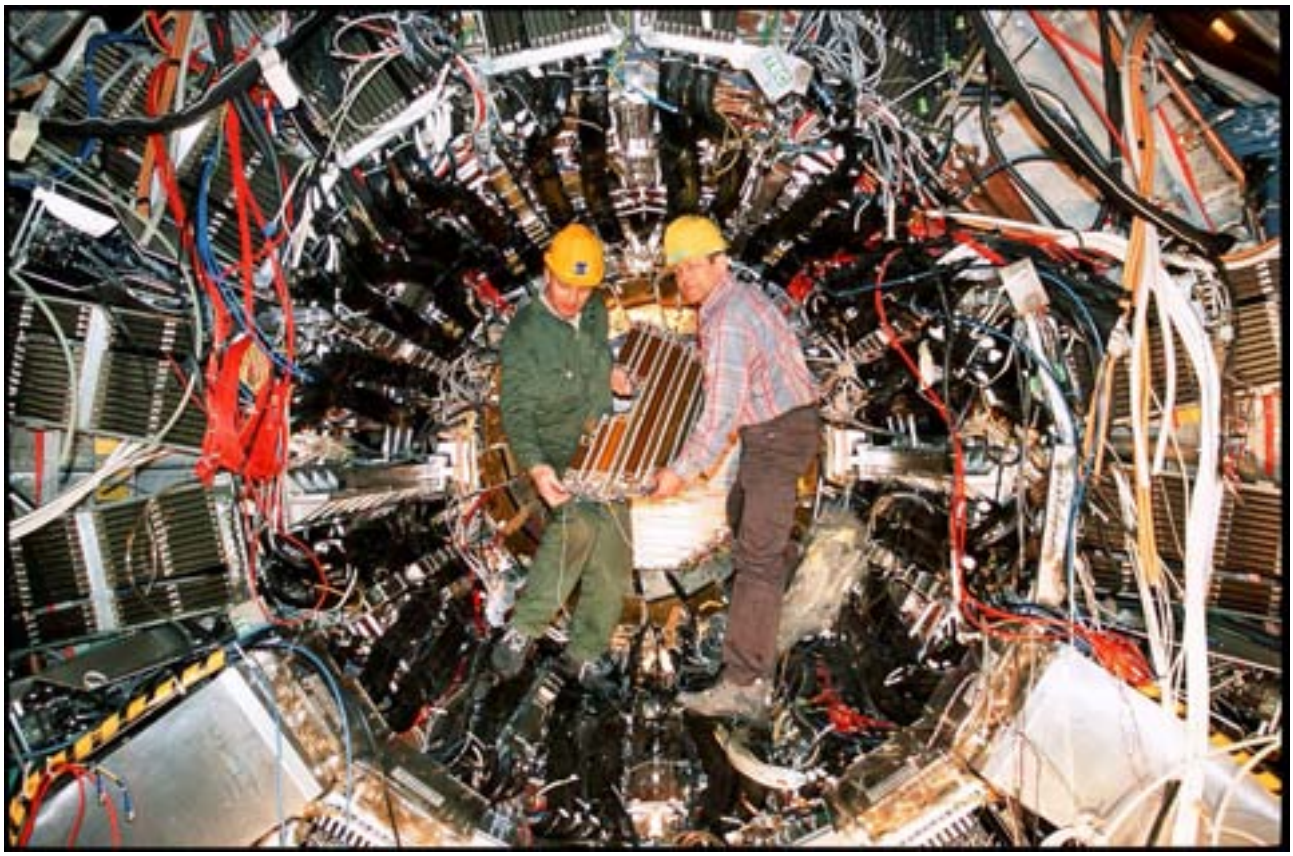

The L3 Detector during dismantling – one of the four experiments of the LEP accelerator.

8 L3

8.1 Introduction

L3 was a general purpose detector designed with good spatial and energy resolution of electrons, photons, muons and jets produced in e^+e^- reactions.

The closure of LEP at the end of 2000 ended the yearly data-taking which began in 1989. Effort in 2002 concentrated on completion of analyses and their publication. In 2002 14 papers were submitted for publication, and a large number of contributions were made to conferences, e.g., 56 to the International Conference on High Energy Physics in Amsterdam. The collaboration expects the analysis of the L3 data sample to last at least until the end of 2003.

The number of physicists working on L3 further declined in 2002. In The Netherlands during 2002, a PhD degree was obtained by six L3 students; there remain five PhD students analysing L3 data,

NIKHEF physicists contribute primarily to analyses of the mass and couplings of the W-boson; QCD, in particular multiplicity correlations and Bose-Einstein correlations; two-fermion production, in particular τ pairs; searches for the Standard Model Higgs; ZZ production; charm and bottom production in two-photon collisions; and studies of the cosmic ray muon flux. Of the PhD theses defended in 2002, one was on the mass of the W-boson, two on Bose-Einstein correlations, one on multiplicity correlations, one on the search for the Higgs boson and the fractality of the QCD parton shower, and one on the cosmic ray muon spectrum.

As in previous years, the computer farm in Nijmegen contributed a large fraction of the L3 Monte Carlo event production, accounting for more than 24 million events.

8.2 Searches

Following the publication, as first of the LEP experiments, of final results on the search for the Standard Model Higgs boson in 2001, attention turned to other possible Higgs scenarios. An example is the so-called fermiphobic Higgs which is predicted in Two Higgs Doublet Models of Type I for certain choices of parameters. Such a Higgs does not decay to fermions at all at tree level. Accordingly, it should decay predominantly to a pair of photons if its mass is below about 90 GeV. In Higgs triplet models one of the neutral scalars has similar behaviour. The superior photon detection capabilities of L3 enable a search for such Higgs bosons in $e^+e^- \to Zh$ where the Z decays to a quark pair, a neutrino pair, or a charged lepton pair and where $h \to \gamma\gamma$. The analysis places a lower limit on the mass of $m_h > 105.4$ GeV at 95% confidence level as shown in Figure 8.1.

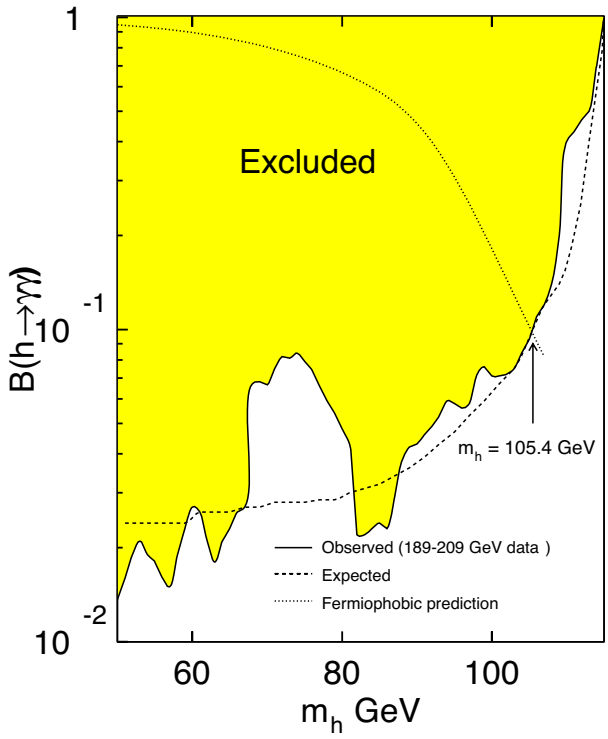

Figure 8.1: *Excluded values at 95% confidence level of the branching ratio of $h \to \gamma\gamma$ under the assumption of the Standard Model production cross section. The expected 95% confidence level limit and the theoretical prediction are also indicated.*

Above a mass of about 90 GeV, the decay modes $h \to ZZ^*$ and $h \to WW^*$ dominate over $h \to \gamma\gamma$. Combining the results of searches in these channels with those of the $\gamma\gamma$ mode results in the limit $m_h > 108.3$ GeV at 95% confidence level.

Limits were also placed on the masses of the neutral Higgs bosons expected in the Minimal Supersymmetric Standard Model as a function of the parameter $\tan\beta$ of this model.

Supersymmetry models often assume R-parity conservation. $R = (-1)^{3B+L+2S}$, where B and L are baryon and lepton number, respectively, and S is the spin.

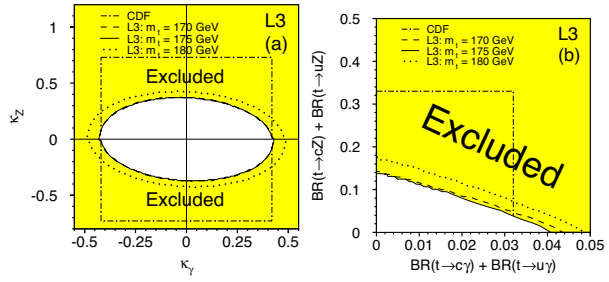

Figure 8.2: *Exclusion regions at 95% confidence level for (a) the anomalous couplings responsible for the flavour-changing neutral currents and (b) the branching ratios. Also shown are the limits from the CDF experiment at the Tevatron.*

Thus, $R = +1$ for ordinary particles and -1 for super-symmetric particles, which means that super-symmetric particles can only be produced in pairs. The main reason for making this assumption is the absence of proton decay. However, R-parity conservation can be relaxed, retaining only the requirement of either B or L conservation and still satisfy the current limits on proton decay. Then a super-symmetric particle could decay to ordinary particles. Limits were placed on the masses of such super-symmetric particles and on their production cross sections.

A search was also performed for single top production, $e^+e^- \to t\bar{c}$, which could have a measurable cross section if new physics includes flavour-changing neutral currents, which are prohibited at tree level in the Standard Model. This is complementary to the studies of flavour-changing neutral current decays of the top performed at the Tevatron.

No evidence for such processes was found, and limits were placed which are more stringent than those from the Tevatron, as shown in Figure 8.2.

Multiphoton final states, $e^+e^- \to n\gamma$ with $n > 1$, were used to set limits on deviations from QED, excited electrons, spin-3/2 leptons, contact interactions, and extra space dimensions.

The measurement of the cross section of $e^+e^- \to Z\gamma\gamma$ was used to put limits on anomalous quartic gauge boson couplings.

8.3 W physics

One of the main goals of the LEP program is the measurement of the properties of the W-boson and its couplings to other gauge bosons. In total some 10000

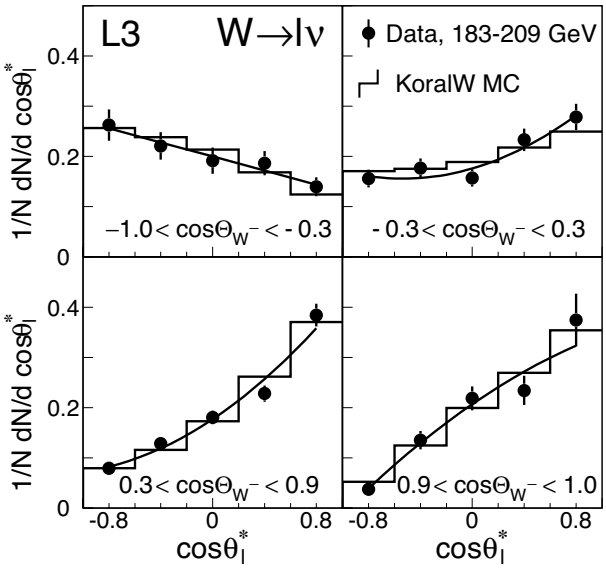

Figure 8.3: *Decay angular distributions for leptonic W decays for four W^- production angle regions. The predictions of the Standard Model, as calculated by the KORALW program are also shown.*

$e^+e^- \to W^+W^-$ candidate events have been selected.

The polarisation of the W bosons and its dependence on the W-boson production angle were measured and found to agree with the Standard Model. For example, the fraction of longitudinally polarised W bosons is $0.218 \pm 0.027 \pm 0.016$. The agreement of the W decay angular distribution for four intervals of the production angle is shown in Figure 8.3

At LEP single-W production, $e^+e^- \to e^+\nu_e W^-\gamma$, provides one of the best experimental measurements of the trilinear gauge boson coupling parameters, in particular of κ_γ. It is complementary to the measurement of the coupling parameters in W-pair production. In the single-W process, only the electromagnetic couplings of the W are probed, whereas in W-pair production also the couplings involving the Z are involved. The result for the two electromagnetic coupling parameters, κ_γ and λ_γ, are shown in Figure 8.4. There is fair agreement with the Standard Model values $\kappa_\gamma = 1$ and $\lambda_\gamma = 0$.

Final results on the mass and width of the W are expected in 2003. In 2002 progress was made on reducing the systematic uncertainties in these measurements. The dominant systematic uncertainty on the measurement of the W mass and width in the four-quark chan-

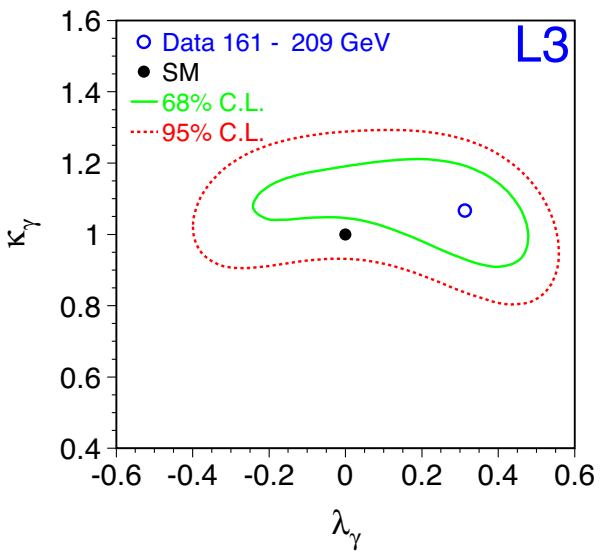

Figure 8.4: *Contours corresponding to 68% and 95% confidence level regions in the κ_γ-λ_γ plane. The result of the fit and the Standard Model prediction are also shown. Systematic uncertainties are included in determining the regions.*

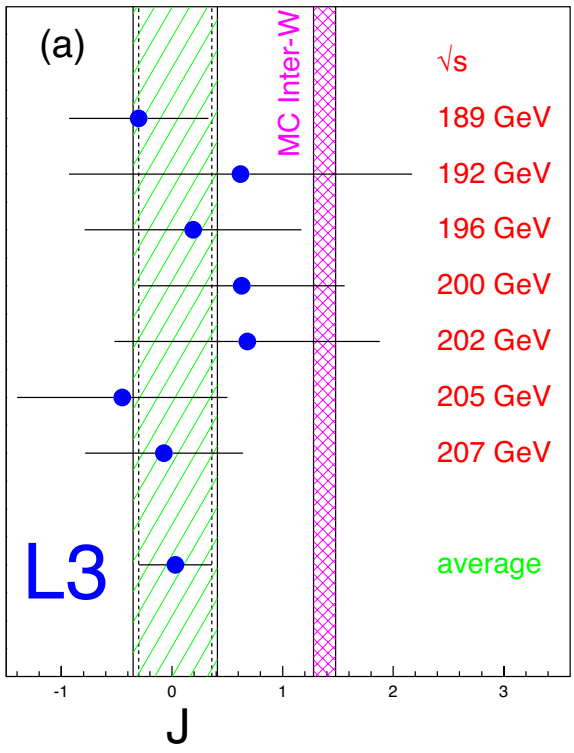

Figure 8.5: *Values of the integral, J, (explained in the text) at different centre-of-mass energies and their average. The error bars are statistical. The bands indicate the average value including systematic uncertainties. The value from a Monte Carlo model including inter-W BEC is also shown.*

nel arises from theoretical uncertainty on two QCD effects. One is the amount and nature of colour flow between gluons arising in the hadronisation of the $q\bar{q}$ from one W, *e.g.*, $W^- \to d\bar{u}$, and those from the other W, *e.g.*, $W^+ \to \bar{s}c$. This is usually referred to as colour reconnection. The other effect is Bose-Einstein correlations (BEC) between identical bosons from different W bosons.

Both of these effects have been intensely studied. Preliminary results have ruled out the most extreme models of colour reconnection. In 2002 L3 published its final result on BEC between identical bosons coming from different W bosons. The study compares the two-particle density, ρ_2, as a function of the four-momentum difference, Q, for like-sign pairs from fully-hadronic, semi-hadronic, and mixed semi-hadronic events. The quantity $\Delta\rho(Q) = \rho_2^{\text{fully}} - 2\rho_2^{\text{semi}} - 2\rho_2^{\text{mix}}$ is expected to be zero in the absence of inter-W BEC and positive otherwise. The value of the integral of $\Delta\rho$ over the low-Q region is shown in Figure 8.5 and compared to the expectation of a Monte Carlo model containing inter-W BEC. The result is consistent with no inter-W BEC and about 3 standard deviations away from the model.

A LEP-wide working group plans to combine the results of all experiments on both colour reconnection and inter-W BEC in order to reduce the systematic uncertainties on the LEP-wide combination of W mass and width.

8.4 QCD

L3 has also studied Bose-Einstein correlations in Z decays. In 2002 results were published on three-particle BEC. Not only are genuine three-particle BEC observed, but a comparison with two-particle BEC results shows consistency with the hypothesis of fully incoherent pion production. Both two- and three-particle BEC is found to be inadequately parametrised by a Gaussian; an Edgeworth expansion is used to fit the data. These results are shown in Figure 8.6.

Final results on the strong coupling constant, α_s, determined using event shapes were published. Combined with previous L3 results at lower energies, α_s is found to "run" as expected in QCD.

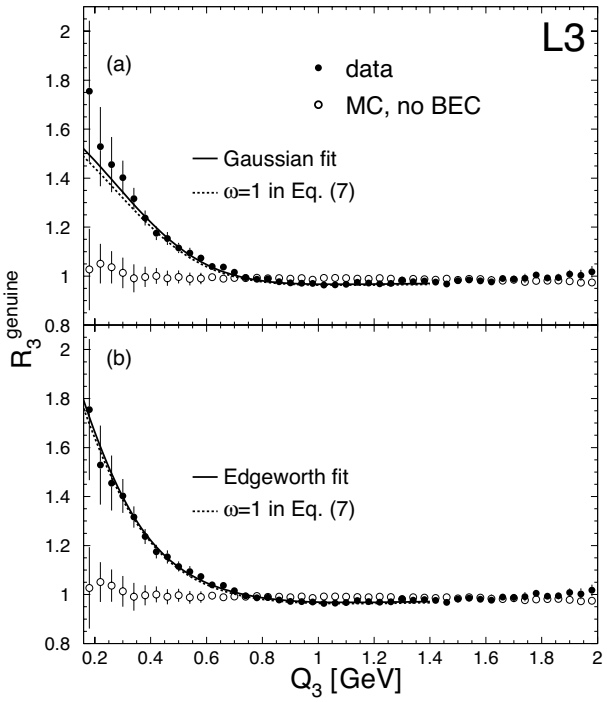

Figure 8.6: *The genuine three-particle BEC correlation function, R_3^{genuine}, as a function of $Q_3 = \sqrt{M_{123}^2 - 9m_\pi^2}$, where M_{123} is the invariant mass of the pion triplet and m_π the mass of the pion. The solid lines are the results of fits to parametrisations with (a) a Gaussian and (b) an Edgeworth expansion. The dotted line shows the prediction of completely incoherent pion production using the results for two-particle BEC. The open circles are from a Monte Carlo model without BEC.*

Various results from $\gamma\gamma$ collisions were published. An example, is a study of Λ and Σ^0 production. The cross sections $\sigma(\gamma\gamma \to Y\bar{Y})$, where Y is a Λ or a Σ^0, are measured as a function of the $\gamma\gamma$ centre-of-mass energy and compared to two models of the structure of the baryon, a quark-diquark model and a three-quark model. Some preference for the quark-diquark model is observed, which is further supported by preliminary evidence from $\sigma(\gamma\gamma \to p\bar{p})$.

8.5 L3+Cosmics

Understanding of the systematic uncertainties on the measurement of the cosmic ray muon spectrum and on the charge ratio of this spectrum has increased considerably in 2002. This resulted in a PhD thesis containing the measurement of the spectrum. This measurement is unique in the sense that the series of measurements presented had never been done before within a single experiment. Furthermore, the precision on the vertical spectrum is as good or better than a combination of all previously existing data above 100 GeV. The final measurement is expected in 2003.

A preliminary combination of air shower and muon detector information indicates large discrepancies with current air shower Monte Carlo models. Final results, expected in 2003, are eagerly awaited by the authors of these models.

A search is being performed for an excess of muons correlated in time and direction with gamma ray bursts observed by the BATSE satellite. Preliminary results are available for 8 gamma ray bursts. Both burst-like signals and signals spread over 24 hours in time around the time of the gamma ray burst have been searched for. No significant signal is seen. A search for signals from unidentified gamma sources is under way.

Using the earth's magnetic field as a charge separator, the shadow of the moon is used to set a limit on the anti-proton to proton ratio. The moon's shadow, observed as a deficit of cosmic ray showers, is seen with a significance of more than 10 standard deviations. However, no deficit of muons is seen in the displaced region which would correspond to the shadow of negative (anti-proton) primary cosmic rays. Preliminary results indicate an upper limit of about 0.2 at 90% confidence level on the ratio of anti-protons to protons of energy in the TeV energy range.

9 Transition Programme

9.1 AmPS: Experiments abroad

Correlations and currents in ^{3}He studied with the $(e, e'pn)$ reaction

(Prop. A1/4-98; with the Universities of Mainz, Tübingen and Glasgow)

In the A1 hall of MAMI, Mainz, data production for the ^{3}He$(e, e'pn)$ experiment has been completed. By means of this investigation, nucleon-nucleon correlations and two-body currents in the three-nucleon system are under study. The choice for ^{3}He as the target is motivated by the availability of continuum-wave Faddeev calculations with realistic NN interactions.

The experimental setup (see Fig. 9.3) was such that the scattered electrons were detected in the magnetic Spectrometer B, proton detection was performed with the highly segmented scintillator array HADRON3, while the neutrons were detected in three time of flight units (TOF) placed at central angles 108°, 125° and 141°. Each TOF unit has an in-plane angular acceptance of 11°.

After detector tuning and calibrations on a ^{2}H target, data were taken for the ^{3}He$(e, e'pn)$ reaction in the kinematics shown in Fig. 9.1, at an incident electron energy of 855 MeV. Five different kinematic settings were employed that encompassed two different energy-transfer ranges (170-270, and 220-320 MeV) and four different momentum transfer ranges with central values 300, 330, 375 and 445 MeV/c. These settings range from the dip region (kinematics A1 and Y1) towards the delta resonance (kinematics B2, A2 and Z2).

The analysis software allowed to monitor on-line the performance of the detectors, as well as to produce on-line spectra containing the physical quantities of the experiment. Missing-energy and missing-momentum spectra were obtained after subtraction of accidental events. A typical result is shown in Fig. 9.2, in which the peak in the missing energy spectrum located at 7.7 MeV corresponds to the three-body break-up of the ^{3}He nucleus.

An estimate of the number of real triple coincident events collected was obtained by integration of the area subtended by the peak, from -10 to 20 MeV. In total, 385 effective hours were spent on ^{3}He$(e, e'pn)$ data taking, collecting 3.107 C of integrated current. The results from the on-line analysis indicated that in total 125000 real triple coincident events were obtained for the five kinematic settings.

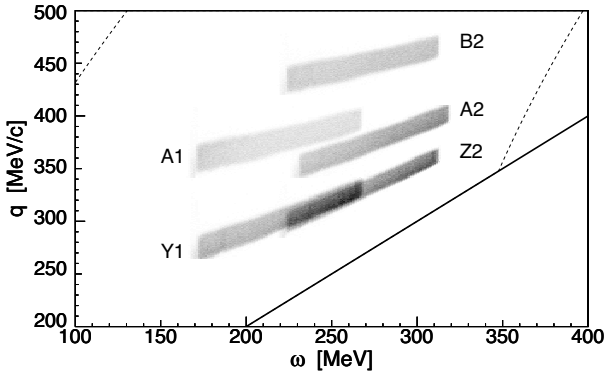

Figure 9.1: *Momentum transfer q vs. energy transfer ω measured in the ^{3}He$(e, e'pn)$ experiment. The dashed lines indicate the centroids of the peaks corresponding to quasi-elastic proton knock-out (left) and excitation of the Δ resonance (right). The solid line corresponds to the coverage of real photons in the (ω, q) plane.*

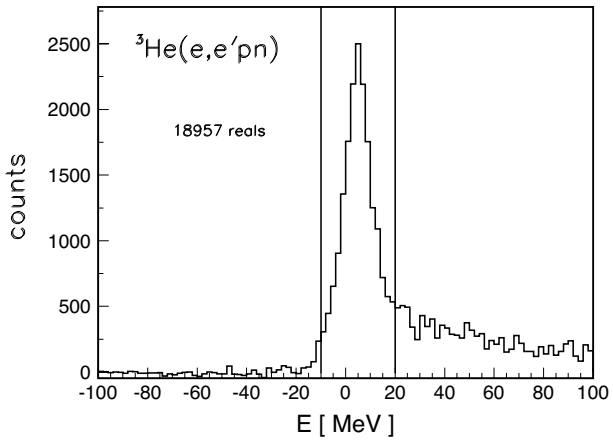

Figure 9.2: *Missing-energy spectrum of kinematics Z2, obtained from the on-line data analysis.*

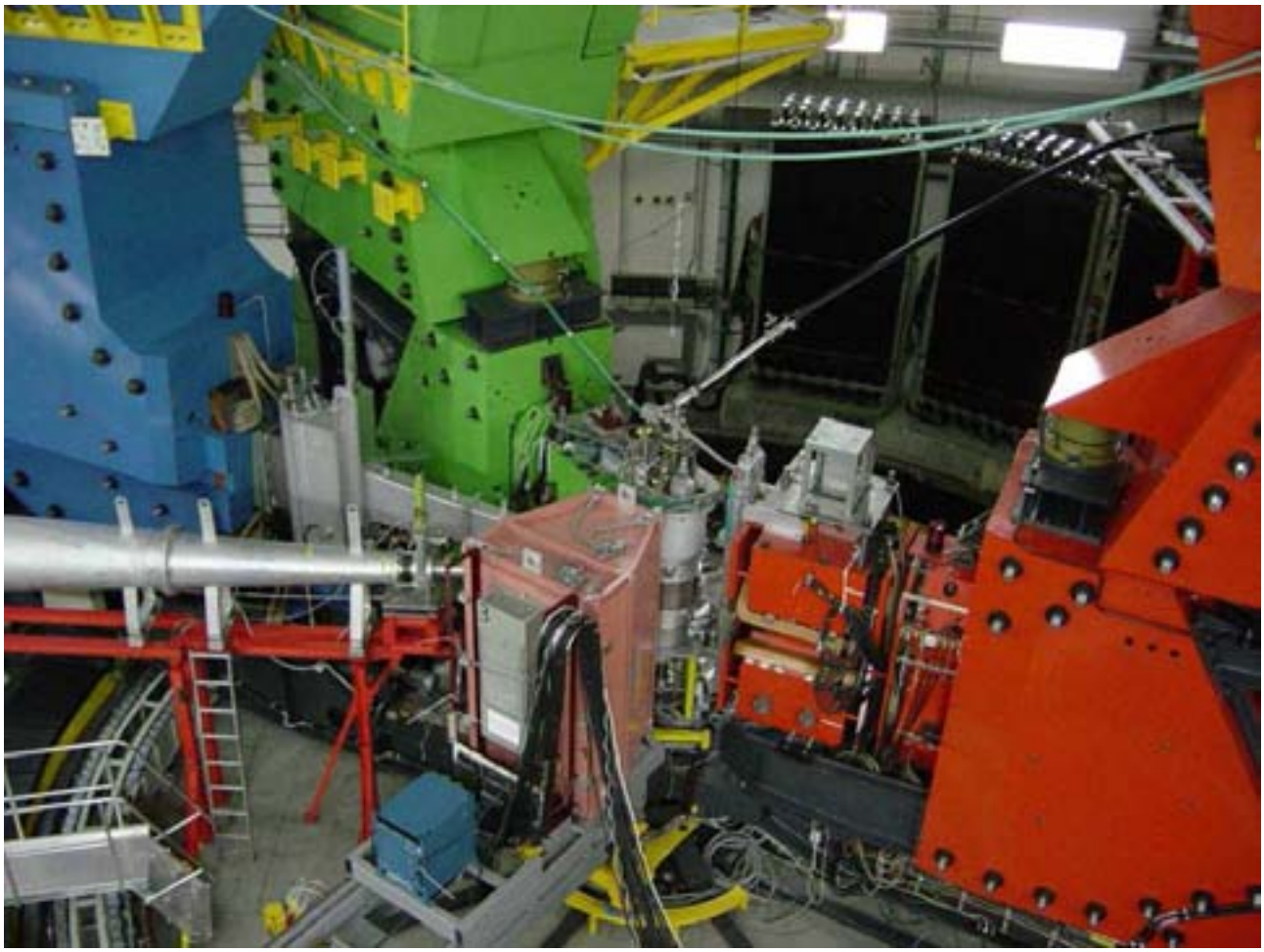

Figure 9.3: *Triple coincidence setup of the (e,e'pn) experiment in the A1 hall at MAMI, Mainz. The blue spectrometer (specB) at the left detects scattered electrons, the HADRON3 detector (center front) measures protons, while the black TOF stands (back) measure the neutrons.*

The off-line calibration of the three detectors is in full progress and will shortly result in experimental cross sections for the ^{3}He$(e, e'pn)$ reaction. The interpretation of these data will be done in combination with the existing data of the complementary ^{3}He$(e, e'pp)$ reaction, obtained at AmPS (D.L. Groep *et al.*, Phys. Rev. **C 63** (2001) 014005). This approach offers the possibility to investigate the relative importance of *pp* and *pn* correlations, as well as the contribution of isobar and meson-exchange currents, in the three-nucleon system.

9.2 Medipix R&D activities: Pixel Detectors

Know-how, obtained by designing semi conducting pixel detectors for high-energy physics, can be used to develop digital X-ray imagers, for use in medical, biological or industrial applications. This "photon-counting" imaging method is up to 50 times more sensitive than current methods based on photographic films or on scintillators combined with CCD's. It means that patients and medical staff using X-rays for diagnostics or therapy, will receive lower doses of ionizing radiation.

NIKHEF participates in several interdisciplinary research projects in the field of semi conducting Pixel Detectors. The activities center around the MediPix Collaboration, an R&D project endorsed by the CERN division for Education and Technology Transfer (ETT). It bundles the research by 16 European universities and research institutes. Apart from that, we have bilateral contacts with two other institutes: with the Czech Academy of Sciences, Prague we obtained an EU-funded Marie Curie fellowship, and with the University of Twente, Enschede, we share two PhD positions in deep submicron chip-design. One such position was funded, back in 1998, by a EU-TMR grant from the European Union, and the second was granted recently by FOM in the framework of "Projectruimte 2002". Further funding requests are pending.

NIKHEF has designed and built the MUROS-2 interface unit, based on a Field Programmable Logic Array (FPLA). This circuit converts between parallel and serial transmission at speeds up to 200 MHz, and performs the needed signal level conversions. Some 18 systems have been delivered to the Medipix members, and to our industrial partner, in 2002. Also the production batch of Medipix-2 chips has been probed at NIKHEF. 12 wafers, out of a total batch of 48, have been probed and show many working chips, although some wafers have an anomalously low yield, which has probably been caused by processing variations in the CMOS foundry. This is being studied further with the CMOS manufacturer. Just before the end of 2002, the first silicon sensor was bump-bonded onto a Medipix-2 chip, and successfully tested. The first images with 256 x 256 pixels at a pitch of 55 μm were obtained and show excellent sensitivity and uniformity.

In collaboration with our Electronics Technology (ET) department, a 2 by 4 Multi-chip carrier has been designed, to carry a tiled array of 8 MEDIPIX-2 chips, allowing an X-ray imager with 28 x 56 mm^2 fully sensitive area. It uses cutting edge high-density interconnect technology (HDI), with a nine-layer printed wire board in stacked microvia buildup technology. Some prototype boards were successfully produced at CERN, and a first production series has been ordered from a company in Belgium. Our goal is to combine eight Medipix-2 chips on a single sensor matrix, to obtain a larger imaging area of 28 x 56 mm^2 and a total of 0.5 million pixels.

Figure 9.4: *The 4th International Workshop on Radiation Imaging Detectors*

Finally, NIKHEF has successfully hosted the 4th International Workshop on Radiation Imaging Detectors (IWORID2002), September 8-12, 2002.

(see also: `http://www.cern.ch/medipix` and `http://www.iworid2002.nl`)

9.3 Future Projects: Linear Collider

Introduction

There is now worldwide consensus in the particle physics community that the next major accelerator after the LHC should be a linear collider.

To realize this Global Linear Collider (GLC) new techniques are under study. One of the projects under study is TESLA (DESY). It is a superconducting e^+e^- collider of 500 GeV total energy, extendable to 800 GeV. Other approaches (SLAC,KEK), focus on a 'warm' technology.

Physics Motivation

The Higgs particle is expected to play a central role in the experimental program of the GLC. At 500 GeV collision energy a Standard Model (SM) Higgs boson of mass up to 400 GeV/c^2 can be observed. This is well above the upper limit of about 200 GeV/c^2 obtained from precision measurements at LEP. If Higgs-boson(s) exist in this mass range they will for sure be discovered at the Large Hadron Collider under construction at CERN (and possibly already at the Fermilab Tevatron collider). However, previous experience has shown that proton-(anti)proton colliders and e^+e^- colliders are complementary. The W and Z bosons were discovered at the Sp$\bar{\text{p}}$S collider of CERN in the early eighties. But precision measurements at LEP of the properties of the Z and W bosons really established the Standard Model, allowing a precise prediction of the top quark mass and to constrain the Higgs boson mass. Even if the Higgs is discovered before at the LHC, the clean experimental conditions of the e^+e^- collider allow precise determination of its properties like mass, width, spin, decay branching fractions. In addition, the GLC offers the unique possibility to establish the coupling of the Higgs boson to itself. The precision of the measurements will be vital for the full understanding of the origin of mass.

Further powerful tests of the Standard Model can be made by comparing the top quark mass, precisely measured from a threshold scan, with much better measurements of the electroweak mixing angle θ_W and of the W boson mass, by lowering the energy of the GLC to 91 GeV (Giga-Z factory) and to around 161 GeV (WW threshold scan), delivering 100 times more data at these energies than collected at LEP.

Supersymmetry (SUSY) predicts many new particles, partners of the matter and force particles that we know today, and more than one Higgs boson. Although there is a large spectrum of masses for these supersymmetric particles, depending on the values of the parameters of the theory, again the GLC is complementary to the LHC in the sense that precision measurements of the masses and other properties of the particles accessible in the energy range of the GLC, will allow an accurate determination of the parameters of the theory.

The physics case for the GLC and a possible detector have been worked out in a series of workshops around the TESLA project and is reported in the TESLA Technical Design Report (See: `http://tesla.desy.de/tdr/`). NIKHEF was involved in the study of the measurement of the branching ratio of the Higgs boson decaying into two photons. This is an important decay mode to measure, as it proceeds through (heavy) particle loops and is therefore very sensitive to new physics. It was shown that a relative uncertainty on this branching ratio of between 10% and 16% could be obtained for a Higgs mass of 120 GeV/c^2. Together with a measurement of the total width of the Higgs boson, possible in the $\gamma\gamma$ mode of operation of TESLA, a precision of 10% on the partial width of the Higgs boson decaying into $\gamma\gamma$ is feasible.

Detector R&D

The ECFA-DESY workshop is continuing with special emphasis on higher energies up to 1 TeV, on $\gamma\gamma$, $e\gamma$ and e^-e^- options, and review of the detector design following further detector R&D. Important aspects of the detector design are related to track momentum resolution, vertexing, energy flow and hermiticity. The proposed TESLA detector therefore consists of a very high precision vertex detector, surrounded and complemented in the forward directions by several additional layers of Si detectors, a large tracking volume covered by a Time Projection Chamber (TPC), and a high granularity calorimeter, all embedded in a 4 Tesla solenoidal magnetic field.

A small NIKHEF group participates in the R&D for a TPC (DESY-PRC R&D 01/03) with groups from Canada, France, Germany, Poland, Russia and the USA. Particular emphasis is put on the R&D for a new type of gas amplification system, based on micropattern gas chambers such as the Gas Electron Multiplier (GEM, see Fig. 9.5) or MicroMEGAS. These devices replace the wire chambers at the end-plates of a classical TPC. They are intrinsically two-dimensional, with a hole or grid spacing similar to the point resolution of around 100 μm.

Instead of using (small) pads to collect the charges

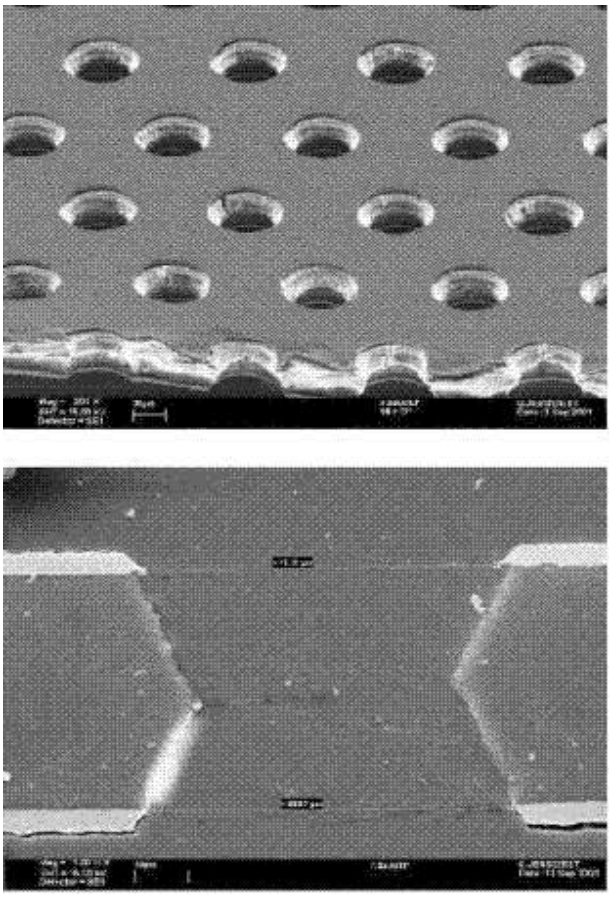

Figure 9.5: *View of a GEM foil (top) and a cross section of a typical GEM hole (bottom).*

after gas multiplication, the NIKHEF group plans to use a pixel readout chip, with a pitch that matches the hole/grid spacing of the GEM/MicroMEGAS. This would allow to collect and detect the charge from single primary electrons liberated by the high-energy charged particle traversing the TPC gas volume. A small ($\sim$1 liter) test TPC was constructed and equipped with two or three successive GEM foils for the gas multiplication and (anode) strips for the readout. With two foils a gas multiplication of about 1100 was obtained. With three foils the gas multiplication reached $\sim$25000 with voltages across the foils between 320 V and 380 V.

The next step is to replace the anode strips by a pixel readout chip. The plan is to use the Medipix2 chip, described elsewhere in this report. This chip has 256×256 pixels of 55×55 μm^2, low noise and a minimum threshold of about 1000 e^-. A gas gain of a few thousand should therefore be sufficient. Preparations are under way to mount one Medipix2 chip on a small readout PCB and mount it on the test chamber.

9.4 Grid Projects

Introduction

The LHC experiments at CERN are adopting the Grid Computing paradigm for their main work of Monte-Carlo event production, data distribution and access, and later for reconstruction and data analysis. Grid Computing works with advanced authorization and authentication methods to allow the HEP software, data, and task execution to be fully distributed among participating institutes. The LHC data and computing centers will no longer be centrally located at CERN but will be distributed across the world. The scheme also has advantages locally, since an institute such as NIKHEF will have substantial local power, which can be deployed according to institute priorities.

NIKHEF is one of the five main sites for the embryonic European HEP Grid (the European DataGrid). NIKHEF also provides effort for tests of transatlantic Grid operation (DataTAG) and for the Dutch National e-Science Infrastructure (VLE, DutchGrid).

Local Facilities

Approximately 270 CPUs are dedicated to Grid (or grid-like) computing service at NIKHEF. An additional 15 machines supply Grid administrative functions like site information services, Grid user databases, distributed file storage, network monitoring, and control of access to local resources by remote Grid users. Local storage amounts to about 0.6 terabyte. We have access to 12 terabyte of Grid-based storage at SARA in the adjacent building.

Roughly half of the 270 CPUs come from the NCF Grid Fabric Research Cluster. These machines (66 dual-CPU AMD boxes) were briefly deployed as part of our EDG (see below) production facility, but they fail under heavy load due to a poor design of the air-cooling flow across the motherboard. As of this writing, NIKHEF is working with the manufacturer to solve this problem.

During 2002 the Networking Group installed a new router for the Grid section of our computing network. This separates our Grid infrastructure from the general NIKHEF user network. The worker CPUs are isolated from the outside world except for connections initiated from the workers themselves. These connections are managed by Network Address Translation (NAT) on board the new router.

The European DataGrid Project

The European DataGrid (EDG) is a project funded by the European Union with the aim of setting up a computational and data-intensive grid of resources for the analysis of data coming from scientific exploration. NIKHEF is one of the five "core sites" of the European DataGrid.

NIKHEF runs both a "production" and a "development" cluster. We also operate virtual-organization servers (databases mapping people onto their experiment organizations for accounting and security purpose) and data catalog servers.

We summarize below the local contribution to the various tasks ("work packages") in EDG.

Data Management

NIKHEF staff made extensive local and remote tests of the EDG Data Management subsystem in 2002. The results of these tests were used to improve the current code and inform the design of the next version of the subsystem (due for release in May 2003).

Fabric Management

It is important that resources, for example compute clusters, are only available to users that are properly authorized. This interface from the Grid to the local systems is taken care of by NIKHEF. This Local Centre Authorization Service (LCAS) has been widely deployed last year, and also plays an important role in securing site access in other Grid projects, e.g. in the PPDG Grid at FermiLab. The more advanced system LCMAPS will recognize experiment membership and roles within the experiments ("MC Production Manager"). It will be developed at NIKHEF in 2003.

In order for the Grid to effectively distribute computational work across the participating computer centers, the centers need to provide some estimate of how available their site is. The current practice is for a site to provide an "estimated traversal time" which indicates that if the queue were to accept a job now, how long will it be before it actually starts to execute. This is a tough problem when there are multiple groups accessing the same pool of queues, and scheduled according to some local policy. NIKHEF is contributing to research in this area (the Masters' Thesis work of H. Li).

Testbed Integration

NIKHEF is one of the five core sites in the EDG project. The NIKHEF development testbed (five machines) is usually (together with Rutherford Lab in the UK) the first site to deploy a new EDG software release after it has been tested at CERN. NIKHEF has provided many

bug fixes to these releases. NIKHEF staff also provide support to both local and remote users in diagnosing run-time problems with computational tasks submitted on the EDG.

This effort also provides central services for Grid "virtual organization" membership to all Grid sites. Furthermore we provide the Grid file-catalog service for the D0, LHCb and Alice experiments, as well as to members of the biomedical and earth-observation communities.

Security services

When interconnecting a multitude of systems worldwide with high-speed connectivity, such a system will instantly become a valuable target for abuse. It is therefore important to do strong authentication of the users of such a system, and to make sure that authorization reflects usage policies.

The user authentication in the Grid is based on public-key cryptography and an associated Public Key Infrastructure (PKI) to distribute the keys. This system is well known from its role in e-commerce transactions, where sensitive financial data (credit card numbers) are encrypted such that only the intended recipient (the web trader) can read it. The Grid takes this technique one step further, and has also the individual end-users authenticate in this way. Using limited-lifetime "proxies", it has been successfully leveraged to provide "single sign-on" for all users on the Grid: you only need to type your pass phrase once at the beginning of the day, and all grid resources can be used without further hassle.

The DutchGrid Certification Authority, run by NIKHEF, provides trusted services to all users in the Netherlands and its statements are trusted world-wide. To promote interoperability between the various counties, in particular with the advance of LHC computing, the DutchGrid CA has worked on definition of common requirements and procedures within the Global Grid Forum.

Networking

Aside from the network monitoring machine on the Testbed, Grid networking activities at NIKHEF are common across projects. They will be described in the DataTAG section below.

HEP Applications

The NIKHEF representative for HEP Applications on the Grid participated in a variety of tasks during 2002.

The first was to produce a "use case" document for the project architecture group. This document has become something of a "Grid bible" in HEP and has been used to drive architectural activities on Grid middleware in both EDG and for the LCG (LHC Computing Grid) project.

Secondly the ATLAS collaboration ran the first Data Challenge on the Grid, and NIKHEF contributed both as a testbed site as well as through assistance from the HEP Applications representative.

The third main contribution was to participate in the EDG Architecture Task Force (ATF) as the HEP application representative.

AliEn

AliEn is a grid prototype constructed by members of the Alice Collaboration at CERN. NIKHEF was the first site (outside of CERN) on which AliEn was successfully installed and this experience contributed valuable corrections to the AliEn design. NIKHEF has continued to contribute one CPU to AliEn production and tests throughout 2002.

D0 Grid

The 104-CPU D0 farm has been running efficiently for the past year; details of the Monte-Carlo production done with the farm can be found in the ATLAS/D0 section of this annual report. Besides D0, the farm has also been used to run Monte-Carlo production for the ANTARES and L3 experiments.

Trials with running the D0 Monte-Carlo production chain under the EDG environment were successfully carried out in late 2002. The EDG platform runs only on an older Linux version for which D0 production software is no longer available, so serious tests are awaiting the release of EDG 2.0 in May 2003.

DataTag

The DataTag project started in 2002. The fundamental objective of the DataTAG project is to create a large-scale intercontinental Grid test bed involving the DataGrid project, several national projects in Europe, and related Grid projects in the USA. This allows exploration of advanced networking technologies and interoperability issues between different Grid domains. The project addresses the issues that arise in the sector of high-performance inter-Grid networking, including sustained and reliable high-performance data replication, end-to-end advanced network services, and novel monitoring techniques. The project has its own dedicated Trans-Atlantic optical link of capacity 2.5 Gbps between

Figure 9.6: *The DataGrid connects the world.*

CERN and Starlight(Chicago). The project directly addresses the issues that arise in the sector of interoperability between the Grid middleware layers such as information and security services. The advances made are being disseminated into each of the associated Grid projects.

DataTag has accomplished upto 1 Gbps transfers between machines (in Amsterdam and Sunnyvale CA, USA) separated by more than 10,000 km. This feat won the world land speed record (in collaboration with UvA and SLAC) in late 2002. Currently 10 Gbps technology is being tested over this same link.

C Theoretical Physics

1 Theoretical Physics Group

1.1 Introduction

The understanding of subatomic phenomena, and the analysis of experiments in this branch of physics, rest heavily on the development and applications of relativistic quantum theory: the description of quantum mechanical properties of particles in the relativistic regime of energies. For point-like particles, the particle-wave duality implies that such theories can be cast in the formalism of quantum field theory: particles are discrete quanta of energy carrying particular values of spin, charge and other quantum numbers, which reflect the properties of the parent field. A very successful quantum field theory exists that describes all known subatomic particles and their observed interactions: the quarks and leptons from which atoms and nuclei are made, and the electro-magnetic, weak and strong subatomic forces that govern their scattering properties, their bound states and their transmutations. This model is simply referred to as the standard model. It is a highly successful theory, not only for qualitative understanding of particle phenomena, but increasingly as a framework for the analysis of precision measurements.

It has been widely speculated in recent years that at the level of smallest imaginable distances —when quantum gravity becomes relevant and space-time starts to behave as a dynamical arena for physical processes— such a quantum-field theory approach is no longer sufficient, and other extended objects such as quantum strings and membranes come into play. So far this has not led to many firm predictions for phenomena observable at particle accelerators, but in all scenarios two ingredients seem required. The first of these new ingredients is supersymmetry, which requires every particle in nature of integral spin to have a partner of half-integral spin and vice-versa. The other requirement is the existence of new dimensions of space in which quantum strings can extend and move. As a result much work is done worldwide on analyzing the consequences of incorporating supersymmetry and extra dimensions into the framework of the present standard model of particle physics.

1.2 QCD

The nuclear particles known as hadrons, including e.g. protons, neutrons and pions, are composite objects; their constituents, generically called partons, are of two types: there are quarks which are of fermionic type and obey the Pauli principle; as such they carry half a unit of spin. In addition there are gluons, massless particles of unit spin, which carry the strong color force binding the partons into the composite nuclear particles. At the short sub-hadronic distance scales these strong interactions are becoming increasingly well-understood. Probing the structure of hadrons with high-energy particles, be they electrons, photons or other hadrons, leads to the creation of new heavy quarks that under ordinary circumstances are not present inside protons and neutrons. Such inelastic scattering teaches us much about the dynamics of strong interactions of partons at short distances.

In the NIKHEF theory program detailed theoretical investigations of the production of heavy quarks, the so-called c, b and t quarks (for charm, bottom and top), are performed. Of special relevance are resummation techniques, which allow the extension of perturbation theory results to a larger kinematical domain. Much expertise in this area has been developed and put to use in the analysis of experiments, e.g. at DESY and FNAL.

Another area of expertise developed under the NIKHEF theory program is the calculation of high-order quantum corrections, encoded in Feynman diagrams with two, three and even four internal loops. In this field the NIKHEF theory program is world leading. The work is technically and computationally very demanding, but the results are likely to be of crucial importance to describe the constitution of particles like the proton with sufficient accuracy that future experiments at the Tevatron (FNAL) and LHC (CERN) can be used for precision tests of the standard model, and possibly discover deviations indicating new physics phenomena outside the standard-model framework.

Finally, the structure of hadrons can change in non-standard environments, for example at finite temperature, pressure and/or particle density. Such environments are created in the collisions of heavy ions. A theoretical study of these thermodynamic properties of hadrons, using lattice field-theory methods, is part of the NIKHEF theory program. The studies are performed in cooperation with the university of Bielefeld.

1.3 Beyond the standard model

A number of experimental observations in the context of the standard model indicate the existence of a new regime of physics at distance scales very short in comparison with hadronic distances; this would imply the existence of new physical forces carried by particles with masses of the order of 10^{15} GeV. These forces subsequently combine with the known forces in the standard model to form one unified theory of particle interactions, a scenario referred to as gauge unification theory (GUT). Such a theory can explain such diverse observations as the variation of the strength of the known interactions with distance *(running couplings)*, charge quantization (including the fractional charges of quarks), and neutrino masses. The NIKHEF theory program focuses in particular on scenarios for unification including supersymmetry.

At the smallest distance scales, characterized by the Planck energy of about 10^{19} GeV, quantum gravitational effects can no longer be ignored and may even become dominant. Although no single model of quantum gravity exists that has sufficient predictive power to be compared with present experimental data, theoretical and mathematical arguments point to the need to start from a quantum theory of one-dimensional objects, *superstrings*. The particles observed in nature could then either be tiny curled up strings, or the end points of strings that extend in extra dimensions and are invisible from within our four-dimensional space-time. The interplay of various dimensions, and the objects that can exist in these dimensions according to the rules of quantum-mechanics, is very intricate and the necessary mathematics is only being developed now. Under the NIKHEF theory program the properties of quantum strings, especially of the open type, and their dynamics are active fields of investigation.

1.4 Cosmology and astrophysics

Particle physics is becoming of increasing importance to understand the properties of the early universe, when it was a very hot and dense fireball. At the same time, theoretical physicists are aware that their theories can be tested by working out its consequences for the evolution of the universe, in addition to the predictions made in the context of laboratory high-energy physics. At the highest energy scales, those of gauge unification and quantum gravity, such cosmological observations may be the only way to test the theoretical framework. For this reason both string theory and supersymmetry/supergravity models are frequently applied to cosmological models. The NIKHEF theory group has been involved in efforts to understand the origins of the expansion of the universe, which may be due to new fundamental scalar fields playing a role in the universe at large.

Another area of high-energy astrophysics where experimental data may become more readily available is provided by neutrino physics. High-energy neutrinos could be a signal of energetic physical processes in the early universe; they may also be produced by annihilation processes of dark matter. Investigations of such phenomena have recently been taken up and will be studied further in the context of the NIKHEF theory program.

D Technical Departments

1 Computer Technology

1.1 Central services

A Sun Enterprise server 3500 provides home and project file service for Unix and MS Windows clients. The server is equipped with three RAID disk storage arrays with a total gross capacity of 1.2 TByte. A Windows-NT server delivers the very same kind of file service exclusively for Window clients. The TSM service at SARA is used to make daily incremental backups of all home and project files on both these server systems.

A new data file server with 2 TByte disk capacity has been installed mid 2002. This server runs under the Linux Red Hat operating system and is meant to store massive data files without backup services and is structured in such a way that the data is accessible from any client in the network using a simple naming scheme based on projects, e.g. /data/atlas.

Mail services, print services and network services like DNS, NIS and DHCP are implemented on Sun server systems running the Solaris operating system. A Dell Windows-NT server delivers network services for the client systems in the Windows network domain. Additionally the web (`http://www.nikhef.nl`) and file transfer services (`ftp://ftp.nikhef.nl`) are implemented on Dell servers with the Linux Red Hat system.

On request of some of our user groups we set up an AFS server pilot project. This AFS server offers wide area network file sharing for users with a local NIKHEF computer account. As an example, when at CERN a NIKHEF computer user can access her/his files from a CERN desktop using the pathname `/afs/nikhef.nl`. AFS is a popular service within the high-energy physics community, but is not widely spread outside this community.

We implemented an LDAP directory server which contains all relevant public coordinates of each individual NIKHEF employee (name, e-mail address, phone number, and so on). The directory server is filled regularly with the data extracted from the personnel database system. A web interface has been made available to make these coordinates accessible from outside NIKHEF.

On request of the ANTARES project group we have installed the Oracle server software on a SUN Solaris system. On request of the NIKHEF management we have installed MeetingMaker service software on a SUN Solaris system. Additionally, we have installed Meeting-Maker client software on a number of Windows desktops.

At the end of the year 2002 we closed the support for the HP-UX system and shut down the two HP server systems. This marked the end of a long period of the usage of HP systems at NIKHEF, which started in the early eighties of the last century with the introduction of the Apollo systems.

1.2 Network infrastructure

The backbone of our local area network and the firewall to the external networks are implemented in a Foundry BigIron 8000, a network device with capabilities for high-speed routing and switching IP traffic. A total of 32 ports with a capacity of 1 Gb/sec and 24 ports with a capacity of 100 Mb/sec are available to connect servers and switches directly to the network backbone. Access from the external networks to the NIKHEF network is controlled by the firewall function of the router. The security level has been increased again: for instance, telnet requests are refused by the firewall while the secure shell protocol is allowed. Stackable switches, with up to 96 ports (100Mb/sec) and a 1 Gb/sec uplink for each stack, are connected to the gigabit backbone of the local area network. The network is partitioned into a number of 'class C' type network segments. Access policies may differ for each individual segment. For instance, the 'guestnet' segment is available to connect laptops and computers that are not under control of the regular Computer Technology (CT) group. The access from this segment to the more secured segments is not enabled for all services. A second Foundry BigIron network router has been installed to separate the regular operational network from the experimental network for grid developments.

This year we started the deployment of a wireless LAN infrastructure in the NIKHEF buildings. The communication is based on the 802.1x protocol. Due to the concrete structure of the NIKHEF buildings, many wireless LAN access points are needed to obtain an overall coverage of the network. Therefore we have decided to limit the coverage of the wireless LAN in this first stage of deployment to the meeting rooms and public spaces such as the Spectrum.

desktop system	number	remark
Windows (98/NT/2000/XP)	220	including instrumentation systems
Linux	180	excluding farm systems
Sun Solaris	30	
Apple Macintosh	3	
Total	433	

Table 1.1: *Desktop systems*

The external connectivity for the NIKHEF community to the internet is provided by a 1 Gb/sec uplink to the access router of SURFnet5 located at the SARA building. The capacity of this link is sufficient and it can easily handle the amount of incoming and outgoing traffic during rush hours. SURFnet5 is the research network within the Netherlands. SURFnet5 is directly linked to a number of international networks. Most relevant for the NIKHEF scientists is the connection from SURFnet5 to the European research network GEANT (e.g. CERN and DESY) and the points of presence in Chicago where a direct link between SURFnet and the research networks in the US and far-east countries exists.

IPv6 is the latest version of the internet protocol and is compared to the current version of the protocol (IPv4) able to cope with a much larger address space. IPv6 traffic can be handled by modern routers in parallel with IPv4 traffic. In collaboration with SURFnet we have set up an IPv6 testbed at NIKHEF and established 'native' IPv6 connections with sites elsewhere in the internet. For this purpose SURFnet provided a dedicated uplink to their IPv6 testbed environment. The aim of this project was to gain experience with this protocol for future use in a compute and data grid infrastructure.

1.3 Desktop systems

Table 1.1 presents a summary of the number of desktop systems for each platform. The total number of desktop systems has increased with almost 20% compared to the last year's numbers. The W2000 edition is the favorite Windows release for the desktop this year, although Windows XP became more popular in the last quarter. The Red Hat versions 6 and 7 have been installed on about 90% of the Linux desktops. Only the HERMES group from DESY prefers the SUSE Linux version 7. The design engineers from the electronic and mechanical groups make use of CAE software that runs on Sun Blade workstations under the Sun Solaris 8 operating system.

Figure 1.1: *The NCF compute node*

1.4 EU-DataGrid testbed

NIKHEF is one of the five core sites for the testbed of the European DataGrid project. This testbed is divided into two parts, on part dedicated to the development of the grid services and one part dedicated to the development of the grid applications provided by the LHC detector groups. The NIKHEF testbed runs grid directory services like a Replica Catalogue and the Certification Authorization for the DutchGrid domain. Grid users can submit their jobs to a Compute Element with 75 worker nodes and store their data sets on a Storage Element in the NIKHEF (or SARA) testbed. The testbed network segment ('farmnet') is separated from the regular NIKHEF network by a gigabit router, which acts as a firewall between the network segments and acts as a collapsed gigabit backbone network for the computers in the farmnet.

We have installed an additional 66 dual-processor worker nodes into the testbed for two purposes:

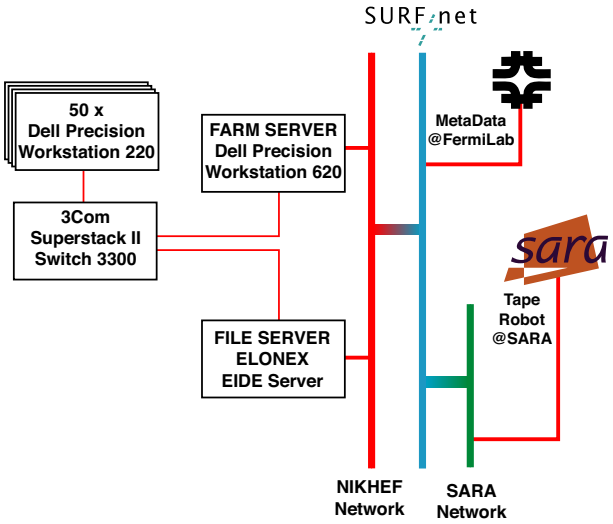

Figure 1.2: *A view of the D0 farm at NIKHEF*

first we wanted to be able to do research on the managements of large clusters and second we wanted to add computing capacity to the testbed. This cluster is known as the NCF research cluster, because the costs for the system have been subsidized by NCF, the Stichting Nationale Computerfaciliteiten, which is part of NWO. Unfortunately the 1U-high rack-mountable compute nodes became overheated during stress tests, due to the high power consumption of the AMD processors. At the end of the year 2002, this problem was still under investigation.

1.5 D0 compute farm

The D0 farm, consisting of 50 dual CP worker nodes, a farm server and a fileserver, produced more than 10 million Monte Carlo events for the D0 experiment. Of these 9.7 M were stored in SAM, the mass store and meta database in Fermilab, 1 million events were stored in the tape robot at SARA.

During the iGrid 2002 Conference in Amsterdam the nodes of the D0 farm were moved to the EDG testbed. During the conference the processing of D0 data was demonstrated, not only the production and storing of MC data but also the retrieval of files from FNAL, the processing of the data at NIKHEF and the storing of the results at FNAL. The MC production during iGrid 2002 resulted in 400 K events.

After iGrid 2002 the D0 nodes had to be detached from the EDG testbed since the testbed runs RedHat version 6 and the latest versions of the D0 software need RedHat version 7. A second SAM station has been installed which is used to fetch files from FNAL to be analyzed at NIKHEF. The 2 NIKHEF SAM stations form part of a worldwide D0 grid. Work is under way to integrate this grid with other grids like the European Datagrid.

1.6 Amsterdam Internet Exchange

The amount of traffic exchanged through the Amsterdam Internet Exchange (AMS-IX) increased from an average throughput of 4 Gb/sec in January to 8 Gbit/sec in December. The AMS-IX has kept its position in 2002 as one of the largest exchanges in the world. NIKHEF is one of the four housing locations of the AMS-IX.

To stay competitive with the other three locations, we have decided to take measures to improve the quality of services for the NIKHEF housing location. The directors of NIKHEF and SARA signed a memorandum of understanding, with the intention to set up a closer collaboration between the housing locations and to harmonize procedures regarding site access, security and installation rules.

Backup power system

In 2001 we took the decision to install a no-break backup power system for the network equipment of the customers of the AMS-IX housing location. In the course of this year the technical facility department started to prepare the installation of the power system. After thorough tests, the backup system became operational at December 16th. Ironically a major power interruption in a large part of Amsterdam happened at November 6th. At that time the backup system was

Figure 1.3: *The 12-cylinder Stamford/Perkins diesel*

not available yet and all AMS-IX and NIKHEF server systems were down for some hours. NIKHEF computer users will benefit of the backup, because the power feed of all major NIKHEF servers is part of the backup system as well.

The system consists of a no- break part (a double UPS battery system including converters) and a short-break part (a diesel generator, see Fig. 1.3). In case of a power failure, the UPS can supply the full AMS-IX electrical power demand for a period of up to five minutes. During this period, typically after a few seconds, the diesel generator will start, supplying electricity to the UPS batteries, the AMS-IX racks, the NIKHEF server systems and the cooling system of the computer rooms.

1.7 Conference support

ICHEP2002

In July 2002 the International Conference on High-Energy Physics ICHEP2002 took place in the RAI Congress Centre in Amsterdam. The CT system group participated in the set up and support of the IT infrastructure during the conference. An Internet Café (see Fig. 1.4) with 50 PC's and a wireless network for laptops has been made available to the about 1000 participants of the conference. Apart from this café, we installed a local web server and scanning equipment for the speakers' corner. The NIKHEF webmaster was involved in the design and implementation of the conference web site.

iGrid2002

In September computer scientists joined the International Grid applications-driven testbed event iGrid2002 at the WTCW campus. 28 teams of scientists showed on this occasion how their applications can utilize multi-gigabit optical networks. A NIKHEF team presented and demonstrated how high-speed optical network connections can be utilized to transport raw data produced by the D0 detector at FNAL to the analysis farm at NIKHEF. On request of the organization of the iGrid event we provided assistance for the IT infrastructure and for the design and implementation of the conference web site.

1.8 Software engineering

ATLAS Detector Control System

The development of the ELMB (Embedded Local Monitor Box), a general purpose front-end device containing an ADC and digital I/O, has continued. Radiation tests proved the design matches the ATLAS constraints. An initial series of around 100 ELMB's has been provided to different sub-detector groups. The experience gained with this model has lead to another, probably final, design, of which around 5000 boxes will be manufactured. Further radiation tests are necessary and the final approval for the production is expected to be given in 2003.

Figure 1.4: *The Internet Café at the ICHEP conference*

The development of the embedded software of the ELMB's is the main responsibility of NIKHEF. A basic version, including the CANopen protocol and handling the ADC and digital I/O, is available on the web.

ATLAS MUON sub-detector

The production of the BOL (Barrel Outer Large) chambers progressed on schedule in 2002. The CT group contributed a variety of software written in LabView and MS-Visual C++. Several Visual C++ applications monitor and guard the production. They also provide the global MS-ACCESS database in which all relevant information of the chambers and tubes in particular is stored. The production of a chamber now takes six days and is highly automated. A special purpose interactive online manual was developped. It performs pre- and post checks of each production step and provided feed back when problems are detected.

During the summer period we tested several types of barrel and end cap chambers at CERN in the H8 test beam environment. DCS and TDAQ integration aspects have been investigated and have been tested on site. A major component of the detector control system is the supervisory control and data acquisition system (usually referred as SCADA), for which the ATLAS col-

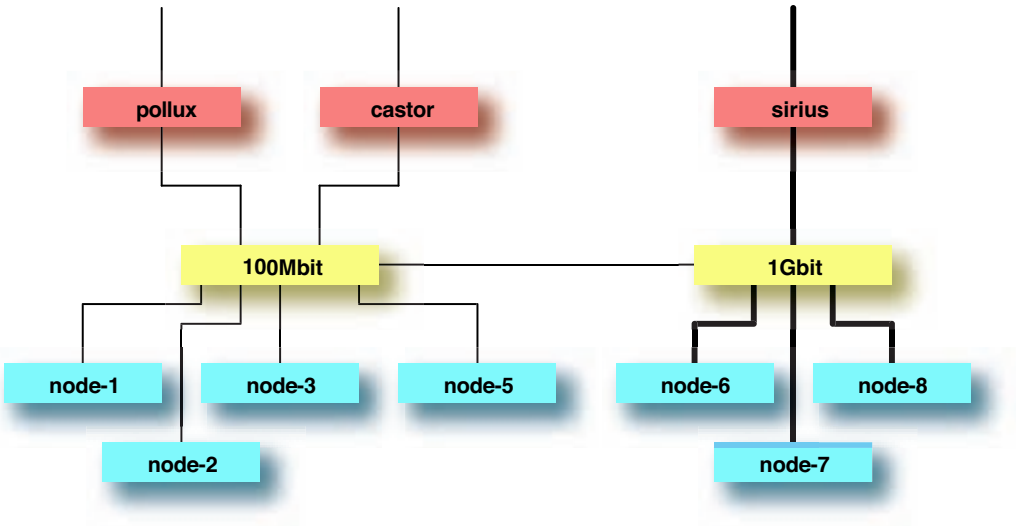

Figure 1.5: *The ANTARES network in La Seyne*

laboration and the other three LHC-detector collaborations selected the PVSS software package of the Austrian company ETM.

The aim of the test beam runs was to perform the temperature readout of the chambers. Each chamber is equipped with an ELMB for the readout of the temperature sensors. The ELMB's are connected into a single CAN field bus network which is interfaced to a PCI CAN controller in a PC. A dedicated OPC driver controls the board and the nodes in the connected CAN field bus network. A PVSS application was made to read, display and store the temperatures as read with a regular time interval from the sensors. The hardware and software of the ELMB is designed to be able to monitor and control other devices such as magnetic field sensors and JTAG registers as well.

ATLAS SCT sub-detector

We started the design of the database to support the production of 20 carbon-fiber discs for the inner tracker silicon sub-detector. During the production all relevant data will be stored into this production database. The implementation of the database will be done in MS ACCESS and is in this respect comparable with the production database for the MUON chambers.

ANTARES IT infrastructure

The CT group configured and installed the computer and network infrastructure for the first string tests of the ANTARES neutrino telescope situated at the borders of the Mediterranean Sea in La Seyne (France). The network comprises a server PC, two PC's for control and monitoring the experiment and a cluster with seven compute nodes. The computers are connected to the network by either a 100 Mb/sec link or, in case the connection is part of the data flow path, a 1000 Mb/sec link. The high- speed Ethernet connection to the neutrino telescope on the bottom of the sea is through the gigabit switch with the compute nodes in the farm. The server PC and both control and monitoring PC's act as a gateway between the internet and the ANTARES online network with the front-end and farm nodes.

The CT group participated in the design and development of software for the ANTARES DAQ system, which is described in more detail in the corresponding chapter in this report.

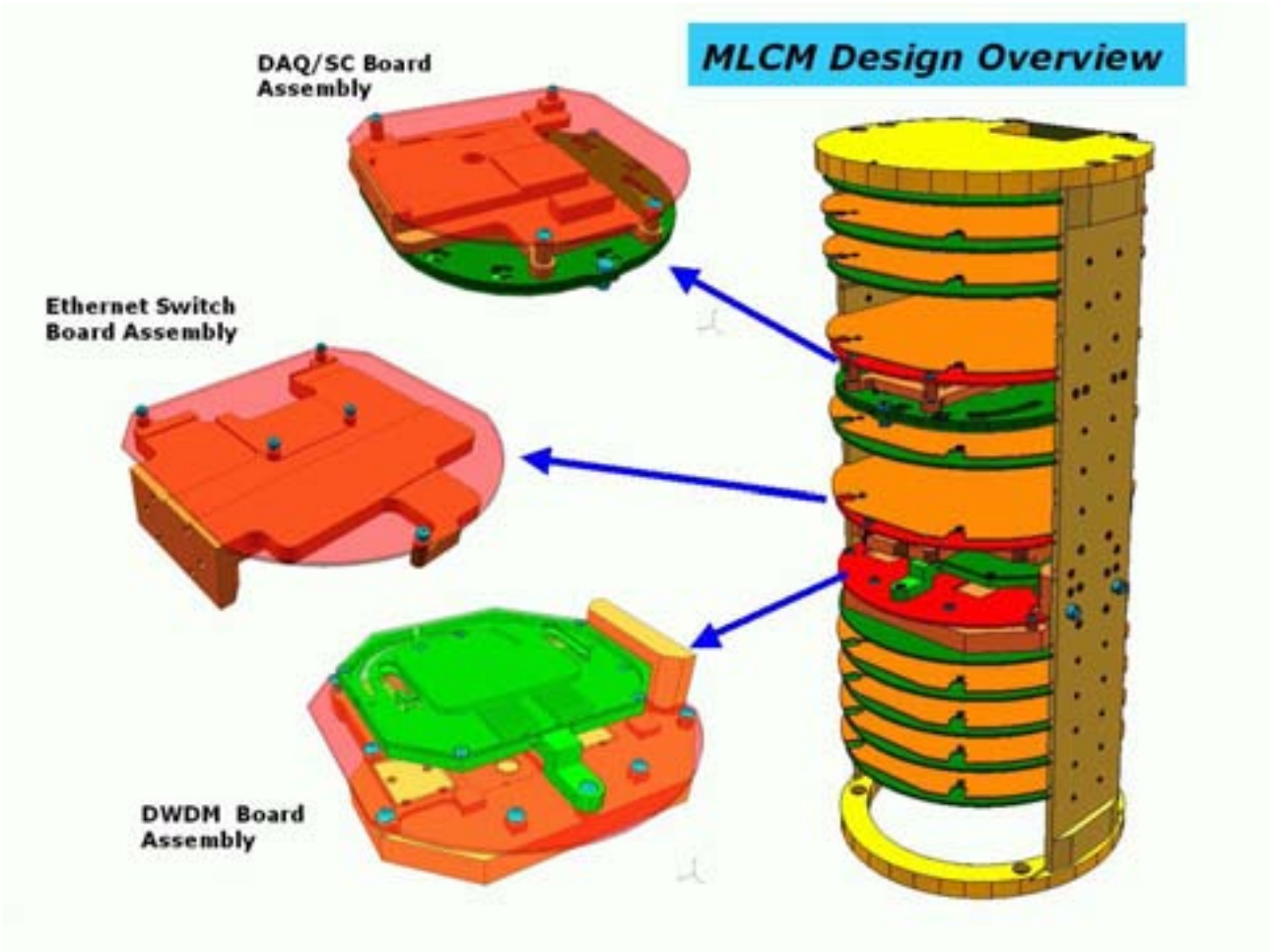

Mechanical design of the Antares MLCM Electronics crate.

2 Electronics Technology

2.1 Introduction

The expertise of the electronics department covers a broad area. It is applied in a number of projects, which can be divided in three main streams:

- Aftercare for the Zeus microvertex detector and the Hermes lambda-wheel detector. Both detectors are running in experiments at DESY.
- Design of components, fabrication of prototypes and production runs for the detectors that will be used in the LHC experiments ATLAS, LHCb and ALICE. For the prototyping the group provides support with high standard instrumentation like signal analyzers, oscilloscopes, power meters, SMD (Surface Mounting Devices) handling tools, etc.
- Design of components for non-accelerator based experiments like ANTARES and Medipix.

Because of this large number of projects there is a permanent high claim on manpower and expertise. In Fig. 2.1 the projects are listed that consumed more than 0.5 FTE.

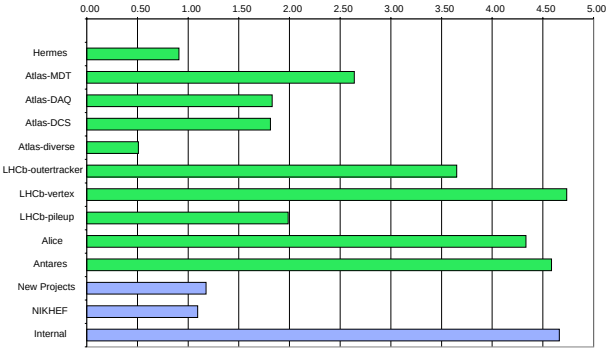

Figure 2.1: *ET manpower distribution in 2002*

2.2 Projects

Information on most projects can be found on the NIKHEF web site and elsewhere in this annual report. Below the involvement of the Electronics Technology Group is described in new developments for each of the projects.

HERMES

The HERMES target magnet was replaced to allow running with a transversely polarized target. However, at the position of the lambda-wheel detector, the stray fields of this magnet are much larger than that of the previously employed longitudinal magnet. At the maximum magnetic field, the stray fields are so large that they inhibit proper operation of the lambda-wheel electronics. The field saturates the ferrite of the pulse transformers that are used to isolate the control signals. Several options to solve the problem have been investigated and it was decided to replace the inductive coupling by a capacitive variant. This implies a reduction of the common-mode rejection, but tests showed an acceptable decrease of less than a factor two. A miniature modification printed circuit board has been designed and taken into production. The electronic modules of the lambda-wheels will be modified during the HERA shutdown period in 2003.

The Beam Loss Monitor has been redesigned, mainly to include integration of the radiation dose with a time constant of one second. This was necessary because a good fraction of the measured radiation can be attributed to long periods (several seconds) with a moderate radiation dose. The new module is currently in production and will also be installed during the 2003 shutdown period.

ATLAS

Monitored Drift Tubes - MDT

For the ATLAS muon spectrometer, NIKHEF builds detectors for the outer layer of the barrel muon detector. These so-called MDTs consist of two times three layers of 72 aluminum detector tubes on top of each other. Five of these detectors, each measuring $6 \times 2.5 \times 0.6$ m, are mounted above each other in a test station, the cosmic ray test stand. Cosmic muons pass through this set up and are detected by the tubes (2160 in total). They are read out by a computer and the reconstructed tracks can be displayed. Especially for the 'Open Day' it seemed more attractive to have a real time display of the tubes' activity. A 3:1 scaled representation of the detector was built, using large LEDs. The display is 80 cm wide and 120 cm high. A dedicated PC spies on the data that are transported on the local area network and sends them to the display via a serial link. The display is updated at an average rate of 30 Hz, the trigger rate of the muon chambers. One can clearly

recognize straight tracks and test signals introduced at a few locations. The display can be viewed from a large distance and a wide angle and attracted many people visiting NIKHEF on the occasion of the 'Open Day'.

Muon Readout Driver - MROD

The MROD-1 prototype supports six optical Input Links, each coming from the Chamber Service Module (CSM) on a Muon MDT chamber, and converts serial data-bits from at maximum 18 Time to Digital Converters (TDC) on a chamber into 32-bit data words. The MROD groups these data words for each TDC and checks whether the data words from all TDC's belonging to the same event number have arrived. The data from this event are formatted and sent via an output link to the Read-Out Buffer (ROB) for further processing by the downstream Trigger and Data Acquisition system.

A small series of MROD-1 modules was produced by external companies and tested. Serious problems concerning the soldering of the Ball Grid Array (BGA) devices showed up. In contrast to what was expected, the soldering process of the BGA devices turned out to be critical. Severe temperature stress in the printed circuit board caused the loss of one module. Furthermore, other modules had to be sent back for resoldering due to bad connections.

The CSM modules on the MDT chambers are located in a high-intensity radiation environment and need radiation tolerant hardware. The six Input Links on the MROD are compatible with the ATLAS S-Link standard, but radiation tolerant S-Link hardware does not exist. To resolve this problem the radiation tolerant Gigabit Optical Link (GOL) device, based on 1.6 Gbit/s point-to-point data transmission technology and developed at CERN, is used on the CSM to drive the optical link. At the MROD side a modified version of the standard S-Link HOLA implementation, receives the data from the CSM. The HOLA hardware is redesigned (now called GOLA) to be compatible with the data format and protocol used by the GOL device.

Read-Out-Buffer - ROBIN

The ATLAS Trigger/DAQ system (TDAQ) is connected via a large number of Read-Out-Buffers to the different sub-detectors of ATLAS. The main hardware component of the Read-Out-Buffers is an intelligent input module called RobIn, that accepts the input data stream consisting of data fragments from the sub-detectors. It provides temporary storage for these data fragments and delivers specific fragments upon request to the downstream system. Logically a total of 1600 RobIn's are required, each one dealing with a maximum input fragment rate of 100 kHz and a maximum input bandwidth of 160 MByte/s, delivered via a standard ATLAS optical link (S-Link). Output rate and bandwidth are of the order of 10% of the input values. Depending on the final TDAQ architecture multiple logical RobIn modules will be assembled into a single physical RobIn component, with multiple inputs and a single output. The physical RobIn can be either connected directly to the main TDAQ Ethernet network or can be attached via a PCI-bus to a host system that provides the Ethernet interface.

As a joint effort of the University of Mannheim, Royal Holloway University London and NIKHEF, a prototype has been developed that accepts data from two input links and that allows to investigate both the fully network based (Ethernet) and fully bus based (PCI) implementation of the RobIn. The final version can be derived from this prototype via small modifications, e.g. by changing the mechanical format and by omitting the unused Ethernet or PCI downstream port.

Semi-Conductor Trackers

Practice shows that it is very difficult to design stable hybrids with front-end chips with a large power-supply. Minimizing the supply-current modulation of the chips is one of the requirements for designing front-end hybrids. A careful analysis of the behavior of the prototype hybrids resulted in a modification that solved the instabilities. For that purpose extra decoupling of the power distribution was required, proving again that a careful layout of the ground system is of basic importance.

B Physics

LHCb Outer Tracker

The current local readout test-system used for the HP TDC is adapted for the new Otis TDC, which was received at the end of the year. The current TDC boards where adapted as readout boards so that the system, including a concentrator, timing and fast control, could still be used. It also involved a new I2C control set, hardware and software. As timing we have provided a Timing and Trigger Control (TTC) generator and receiver to trigger the present and future front ends in a CERN compatible way (on glass fiber). Furthermore a first proposal was worked out for signal and power distribution at the LHCb outer tracker detector. This means distribution of supply, slow control, timing signals, and data fibers.

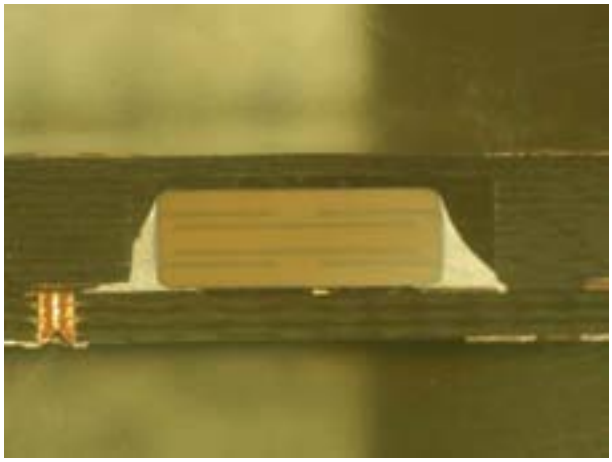

Figure 2.2: *HV board with capacitor for LHCb-OT, cut in half*

For the detector straw module several models have been constructed for end pieces, electronics boards, housings and mechanics including gas in- and outputs. Special attention had to be given to the limited space available between modules.

Special High Voltage boards have been constructed with capacitors inside the board for improved low current-leakage characteristics. Together with the board manufacturer the production process has been improved in order to ensure low dropout of HV-channels. This has the advantage that the low leakage current of the capacitors can not be spoiled by external influences (see Fig. 2.2).

Additional Rasnik units (from ATLAS) have been delivered to the collaboration for a prototype setup of an alignment system.

The ET group has joined the LHCb electronics steering work group, in which the electronics for all LHCb detectors is reviewed and the design of electronics that can be common for all detectors is worked out.

LHCb-Vertex RF measurements

As required by the CERN RF experts the frequency measurement range is enlarged from 150 MHz-1.5 GHz to 300 kHz-1.5 GHz because of the importance of the impedance behavior in the lower frequency part of the band. The higher signal levels give a lower noise level in the output results. During beam fill time of the LHC the two silicon strip detector boxes will be set in open condition (60 mm maximum distance) for the maximum beam-stay-clear situation. In order to reduce the RF coupling between beam path and suppressor the Wakefield suppressor has been extended with side flaps (see the figure in the LHC*b* section).

Measurements show that the coupling impedance for the open condition is improved such that it has a real part of 150 Ω for a single resonance at about 800 MHz. There is still a low-Q resonance at about 800 MHz that did not change in frequency but only in amplitude for a change of the detector box distance from 2 to 60 mm. This effect is not a serious problem, but nevertheless some time will be spent to discover the cause of this resonance.

The setup in the mockup tank will be changed. The detector boxes will be covered with the realistic corrugated RF foil and the Wakefield suppressors will be modified such as to contain less material.

LHCb-Vertex Silicon detector shielding

We simulate the beam in the frequency domain by a coaxial RF power line at 50 Ω. The outer conductor of the coax consists of 30 μm aluminum. The CW signal level in the coax was 10 W at 40 MHz. At 5 mm from the coaxial outer conductor the prototype silicon strip detector is mounted. As a second step we made a hole in the aluminum outside conductor just in front of the silicon strip detector, which gives much higher EM field levels.

In both situations we do not see an influence on the working of the silicon in combination with the electronics of the test setup. There was no change in noise level. Further tests will be concentrated on that part of the frequency spectrum in the beam that is related to the circumference of LHC (kHz band).

LHCb-Pile up Veto system

For the pile-up veto system a full-scale prototype of the vertex processor was designed. Presently the printed circuit board is being developed. The central part of this board consists of two large Field-Programmable Gate Arrays (FPGA), consisting of 3.2 million logic gates each. These FPGA's contain the correlation matrices that produce the trigger decision as input for the level0 trigger logic.

The pile-up veto system supplies a trigger decision to the level0 trigger of LHCb. As such, digital data are required prior to level0 buffering. The only readout chip for strip detectors that can deliver these discriminated signals is the *Beetle* chip. This device is a 128 channel analogue pipeline chip for silicon strip detectors. It has been designed by the ASIC Labor in Heidelberg in

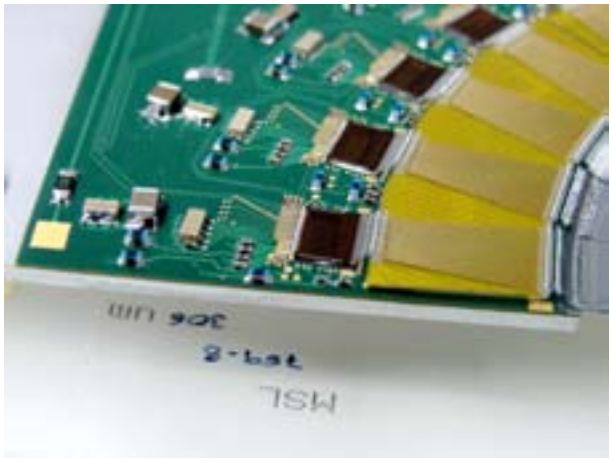

Figure 2.3: *Test hybrid with the Beetle front end chip and detector*

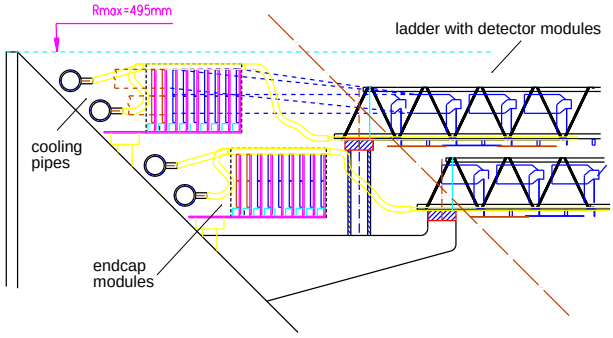

Figure 2.4: *Two Detector Layers with ladders connected to two EndCap Modules*

cooperation with NIKHEF. This year several new front-end test chips have been characterized. Based on these results, the final front-end for the complete *Beetle* chip was chosen. The 16 chip hybrid that was designed at the end of 2001, was fully equipped with a *Beetle* chip and bonded to a silicon detector of the Vertex Locator (VELO) (see Fig. 2.3). This prototyped hybrid was tested extensively with a 120 GeV pion beam at the CERN X7 facility. All 16 chips have been characterized and the noise contribution of the hybrid is negligible. Based on the laboratory and beam test results the VELO group has chosen the *Beetle* as the preferred front-end chip.

The comparator circuits in the *Beetle* chip, which are necessary for the pile-up veto project, have been characterized. The offset variation between different circuits in the same chip was found to be too large. With Monte-Carlo techniques we discovered that the main contribution to the offset results from the threshold variation of the deep sub-micron process. An improvement can only be made by extending the range of the digital to analogue converters of the threshold from 3 to 5 bits. A redesign is in progress and will be submitted a next run.

A full scale hybrid for the pile-up project has been designed. The hybrid has an additional 256 differential digital signal as compared to the VELO hybrid mentioned before. An 8-layer design with kapton as base material is needed. This hybrid is being produced at CERN. To test the vertex finder board, a dedicated pattern generator was designed, produced and tested. The large FPGA's on the vertex finder are being reprogrammed to reach the operating frequency of 40 MHz for LHC operation. The prototype design of the kapton cables for the VELO is in progress. The cables must meet the stringent requirements on shape, flexibility, radiation hardness and outgassing, and at the same time provide a controlled impedance path for the signals and act as shield for electro-magnetic pick-up.

ALICE

For the Silicon Strip Detector (SSD) in the Inner Tracker System (ITS) of the ALICE experiment we design electronics that handles the signals between the front-end hybrids in the detector and the data acquisition outside the detector. This electronics is placed at both ends of each detector ladder and is called an EndCap module. In total 144 modules are needed. In the design of the EndCap module the amount of power consumption and spacial extensions are very important restrictions. The electronics must be radiation tolerant and therefore application specific IC's (ASIC's) are being developed using a special IC technology employing 0.25 μm CMOS. Low-power ASIC's reduce the power consumption and spacial dimensions, as compared to a solution employing commercial IC's.

Two types of ASIC's are necessary, a control and buffer chip (ALCAPONE) for all signals that are needed for the front-ends on the detectors, and an analog buffer (ALABUF) to send the analogue data from the detector to the data-acquisition system.

The ALCAPONE chip has functions for buffering digital (LVDS and CMOS) signals, for the control of configuration data of the front-end chip and the chip itself, and for power regulation in the EndCap and the front-end

Hybrid. This makes this ASIC a "mixed signal" design with analogue and digital functions. Both the analogue- and digital parts are verified with simulations. The digital part is designed using Verilog as the description language, and then synthesized to a schematic of standard gates by software. The digital layout is generated "automatically", whereas the analogue part must be laid out by hand completely. The ALCAPONE0 design has been prototyped and successfully tested. Small improvements are necessary, but no major design changes have to be made before going into production in 2003. The ALABUF is a complete analogue design, consisting of two differential fixed gain signal amplifiers preceded by a two-channel analogue multiplexer. The ALABUF1 design has now been verified and accepted to go into production early 2003.

To verify the functional behavior of the complete EndCap module, a test board was designed for the ALCAPONE0 and ALABUF1 chips. With 7 of these boards connected, all functions could be tested in a setup controlled by a LabView program. The results will be included in the next ALCAPONE design.

ANTARES

Optical network

The Gigabit Ethernet (GbE) electric-optical conversion boards used in the connection between the offshore GbE switch and its counterpart at the shore station has been developed and realized. Commercially available GbE-PCI adapters together with an in-house designed electric-optical GbE retimer are used to make an Ethernet connection with a PC. A GbE test-bench has been set up and consists of two PCs that maintain a GbE connection between them, over 50 km with a dispatched

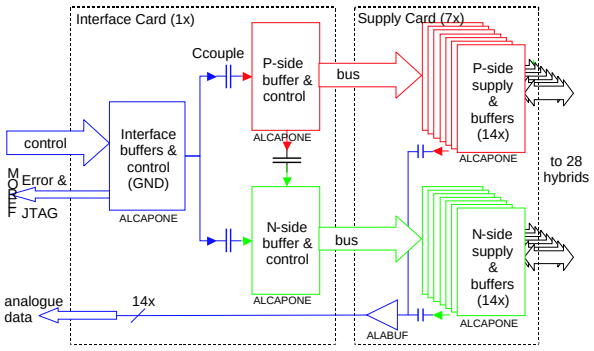

Figure 2.5: *Block diagram of the interface part of the EndCap module*

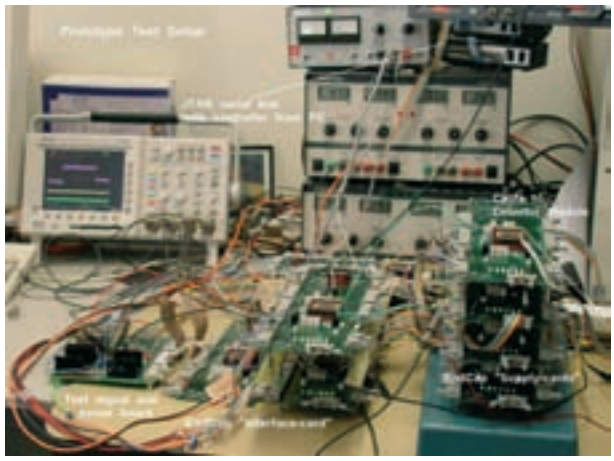

Figure 2.6: *Test setup for the Alice chips*

data transfer speed of 80 MB/s. Measurements with the produced boards over the link at minimum optical input level show a bit-error rate of one per 10^{22} transferred bits. Three independent optical data links have been produced for the test-sector line; GbE boards for the two MLCM (Master Local Control Modules) connections and 100 MHz Ethernet boards for the SCM (String Control Module) link. The entire setup is multiplexed and de-multiplexed with DWDM filters to a single fiber to shore and vice versa.

Figure 2.7: *Transmitter and receiver board for the optical communication in ANTARES*

Power distribution

Based on the anticipated power distribution from the conceptual design report the string power distribution topology has been designed. It consists of two parts: a string power module and a local power box. The string power module will convert the power from shore to a DC power in such a way that it minimizes noise and optimizes efficiency. This power will be converted by the local power box in each module to the voltage levels needed by the various electronic boards (see Fig. 2.8). Both items are realized in an extremely tight planning scheme with the Dutch firm BF-Power Concepts.

Figure 2.8: *Local power box of an Antares module.*

Medipix

A High-Density-Interconnect board to support 8 particle-detection chips, each containing 64,536 pixels is being made in collaboration with the firm Electronic Workbench and CERN. These dense chips required Chip-On-Board Technology and wire bond the chips in the same way as used for the hybrids of the LHCb-Pile up detector. A maximum number of 1601 wire bonds are used to the gold plating top layer of the PCB.

2.3 Department development

For all projects described above a wide field of electronic expertise is required. To keep the expertise on the required level and to increase the employability of the members of the electronic department various courses were attended by members of the group. For instance, knowledge about electromagnetic compatibility is a very important factor in the high-frequency designs of communication electronics and electronics in a noisy environment. This is especially necessary for near-beam experiments and when switching power is close to the electronic circuits. An ET-member joined a reference team to judge the grounding and shielding solution in the ZEUS straw tube tracker.

Other fields in which expertise is required are VLSI-design, PCB-design and optical networks. The electronics group participates in two projects concerning microelectronics. One is for ALICE, for which two ASIC's are in development, and the other is for LHC-B. In the latter case, design support is given to the NIKHEF group that contributes to the development of the *Beetle* chip (responsibility : "ASIC Labor in Heidelberg"). This work contains besides the design also improvements of the comparator. In addition, software support is given for the Medipix project, in which a new ADC is designed for future pixel-based detector chips using a deep-submicron IC technology.

In the field of PCB layout most of the board layout is done in house because of the specific electronic constraints on printed circuit boards. This means a high claim on expertise and tools. Several courses to optimize the PCB designs have been followed by members of the group.

In order to fully exploit the expertise in the group the instrumentation has to meet the highest standards and performance. Therefore, periodically new instrumentation is purchased as replacement and upgrading.

The ergonomic aspects of the office furniture and the workshop furniture are being evaluated on a continuous basis. New desks are in accordance with the latest ergonomic and safety regulations.

3 Mechanical Workshop

3.1 Introduction

The mechanical workshop has contributed to several projects in the experimental programs. For the LHC experiments the emphasis is changing from prototyping to production and production-startup. This production stage will require additional manpower for the coming two years.

3.2 Projects

ATLAS Muon Chambers

During the first part of this year 12 Muon Chambers were completed. In July 2002, material problems with the small brass gas-inlet tubes were detected. Therefore, it was decided to use stainless steel inlet tubes instead of the previously used brass ones. In total approximately 320.000 O-ring joints will have to be made gas tight. The first shipment of these gas tubes will arrive in April 2003.

A small fraction of the wires in the drift tubes was observed to break. This problem is caused by high gas flows but it can now be avoided by reducing the gas inlet speed. Moreover, a technique was developed to repair broken wires in an already completed Muon Chamber.

The Muon-Chamber production itself is now running smoothly. During production in the year 2002, 32 of the largest chambers have been built (see Fig. 3.1). The first chamber (built in 2001) took 18 days completion time. Meanwhile we have managed to reach a 6 days cycle for completing a chamber by partially assembling it outside the cleanroom (see Fig. 3.2).

Figure 3.1: *Storage of the ATLAS Muon Chambers in the former accelerator-building.*

We expect to complete the last of the 96 chambers in July 2004, after which the electronics, the gas-system and Faraday cages have to be mounted. It is planned to have all chambers ready in October 2004.

Finally, for the ATLAS muon spectrometer 1200 magnetic field sensors have to be calibrated with a relative accuracy of 10^{-4}. The workshop started to build the mechanics for a calibration stand.

ATLAS Semi-Conductor Tracker

This year two experimental support discs have been constructed with inserts to test the glueing methods and tooling, and to test their strength and accuracy. Ordering of all inserts has been done. Meanwhile, the first (small) delivery of inserts is being used on these discs, which form the support structure of the tracker. Since the delivery of the end caps at CERN is planned for March 2005, the assembly schedule shows a large need for manpower in 2003 and 2004. To get both end caps delivered in time two assembly lines (in The Netherlands and United Kingdom) are being set up. NIKHEF is producing the 80 modules that will be mounted on the discs. For this purpose, a cooled test box has been constructed (see Fig. 3.3).

Figure 3.2: *Construction of the Muon-Chamber frame outside the cleanroom. The lower two spacers form the basis of the station. The upper one is copied using precision parts.*

Figure 3.3: *The test box with two modules to be tested.*

The starting point of the assembly schedule is the expected delivery date of bare discs. A manufacturer for these discs was selected, and the first discs arrived in November. The first disc had a flatness within specifications, but the second one did not meet these specifications. Therefore, the manufacturer changed his tooling, which resulted in a satisfactory improvement. Disc reception measurements are being performed at NIKHEF, while also machining of all 20 raw discs, which takes several days per disc, will be carried out in the NIKHEF mechanical workshop. Each assembly line (at NIKHEF and in the UK) will handle nine discs, two discs will be kept as spares. After machining, all inserts must be glued on, and again machined flat within specification. For this purpose, a stiff support disc has been produced onto which the discs will be mounted during machining (see Fig. 3.4).

Between the steps in the machining process all specifications will be checked with a 3D measuring machine. The "mass production" for this project will start in the beginning of 2003. Part of the tooling has still to be produced, but has already been (pre-)designed. Installation of services and installation of modules onto nine discs will be performed in the room that has been conditioned especially for the Semi-Conductor Tracker project. Test and quality control activities will also take place in this room. Furthermore, assembly of the end cap cylinder will also need cooling and other environmental conditioning.

LHCb Vertex detector

In 2002 several new prototypes for the wake-field suppressors have been produced, and a new mold has been developed. The latest tests show that the prototypes function satisfactorily and that they could stand endurance tests. The attachment piece to the vacuum box has also been finalized and is ready for production.

At the Vrije Universiteit Amsterdam a full-size mold has been produced for forming the RF foil, that is used to separate the silicon modules from the primary vacuum. Several RF foils have been formed and were tested to be gas-tight.

The smallest bending radius of the RF foils that we can produce is 8 mm. With this radius the present design of the silicon modules cannot be accommodated, especially for the phi-detector, so re-design of the silicon modules seems necessary.

The constitution of the material plays a dominant role: both the chemical composition and the conditions of the fabrication are very important. Methods presently being investigated are:

- Cold formation: press-heat-cool-press (more than 15 cycles, 2 - 70 bar)
- Forming after heating to 350 degrees (Hot Metal Gas Forming)
- Heat to 520 degrees (Superplastic formation, pressure up to 10 bar - one step)
- Explosive forming

The first and second method turn out to produce good foils. The third method yields a material that is too hard; it easily breaks at larger deformations. The explosive forming technique (an experimental process carried out by an external firm) did not come near the deformation that is needed. Since the second method requires less steps in the production process than the first one, it has been chosen for the final production.

In order to cure possible pinholes in the foils we have also investigated the use of a poly-amide-imide coating. This kapton-like coating makes the foil vacuum tight, it is a good electric insulator and is radiation resistant (it is used in space research). It is not yet sure whether it is necessary to apply this coating in the secondary vacuum.

The test set-up for the motion control of the RF foils has been produced and is presently being tested in the Electronics Technology Department.

Figure 3.4: *Machining a disc with inserts, mounted on a stiff support.*

The production of prototype bellows was not yet successful; we performed two experiments to solder a complete bellow in a vacuum-oven. Both failed because of deformation during heating up, even though the second time a mold was made to fix all parts during the heating process.

One of these bellows has been exposed to an endurance test; no signs of rupture were observed after the (required) 10000 movements by 30 mm. Only after 50000 such movements small cracks appeared at places that showed already folding marks in the beginning.

It has been decided to weld the bellow parts together by using molds to lead away the heat in the 0.15 mm thick stainless steel shells. First experiments for such a welding process have been started (see Fig. 3.5). The total welding length per bellow is approximately 70 meter. Six bellows are needed in total.

LHCb Outer Tracker

For the LHCb Outer Tracker, the emphasis was on the preparation of the new cleanroom (see Fig. 3.6) and the development of tooling for the production of the straw chambers in the coming two years.

The wire locators and end-pieces that support the wires have been finished and the first pre-series are being produced. Molds that keep the straws in place during gluing have been developed and ordered. A module of 2500 mm length has been built and parts for a 1 meter prototype chamber were produced at the end of the year. The first chamber will be built in the beginning of 2003 and will contain only final parts.

Figure 3.5: *Bellow parts (2 x 0.15 mm thickness) for the LHCb vertex detector being welded together in a mold.*

Figure 3.6: *The new LHCb cleanroom with some production tooling.*

ANTARES

For Antares we constructed cooling blocks that will hold and cool the electronics boards for the test-string in the Mediterranean sea.

DUBBLE

Based upon the prototype slit constructed in 2001 twelve slits have been produced and tested this year. They will be installed at ESRF in Grenoble in the beginning of 2003.

AMS

The flexible thermal connectors for connecting the modules to the cooling ring were developed and 120 sets have been produced.

ALICE

The development of a production tool for folding and gluing the kapton flat-cable to the read-out modules for the ALICE detector has been started.

4 Engineering Department

4.1 Atlas muon chambers

The production drawings for 7 types of muon chambers (MDTs) are ready to send to the Engineering Data Management system at CERN. The design of the tooling for the gluing of the small MDT version has been finalised. The design of the transport frames of these chambers is ready.

At NIKHEF, 96 large chambers are constructed. In collaboration with Frascati (Italy) the design of a station to construct the spacer outside the cleanroom has been finalised. This station is operational and allows to prepare the spacers independly of the assembly in the cleanroom. We optimised the production site leak test set-up included in the integral test set-up. The procurement of gas bars, cross plates and transport frames has been realised. Studies of broken wires have been ongoing. We designed the projective alignment components.

The design of the common support structure to couple the trigger chambers (RPCs) with the MDT detectors has been completed.

4.2 Atlas silicon tracker

In July 2002 the contract with Programmed Composites, Inc. to produce 20 carbon fibre discs according to the European community standards was finalized. The discs function as a support structure and will be equipped with high precision silicon dectector modules. The first disc was delivered and accepted in December 2002. To study the routing of the necessary cabling and cooling pipes, a so called 'Cheap O' disc (Fig. 4.1) was designed and constructed. The design of the inserts that hold the services and modules made out of Torlon is finished and the first prototypes are available. We designed the disc tooling to machine both sides of the discs and its inserts within 0.1 mm flatness. Work on the design of the assembly tools, needed to mount the modules on the discs is in progress. The design of the storage box for the discs has been updated.

4.3 LHCb Outer tracker

The main issue for the LHCb detector in 2002 was the change to the so called 'light version' of the outer tracker. The final design of the straw assembly with respect to the electrical and mechanical compatibility required close collaboration of the mechanical group and the colleagues from the electronic department. A 2.5 m prototype module has been manufactured in order to optimise the fabrication procedure. Some modifications to the modules were made to ensure gas tightness and grounding of the straws. The procedure for injection molding of the wire locators has been updated. A first set was successfully produced as can be seen in

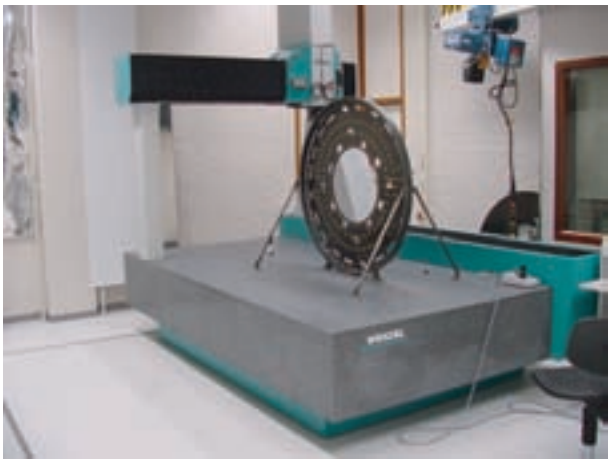

Figure 4.1: *Photograph of the 'Cheap O' disc on the 3D measuring device at NIKHEF.*

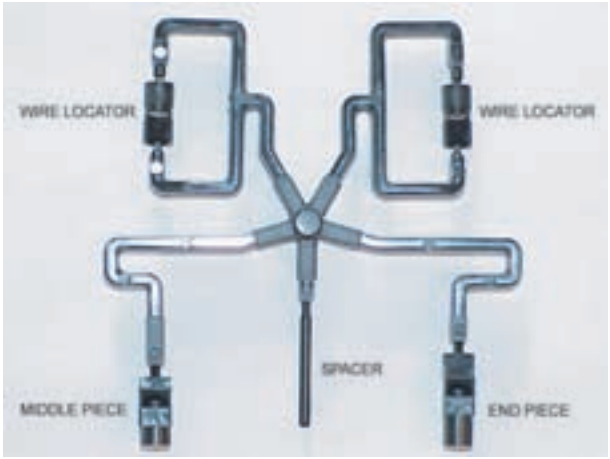

Figure 4.2: *Injection molding prototype of two wire locators (black cylinders at top left and right), one end- and one middle-block (black cylinders at bottom left and right), produced with a four-fold injection mould at Philips CFT. Still visible is the plastic frame that holds the various parts together during the production process.*

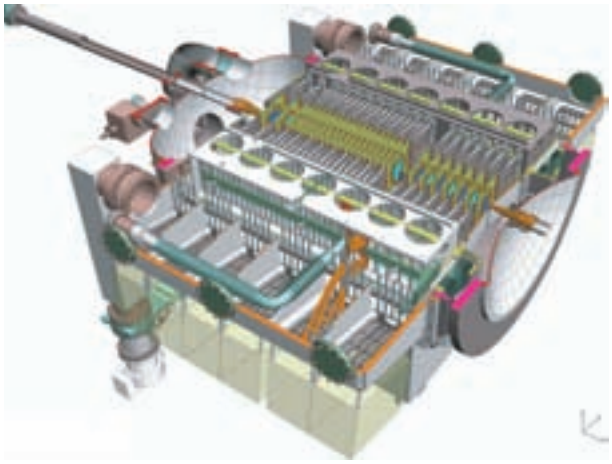

Figure 4.3: *The cross section of the present design of the LHCb vertex detector.*

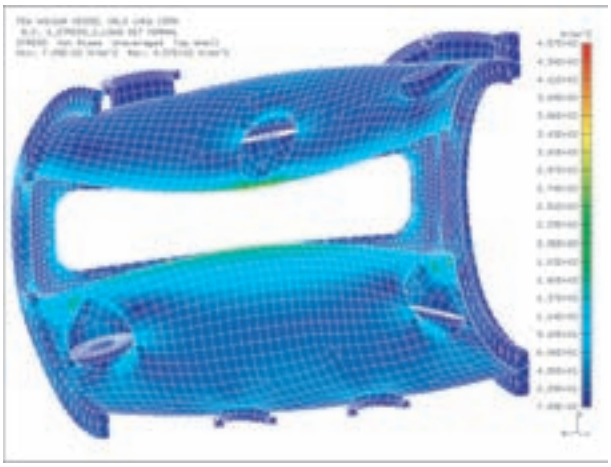

Figure 4.4: *A graph of the mechanical stress of the LHCb vacuum tank, obtained in a study using the finite element method.*

Fig. 4.2. The integration with the inner tracker has been designed. A clean room for the production of the 5 m modules has been prepared. Part of the production tooling is designed and manufactured. The collaboration with our colleagues in Heidelberg (Germany) and Warshaw (Poland) resulted in an optimal sharing of the production tasks.

4.4 LHCb vertex

The design of the vertex detector of LHCb has evolved to a complex but feasible set-up. A drawing of this setup is shown in figure 4.3. We contribute to the design of the vacuum vessel. Fig. 4.4 shows the result of a study using the finite element method to minimise the mechanical stresses. The main issues were the development of the aluminium separation foil and the large bellows. Our work on the foil led to a promising solution while the bellows are still in the prototyping stage.

The functioning of the 'gravity valve' still is being studied. This safety valve protects the primary vacuum against back streaming from the secondary housing using only mechnical components. See also the LHCb section elsewhere in this report.

In December, the the total setup was reviewed by the Engineering Design Review committee, which concluded in the 'go ahead' signal.

4.5 ALICE

NIKHEF is responsible for the assembly of ALICE silicon strip detection modules (SSD) on carbon fibre support structures and the subsequent mounting of these ladders on carbon fibre support cones.

NIKHEF is also involved in the discussions about integration of the detectors in the inner tracking system (ITS) with the Time Projection Chamber (TPC). The TPC directly surrounds the SSD system, which itself forms the outer layers of the ITS. Therefore integration issues directly affect the production procedures of the SSD system.

During 2002, the corrosion properties of the Phynox tubes (40 μm wall thickness) selected for the cooling system on the detection modules were verified. The design of the detection modules was frozen and a first prototype was constructed.

For the positioning of the modules on the suppport frames, it is required that the modules, which consist of a hybrid and the actual sensor, are assembled with high mechanical precision. NIKHEF developped the tool to assemble the modules, which is now nearly completed.

The carbon support frames for the modules were produced in St. Petersburg. The engineering department has prepared tools for quality control of these frames, assuring that mounting of the modules on these frames will result in a system with the required accuracy.

The design of the tools for assembling ladders on their support cones was started. Possible locations for this assembly activity are being investigated.

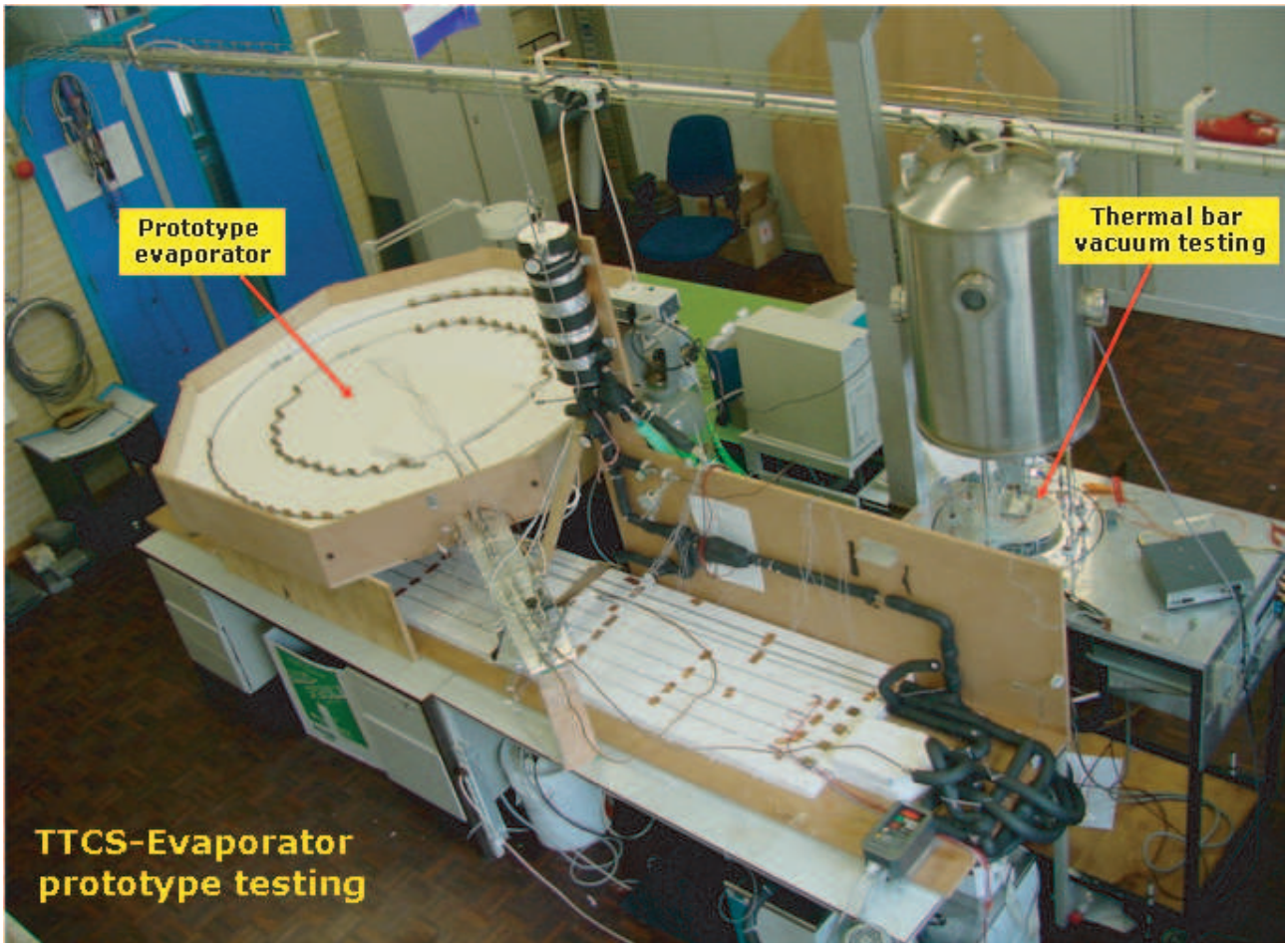

Figure 4.5: *Photograph of the cooling circuit for the AMS silicon tracker.*

4.6 Antares

The engineering group contributed to the analysis of the thermal management of the crates that house an important part of the read-out electronis of Antares. A prototype electronics set-up was build and tested in a water reservoir to study the temperature behaviour. Our prediction based on computer simulations appeared to be in close agreement with the measurements.

4.7 AMS

The engineering of the AMS cooling circuit is finalised (see Fig. 4.5) and the production drawings are available. Integration issues still have to be solved while the manufacturing phase is started. In collaboration with NLR and AMS the design of the TTCS (Tracker Thermal Control System) circulation unit is being developed.

4.8 ESRF-Dubble

In 2002 the redesign, the manufacturing and the installation of several precision components has been realised. Herewith, a successful collaboration of 12 years with ESRF in Grenoble came to a conclusion.

The ICHEP 2002 poster.

E Publications, Theses and Talks

1 Publications

ALICE

[1] Aggarwal, M.M. *et al.*; N.J.A.M. van Eijndhoven, R. Kamermans, E.C. van der Pijll; WA98 Collaboration
Transverse mass distributions of neutral pions from ^{208}Pb-induced reactions at 158 AGeV
Eur. Phys. J. **C23** (2002) 225

[2] Aggarwal, M.M. *et al.*; N.J.A.M. van Eijndhoven, R. Kamermans, E.C. van der Pijll; WA98 Collaboration
Event-by-Event Fluctuations in Particle Multiplicities and Transverse Energy Produced in 158 AGeV Pb+Pb Collisions
Phys. Rev. **C65** (2002) 054912

[3] Lebedev, A. *et al.*; N.J.A.M. van Eijndhoven, R. Kamermans, E.C. van der Pijll; WA98 Collaboration
Direct Photons in WA98
Nucl. Phys. **A698** (2002) 135

[4] Eijndhoven, N.J.A.M. van, and Wetzels, W.
In-event background and signal reconstruction for two-photon invariant-mass analyses
Nucl. Instr. and Meth. **A482** (2002) 513

[5] Carrer, N. *et al.*; R. Kamermans, P.G. Kuijer, E. Schillings; NA57 collaboration
First results on strange baryon production from the NA57 experiment
Nucl. Phys. **A698** (2002) 118C

[6] Fanebust, K. *et al.*; N.J.A.M. van Eijndhoven, R. Kamermans, P.G. Kuijer, E. Schillings, P.C. de Rijke; NA57 Collaboration
Results on Hyperon Production from NA57
J. Phys. **G28** (2002) 1607

[7] Afanasiev, S.V. *et al.*; M. van Leeuwen, M. Botje; NA49 Collaboration
Energy dependence of pion and kaon production in central pb+ collisions
Phys. Rev. **C66** (2002) 054902

[8] Afanasiev, S.V. *et al.*; M. van Leeuwen, M. Botje; NA49 Collaboration
Cascade and anti-cascade+ production in central Pb+Pb collisions at 158-GeV/C per nucleon
Phys. Lett. **B538** (2002) 275

[9] Rybicki, A. *et al.*; M. van Leeuwen, M. Botje; NA49 Collaboration
Baryon number transfer in nuclear collisions at SPS energie
Acta Phys. Polon. **B33** (2002) 1483-1494

[10] Fischer, H.G. *et al.*; M. van Leeuwen, M. Botje; NA49 Collaboration
Baryon number transfer and central net baryon density in elementary hadronic interactions
Acta Phys. Polon. **B33** (2002) 1473

[11] Susa, T. *et al.*; M. van Leeuwen, M. Botje; NA49 collaboration
Cascade production in p+p, p+A and A+A interactions at 158 AGeV
Nucl. Phys. **A698** (2002) 491

[12] Friese, V. *et al.*; M. van Leeuwen, M. Botje; NA49 collaboration
Production of strange resonances in C+C and Pb+Pb collisions at 158 AGeV
Nucl. Phys. **A698** (2002) 487

[13] Blume, C. *et al.*; M. van Leeuwen, M. Botje; NA49 collaboration
New results from NA49
Nucl. Phys. **A698** (2002) 104

[14] Kollegger, T. *et al.*; M. van Leeuwen, M. Botje; NA49 collaboration
Energy dependence of kaon production in central Pb+Pb collisions
J. Phys. **G28** (2002) 1689

[15] Mischke, A. *et al.*; M. van Leeuwen, M. Botje; NA49 collaboration
Lambda production in central Pb+Pb collisions at CERN SPS energies
J. Phys. **G28** (2002) 1761

[16] Kadija, K. *et al.*; M. van Leeuwen, M. Botje; NA49 collaboration
Strange particle production in p+p, p+Pb and Pb+Pb interactions from NA49
J. Phys. **G28** (2002) 1675

[17] Botje, M.
Error estimates on parton density distributions
J. Phys. **G28** (2002) 779

[18] Haas, A.P. de *et al.*
Aluminium microcable technology for the Alice silicon strip detector: a status report
Proc. 8th workshop on electronics for LHC experiments, Colmar, France, Sept. 9-13, 2002

ANTARES

[19] Carloganu, C. *et al.*; R. van Dantzig, J. Engelen, A. Heijboer, M. de Jong, P. Kooijman, G.J. Nooren, J.E.J. Oberski, P. de Witt Huberts, E. de Wolf
The ANTARES optical module
Nucl. Instrum. Meth. **A484** (2002) 369-383

ATLAS

[20] Abazov, V.M. *et al.*; Balm, P.W.; Bos, K.; Peters, O.; Ahmed, S.N.; Jong, S.J.; Duensing, S.; Filthaut, F.; Wijngaarden, D.A.; D0 collaboration
Hard single diffraction in $\overline{p}p$ Collisions at $\sqrt{s}$ = 630 and 1800 GeV
Phys. Lett. **B531** (2002) 52-60

[21] Abazov, V.M. *et al.*; Balm, P.W.; Bos, K.; Peters, O.; Ahmed, S.N.; Jong, S.J.; Duensing, S.; Filthaut, F.; Wijngaarden, D.A.; D0 collaboration
Improved W boson mass measurement with the D0 detector
Phys. Rev. **D66** (2002) 012001

[22] Abazov, V.M. *et al.*; Balm, P.W.; Blekman, F.; Bos, K.; Peters, O.; Ahmed, S.N.; Jong, S.J.; Duensing, S.; Filthaut, F.; Naumann, N.A.; Wijngaarden, D.A.; D0 collaboration
Direct measurement of the W boson decay width
Phys. Rev. **D66** (2002) 032008

[23] Abazov, V.M. *et al.*; Balm, P.W.; Bos, K.; Peters, O.; Ahmed, S.N.; Jong, S.J.; Duensing, S.; Filthaut, F.; Wijngaarden, D.A.; D0 collaboration
The inclusive jet cross section in $p\bar{p}$ collisions at $\sqrt{s}$ = 1.8 TeV using the kT algorithm
Phys. Lett. **B525** (2002) 211-218

[24] Abazov, V.M. *et al.*; Balm, P.W.; Bos, K.; Peters, O.; Ahmed, S.N.; Jong, S.J.; Duensing, S.; Filthaut, F.; Wijngaarden, D.A.; D0 collaboration
Subjet multiplicity of gluon and quark jets reconstructed with the $k_\perp$ Algorithm in $p\bar{p}$ collisions
Phys. Rev. **D65** (2002) 052008

[25] Abazov, V.M. *et al.*; Balm, P.W.; Bos, K.; Peters, O.; Ahmed, S.N.; Jong, S.J.; Duensing, S.; Filthaut, F.; Wijngaarden, D.A.; D0 collaboration
Direct search for charged Higgs bosons in decays of top quarks
Phys. Rev. Lett. **88** (2002) 151803

[26] Abazov, V.M. *et al.*; Balm, P.W.; Bos, K.; Peters, O.; Ahmed, S.N.; Jong, S.J.; Duensing, S.; Filthaut, F.; Wijngaarden, D.A.; D0 collaboration
Search for the scalar top quark in $p\bar{p}$ collisions at $\sqrt{s}$ = 1.8 TeV
Phys. Rev. Lett. **88** (2002) 171802

[27] Abazov, V.M. *et al.*; Balm, P.W.; Bos, K.; Peters, O.; Ahmed, S.N.; Jong, S.J.; Duensing, S.; Filthaut, F.; Wijngaarden, D.A.; D0 collaboration
Search for leptoquark pairs decaying into $\nu\nu$ plus jets in $p\bar{p}$ collisions at TeV at root s=1.8 TeV
Phys. Rev. Lett. **88** (2002) 191801

[28] Adam, W. *et al.*; Eijk, B. van; Hartjes, F.; Noomen, J.; RD42 collaboration
Radiation tolerance of CVD diamond detectors for pions and protons
Nucl. Instr. Meth. **A476** (2002) 686-693

[29] Adam, W. *et al.*; Eijk, B. van; Hartjes, F.; Noomen, J.; RD42 collaboration
Performance of irradiated CVD diamond microstrip sensors
Nucl. Instr. Meth. **A476** (2002) 706-712

[30] Blair, R. *et al.*; Boterenbrood, H.; Jansweijer, P.; Kieft, G.; Scholte, R.; Slopsema, R.; Vermeulen, J.
The ATLAS Level-2 Trigger Pilot Project
IEEE Trans. Nucl. Sci. **49** (2002) 851-857

[31] Dolbnya, I.P. *et al.*; Hartjes, F.G.; Udo, F.
A fast position sensitive microstrip-gas-chamber detector at high count rate operation
Rev. Sci. Instrum. **73** (2002) 3754-3758

[32] Gschwendtner, E. *et al.*; Hessey, N.
Benchmarking the particle background in the large hadron collider experiments
Nucl. Instr. Meth. **A482** (2002) 573-580

[33] Gschwendtner, E.; Fabjan, C.W.; Hessey, N.; *et al.*
Measuring the photon background in the LHC experimental environment
Nucl. Instr. Meth. **A476** (2002) 222-224

B Physics

[34] Ketel, T., *et al.*
Performance of an irradiated LHCb prototype p-on-n silicon microstrip detector
Nucl. Instr. Meth. **A478** (2002) 291-295

[35] Brand, J.F.J. van den, Doets, M., Kraan, M., Klous, M.S., Kaan, A.P.
The vacuum system of the LHCb vertex detector
Vacuum **67** (2002) 363-371

DATAGRID

[36] Afsarmanesh, H., R.G. Belleman, A.S.Z. Belloum, A. Benabdelkader, J.F.J. van den Brand, G.B. Eijkel, A. Frenkel, C. Garita, D.L. Groep, R.M.A. Heeren, Z.W. Hendrikse, L.O. Hertzberger, J.A. Kaandorp, E.C. Kaletas, V. Korkhov, C.T.A.M. de Laat, P.M.A. Sloot, D.Vasunin, A. Visser and H.H. Yakali; VLAM-G
A Grid-based virtual laboratory
Scientific Programming **10** (2) 173-181, 2002

[37] Belloum, A., Z.W. Hendrikse, D.L. Groep, E.C. Kaletas, A.W. van Halderen, L.O. Hertzberger; VLAM
A Data & Process Handling System on the Grid
Proc. 9th Int. Conf. HPCN Europe, 2001, Springer Verlag 2002, pg. 81-93.

[38] Eijkel, G.B., H. Afsarmanesh, D. Groep, A. Frenkel, R.M.A. Heeren
Mass spectrometry in the Amsterdam Virtual Laboratory: development of a high-performance platform for meta-data analysis
Proc. 13th Sanibel Conf. on Mass Spectrometry: informatics and mass spectrometry, Sanibel Island, Florida (USA) 2001.

[39] Belloum, A.S.Z., D.L. Groep, Z.W. Hendrikse, L.O. Hertzberger, V. Korkhov, C.T.A.M. de Laat, D. Vasunin; VLAM-G
A Grid-Based Virtual Laboratory
Proc. TERENA Networking Conf., Limerick, 2002

HERMES

[40] Airapetian, A. *et al.*; Bouhali, O.; Bulten, H.J.; Witt Huberts, P.K.A. de; Ferro-Luzzi, M.; Garutti, E.; Heesbeen, D.; Hesselink, W.H.A.; Kolster, H.; Laziev, A.; Mexner, V.; Simani, C.; Steijger, J.J.M.; Brand, J.F.J. van den; Steenhoven, G. van der; Hunen, J.J. van; Visser, J.; HERMES collaboration
Single-spin azimuthal asymmetry in exclusive electroproduction of π^+ mesons
Phys. Lett. **B535** (2002) 85-92

[41] Amarian, M.
DVCS and exclusive Meson production at HERMES
Nucl. Phys. **B105** (2002) 100-104

[42] Baumgarten, C. *et al.*; Kolster, H.
Molecular flow and wall collision age distributions
Eur. Phys. J. **D18** (2002) 37-49

[43] Baumgarten, C. *et al.*; Kolster, H.; Simani, M.C., *Time-of-flight measurements in atomic beam devices using adiabatic high frequency transitions and sextupole magnets*
Nucl. Instr. Meth. **A489** (2002) 1-9

[44] Baumgarten, C. *et al.*; Kolster, H.; Simani, M.C.
An atomic beam polarimeter to measure the nuclear polarization in the HERMES gaseous polarized hydrogen and deuterium target
Nucl. Instr. Meth. **A482** (2002) 606-618

[45] Garutti, E.
Hadron formation in nuclei in DIS
Acta Phys. Pol. **B33** (2002) 3013-3017

[46] Simani, M.C.
Recent results on the helicity structure of the nucleon form HERMES
Acta Phys. Pol. **B33** (2002) 3731-3735

[47] Steenhoven, G. van der
Concluding remarks on the QCD-N'02 Workshop
Nucl. Phys. **A711** (2002) 363c-372c

[48] Visser, J. *et al.*; HERMES collaboration
The cross-section ratio of deuterium over hydrogen in DIS at HERMES
Nucl. Phys. **A699** (2002) 136-139

[49] Garrow, K. *et al.*; Blok H.P., B. Zihlmann
Nuclear transparency from quasielastic $A(e,e'p)$ reactions up to $Q^2 = 8.1$ (GeV/c)^2
Phys. Rev. **C66** (2002) 044613

LEP-DELPHI

[50] Kluit, P.
B_s oscillations

Proc. Int. Conf. on Flavor Physics ICFP2001, (ed. Y-L Wu) World Scientific, Singapore 2002, p. 275-279

[51] Kluit, P., and Stocchi, A.
Heavy quarks and the CKM matrix
Comptes Rendues Academie des Sciences, C.R. Physique **3** (2002) 1203-1210

[52] Abdallah, J. *et al.*; Blom, H.M.; Kluit, P.; Montenegro, J.; Mulders, M.; Reid, D.; Timmermans, J.; Dam, P. van; Eldik, J. van; Vulpen, I. van; DELPHI Collaboration
Search for charged Higgs bosons in e^+e^- collisions at $\sqrt{s}$ = 189-202 GeV
Phys. Lett. **B525** (2002) 17-28

[53] Abdallah, J. *et al.*; Blom, H.M.; Kluit, P.; Montenegro, J.; Mulders, M.; Reid, D.; Timmermans, J.; Dam, P. van; Vulpen, I. van; DELPHI Collaboration
Searches for neutral Higgs bosons in $\mathrm{e^+e^-}$ collisions from $\sqrt{s} = 191.6$ to 201.7 GeV
Eur. Phys. J. **C23** (2002) 409-435

[54] Abdallah, J. *et al.*; Blom, H.M.; Kluit, P.; Montenegro, J.; Mulders, M.; Reid, D.; Timmermans, J.; Dam, P. van; Vulpen, I. van; DELPHI Collaboration
Rapidity-alignment and $\mathrm{p_T}$ compensation of particle pairs in hadronic Z^0 decays
Phys. Lett. **B533** (2002) 243-252

LEP-L3

[55] Achard, P., *et al.*; S.V. Baldew, G.J. Bobbink, A. Buijs, M. Dierckxsens, M. van Dierendonck, P. Duinker, R. van Gulik, P. de Jong, F.L. Linde, A.J.M. Muijs, J.A. van Dalen, F. Filthaut, R.S. Hakobyan, Y. Hu, W. Kittel, A.C. König, D. Mangeol, W.J. Metzger, B. Petersen, M. Pohl, B. Roux, M.P. Sanders, D.J. Schotanus, C. Timmermans, R.T. Van de Walle, H. Wilkens; L3 Collaboration
Inclusive π^0 and K^0_S production in two-photon collisions at LEP
Phys. Lett. **B524** (2002) 44

[56] Achard, P., *et al.*; S.V. Baldew, G.J. Bobbink, A. Buijs, M. Dierckxsens, M. van Dierendonck, P. Duinker, R. van Gulik, P. de Jong, F.L. Linde, A.J.M. Muijs, J.A. van Dalen, F. Filthaut, R.S. Hakobyan, Y. Hu, W. Kittel, A.C. König, D. Mangeol, W.J. Metzger, B. Petersen, M. Pohl, B. Roux, M.P. Sanders, D.J. Schotanus, C. Timmermans, R.T. Van de Walle, H. Wilkens; L3 Collaboration
Bose-Einstein correlations of neutral and charged pions in hadronic Z decays
Phys. Lett. **B524** (2002) 55

[57] Achard, P., *et al.*; S.V. Baldew, G.J. Bobbink, A. Buijs, M. Dierckxsens, M. van Dierendonck, P. Duinker, R. van Gulik, P. de Jong, F.L. Linde, A.J.M. Muijs, J.A. van Dalen, F. Filthaut, R.S. Hakobyan, Y. Hu, W. Kittel, A.C. König, D. Mangeol, W.J. Metzger, B. Petersen, M. Pohl, B. Roux, M.P. Sanders, D.J. Schotanus, C. Timmermans, R.T. Van de Walle, H. Wilkens; L3 Collaboration
Search for R-parity violating decays of supersymmetric particles in e^+e^- collisions at LEP
Phys. Lett. **B524** (2002) 65

[58] Achard, P., *et al.*; S.V. Baldew, G.J. Bobbink, A. Buijs, M. Dierckxsens, M. van Dierendonck, P. Duinker, R. van Gulik, P. de Jong, F.L. Linde, A.J.M. Muijs, J.A. van Dalen, F. Filthaut, R.S. Hakobyan, Y. Hu, W. Kittel, A.C. König, D. Mangeol, W.J. Metzger, B. Petersen, M. Pohl, B. Roux, M.P. Sanders, D.J. Schotanus, C. Timmermans, R.T. Van de Walle, H. Wilkens; L3 Collaboration
f1(1285) formation in two photon collisions at LEP
Phys. Lett. **B526** (2002) 269

[59] Achard, P., *et al.*; S.V. Baldew, G.J. Bobbink, A. Buijs, M. Dierckxsens, M. van Dierendonck, P. Duinker, R. van Gulik, P. de Jong, F.L. Linde, A.J.M. Muijs, J.A. van Dalen, F. Filthaut, R.S. Hakobyan, Y. Hu, W. Kittel, A.C. König, D. Mangeol, W.J. Metzger, B. Petersen, M. Pohl, B. Roux, M.P. Sanders, D.J. Schotanus, C. Timmermans, R.T. Van de Walle, H. Wilkens; L3 Collaboration
Study of the $W^+W^-\gamma$ process and limits on anomalous quartic gauge boson couplings at LEP
Phys. Lett. **B527** (2002) 29

[60] Achard, P., *et al.*; S.V. Baldew, G.J. Bobbink, A. Buijs, M. Dierckxsens, M. van Dierendonck, P. Duinker, R. van Gulik, P. de Jong, F.L. Linde, A.J.M. Muijs, J.A. van Dalen, F. Filthaut, R.S. Hakobyan, Y. Hu, W. Kittel, A.C. König, D. Mangeol, W.J. Metzger, B. Petersen, M. Pohl, B. Roux, M.P. Sanders, D.J. Schotanus, C. Timmermans, R.T. Van de Walle, H. Wilkens; L3 Collaboration

Study of multiphoton final states and tests of QED in e^+e^- collisions at $\sqrt{s}$ up to 209 GeV
Phys. Lett. **B531** (2002) 28

[61] Achard, P., *et al.*; S.V. Baldew, G.J. Bobbink, A. Buijs, M. Dierckxsens, M. van Dierendonck, P. Duinker, R. van Gulik, P. de Jong, F.L. Linde, A.J.M. Muijs, J.A. van Dalen, F. Filthaut, R.S. Hakobyan, Y. Hu, W. Kittel, A.C. König, D. Mangeol, W.J. Metzger, B. Petersen, M. Pohl, B. Roux, M.P. Sanders, D.J. Schotanus, C. Timmermans, R.T. Van de Walle, H. Wilkens; L3 Collaboration
Double-tag events in two-photon collisions at LEP
Phys. Lett. **B531** (2002) 39

[62] Achard, P., *et al.*; S.V. Baldew, G.J. Bobbink, A. Buijs, M. Dierckxsens, M. van Dierendonck, P. Duinker, R. van Gulik, P. de Jong, F.L. Linde, A.J.M. Muijs, J.A. van Dalen, F. Filthaut, R.S. Hakobyan, Y. Hu, W. Kittel, A.C. König, D. Mangeol, W.J. Metzger, B. Petersen, M. Pohl, B. Roux, M.P. Sanders, D.J. Schotanus, C. Timmermans, R.T. Van de Walle, H. Wilkens; L3 Collaboration
Search for a Higgs boson decaying into two photons at LEP
Phys. Lett. **B534** (2002) 28

[63] Achard, P., *et al.*; S.V. Baldew, G.J. Bobbink, A. Buijs, M. Dierckxsens, M. van Dierendonck, P. Duinker, R. van Gulik, P. de Jong, F.L. Linde, A.J.M. Muijs, J.A. van Dalen, F. Filthaut, R.S. Hakobyan, Y. Hu, W. Kittel, A.C. König, D. Mangeol, W.J. Metzger, B. Petersen, M. Pohl, B. Roux, M.P. Sanders, D.J. Schotanus, C. Timmermans, R.T. Van de Walle, H. Wilkens; L3 Collaboration
Inclusive $D^*\pm$ production in two-photon collisions at LEP
Phys. Lett. **B535** (2002) 59

[64] Achard, P., *et al.*; S.V. Baldew, G.J. Bobbink, A. Buijs, M. Dierckxsens, M. van Dierendonck, P. Duinker, R. van Gulik, P. de Jong, F.L. Linde, A.J.M. Muijs, J.A. van Dalen, F. Filthaut, R.S. Hakobyan, Y. Hu, W. Kittel, A.C. König, D. Mangeol, W.J. Metzger, B. Petersen, M. Pohl, B. Roux, M.P. Sanders, D.J. Schotanus, C. Timmermans, R.T. Van de Walle, H. Wilkens; L3 Collaboration
Λ and Σ^0 pair production in two photon collisions at LEP
Phys. Lett. **B536** (2002) 24

[65] Achard, P., *et al.*; S.V. Baldew, G.J. Bobbink, A. Buijs, M. Dierckxsens, M. van Dierendonck, P. Duinker, R. van Gulik, P. de Jong, F.L. Linde, A.J.M. Muijs, J.A. van Dalen, F. Filthaut, R.S. Hakobyan, Y. Hu, W. Kittel, A.C. König, D. Mangeol, W.J. Metzger, B. Petersen, M. Pohl, B. Roux, M.P. Sanders, D.J. Schotanus, C. Timmermans, R.T. Van de Walle, H. Wilkens; L3 Collaboration
Determination of α_s from Hadronic Event Shapes in e^+e^- Annihilation at $192 < \sqrt{s} < 208$ GeV
Phys. Lett. **B536** (2002) 217

[66] Achard, P., *et al.*; S.V. Baldew, G.J. Bobbink, A. Buijs, M. Dierckxsens, M. van Dierendonck, P. Duinker, R. van Gulik, P. de Jong, F.L. Linde, A.J.M. Muijs, J.A. van Dalen, F. Filthaut, R.S. Hakobyan, Y. Hu, W. Kittel, A.C. König, D. Mangeol, W.J. Metzger, B. Petersen, M. Pohl, B. Roux, M.P. Sanders, D.J. Schotanus, C. Timmermans, R.T. Van de Walle, H. Wilkens; L3 Collaboration
The $e^+e^- \to Z\,\gamma\gamma \to q\bar{q}\gamma\gamma$ reaction at LEP and constraints on anomalous quartic gauge boson couplings
Phys. Lett. **B540** (2002) 43

[67] Achard, P., *et al.*; S.V. Baldew, G.J. Bobbink, A. Buijs, M. Dierckxsens, M. van Dierendonck, P. Duinker, R. van Gulik, P. de Jong, F.L. Linde, A.J.M. Muijs, J.A. van Dalen, F. Filthaut, R.S. Hakobyan, Y. Hu, W. Kittel, A.C. König, D. Mangeol, W.J. Metzger, B. Petersen, M. Pohl, B. Roux, M.P. Sanders, D.J. Schotanus, C. Timmermans, R.T. Van de Walle, H. Wilkens; L3 Collaboration
Measurement of genuine three-particle Bose-Einstein correlations in hadronic Z decay
Phys. Lett. **B540** (2002) 185

[68] Achard, P., *et al.*; S.V. Baldew, G.J. Bobbink, A. Buijs, M. Dierckxsens, M. van Dierendonck, P. Duinker, R. van Gulik, P. de Jong, F.L. Linde, A.J.M. Muijs, J.A. van Dalen, F. Filthaut, R.S. Hakobyan, Y. Hu, W. Kittel, A.C. König, D. Mangeol, W.J. Metzger, B. Petersen, M. Pohl, B. Roux, M.P. Sanders, D.J. Schotanus, C. Timmermans, R.T. Van de Walle, H. Wilkens; L3 Collaboration
Search for neutral Higgs bosons of the minimal supersymmetric standard model in e^+e^- interactions at $\sqrt{s}$ up to 209 GeV
Phys. Lett. **B545** (2002) 30

[69] Achard, P., *et al.*; S.V. Baldew, G.J. Bobbink, A. Buijs, M. Dierckxsens, M. van Dierendonck, P. Duinker, R. van Gulik, P. de Jong, F.L. Linde, A.J.M. Muijs, J.A. van Dalen, F. Filthaut, R.S. Hakobyan, Y. Hu, W. Kittel, A.C. König, D. Mangeol, W.J. Metzger, B. Petersen, M. Pohl, B. Roux, M.P. Sanders, D.J. Schotanus, C. Timmermans, R.T. Van de Walle, H. Wilkens; L3 Collaboration
Measurement of Bose-Einstein Correlations in $e^+e^- \to W^+W^-$ Events at LEP
Phys. Lett. **B547** (2002) 139

[70] Achard, P., *et al.*; S.V. Baldew, G.J. Bobbink, A. Buijs, M. Dierckxsens, M. van Dierendonck, P. Duinker, R. van Gulik, P. de Jong, F.L. Linde, A.J.M. Muijs, J.A. van Dalen, F. Filthaut, R.S. Hakobyan, Y. Hu, W. Kittel, A.C. König, D. Mangeol, W.J. Metzger, B. Petersen, M. Pohl, B. Roux, M.P. Sanders, D.J. Schotanus, C. Timmermans, R.T. Van de Walle, H. Wilkens; L3 Collaboration
Production of Single W Bosons at LEP and Measurement of $WW\gamma$ Gauge Coupling Parameters
Phys. Lett. **B547** (2002) 151

[71] Achard, P., *et al.*; S.V. Baldew, G.J. Bobbink, A. Buijs, M. Dierckxsens, M. van Dierendonck, P. Duinker, R. van Gulik, P. de Jong, F.L. Linde, A.J.M. Muijs, J.A. van Dalen, F. Filthaut, R.S. Hakobyan, Y. Hu, W. Kittel, A.C. König, D. Mangeol, W.J. Metzger, B. Petersen, M. Pohl, B. Roux, M.P. Sanders, D.J. Schotanus, C. Timmermans, R.T. Van de Walle, H. Wilkens; L3 Collaboration
Search for single top production at LEP
Phys. Lett. **B549** (2002) 290

[72] Adriani, O., *et al.*; S.V. Baldew, G.J. Bobbink, A. Buijs, M. Dierckxsens, M. van Dierendonck, P. Duinker, R. van Gulik, P. de Jong, F.L. Linde, A.J.M. Muijs, J.A. van Dalen, F. Filthaut, R.S. Hakobyan, Y. Hu, W. Kittel, A.C. König, D. Mangeol, W.J. Metzger, B. Petersen, M. Pohl, B. Roux, M.P. Sanders, D.J. Schotanus, C. Timmermans, R.T. Van de Walle, H. Wilkens; L3+C Collaboration
The L3+C Detector, A Unique Tool-Set to Study Cosmic Rays
Nucl. Instrum. Meth. **A488** (2002) 209

[73] Metzger, W.J.
New Bose-Einstein Results from L3
Proc. XXXI Int. Symposium on Multiparticle Dynamics (ISMD 2001) Datong, China, eds. Bai Yuting, Yu Mailing and Wu Yuanfang, (World Scientific, Singapore, 2002) p.313

[74] Dalen, J. van
Bose-Einstein Correlations in WW Events at LEP2
Proc. XXXI Int. Symposium on Multiparticle Dynamics (ISMD 2001) Datong, China, eds. Bai Yuting, Yu Mailing and Wu Yuanfang, (World Scientific, Singapore, 2002) p.317

[75] Chen, G.
Measurement of the Scaling Property of the Factorial Moments in Hadronic Z Decays
Proc. XXXI Int. Symposium on Multiparticle Dynamics (ISMD 2001) Datong, China, eds. Bai Yuting, Yu Mailing and Wu Yuanfang, (World Scientific, Singapore, 2002) p.361

Transition Program (AmPS, CHORUS, Medipix)

[76] Ponchut, C., Visschers, J.L., Fornaini, A., Graafsma, H., Maiorino, M., Mettivier, G., Calvet, D.
Evaluation of a photon-counting hybrid pixel detector array with a synchrotron X-ray source
Nucl. Instr. Meth. **A484** (2002) 396-406

[77] Vavrik, D., Jakubek, J., Visschers, J., Pospisil, S., Ponchut, C., Zemankova, J.
First tests of a Medipix-1 pixel detector for X-ray dynamic defectoscopy
Nucl. Instr. Meth. **A487** (2002) 216-223

[78] Bertolucci E., Boerkamp, T., Maiorino, M., Mettivier, G., Montesi, M.C., Russo, P.
Portable system for imaging of alpha, beta, and x-ray sources with silicon pixel detectors and medipix1 readout
IEEE Transactions on Nuclear Science **49** (2002) 1845

[79] Llopart, X., Campbell, M., Dinapoli, R., San Segundo, D., Pernigott I, E.
Medipix2: a 64-k pixel readout chip with 55-um square elements working in single photon counting mode
IEEE Transactions on Nuclear Science **49** (2002) 2279

[80] San Segundo Bello, D., Nauta, B., Visschers, J.
Towards a Single-Photon Energy-Sensitive Pixel Readout Chip: pixel level ADCs and digital readout circuitry

Proc. ProRISC 2002, Veldhoven (ISBN: 90-73461-33-2) p444

[81] Buuren, L.D. van, D.J. Boersma, J.F.J. van den Brand, H.J. Bulten, S. Klous, I. Passchier, H.R. Poolman, M.C. Simani, H. de Vries
Spin-dependent electron proton scattering in the Delta-excitation region
Phys. Rev. Lett. **89** (2002) 012001

[82] Spaltro, C.M., Th.S. Bauer, H.P. Blok, E. Jans, W.J. Kasdorp, L. Lapikas, G.J. Nooren, C.J.G. Onderwater, M. van Sambeek, R. Starink, G. van der Steenhoven, M.A. van Uden, H. de Vries
The ^{3}He(e,e'd)p reaction in (q,ω) constant kinematics
Nucl. Phys. **A706** (2002) 403-417

[83] Misiejuk, A., Z. Papandreou, E. Voutier, Th.S. Bauer, H.P. Blok, D.J. Boersma, H.W. den Bok, E.E.W. Bruins, W.H.A. Hesselink, E. Jans, N. Kalantar-Na-yestanaki, W.-J. Kasdorp, J. Konijn, J.-M. Laget, L. Lapikas, G.J.G. Onderwater, A. Pellegrino, R. Schroevers, C.M. Spaltro, R. Starink, G. van der Steenhoven, J.J.M. Steiger, J.L. Visschers
Electron-induced neutron knockout from ^{4}He
Phys. Rev. Lett. **89** (2002) 172501

[84] Passchier, I., L. D. van Buuren, D. Szczerba, R. Alarcon, Th. S. Bauer, D. J. Boersma, J. F. J. van den Brand, H. J. Bulten, R. Ent, M. Ferro-Luzzi, M. Harvey, P. Heimberg, D. W. Higinbotham, S. Klous, H. Kolster, J. Lang, B. L. Militsyn, D. Nikolenko, G. J. L. Nooren, B. E. Norum, H. R. Poolman, I. Rachek, M. C. Simani, E. Six, H. de Vries, K. Wang, and Z.-L. Zhou
Spin-Momentum Correlations in Quasielastic Electron Scattering from Deuterium
Phys. Rev. Lett. **88** (2002) 10230

[85] Kayis-Topaksu, A. *et al.* ;R. van Dantzig, M. de Jong, O. Melzer, R.G.C. Oldeman, E. Pesen, J.L.Visschers ; CHORUS Collaboration
Measurement of D^0 production in neutrino charged-current interactions
Phys. Lett. **B527** (2002) 173-81

[86] Jong, M. de, R.G.C. Oldeman, C.A.F.J. van der Poel, J.W.E. Uiterwijk; CHORUS Collaboration
The data acquisition system of the CHORUS experiment
Nucl. Instr. Meth. **A479** (2002) 412-438

[87] Penel-Nottaris, E. *et al.* ; J.A. Templon; JLab Hall A Collaboration and E89-044 Collaboration
Bound nucleon properties through ^{3}He(e,e'p) at high Q^2
Nucl. Phys. **A711** (2002) 274c-278c

Theory

[88] Eynck, T.O., E. Laenen, L. Phaf, S. Weinzierl
Comparison of Phase Space Slicing and Dipole Subtraction Methods for $\gamma^* \to Q\bar{Q}$
Eur. Phys. J. **C23** (2002) 259-266

[89] Harris, B.W., E. Laenen, L. Phaf, Z. Sullivan, S. Weinzierl
The fully differential single-top-quark cross section in next-to-leading order QCD
Phys. Rev. **D66** (2002) 054024

[90] Holten, J.W. van
Cosmological Higgs fields
Phys. Rev. Lett. **89** (2002) 201301

[91] Holten, J.W. van
Cosmic scalar fields with flat potential
Mod. Phys. Lett. **A17** (2002) 1383-1392

[92] Holten, J.W. van
Worldine deviations and epicycles
Int. J. Mod. Phys. **A17** (2002), 2764

[93] Huiszoon, L.R., K. Schalm, A.N. Schellekens
Geometry of WZW Orientifolds
Nucl. Phys. **B624** (2002) 219-252

[94] Koch, J.H., V. Pascalutsa, S. Scherer
Hadron structure and the limitations of phenomenological models in electromagnetic reactions
Phys. Rev. **C65** (2002) 045202

[95] Moch, S., J.A.M. Vermaseren, A. Vogt
Non-Singlet Structure Functions at Three Loops: Fermionic Contributions
Nucl. Phys. **B646** (2002) 181-200

[96] Moch, S., J.A.M. Vermaseren
Towards deep-inelastic structure functions at three loops
Acta Phys. Polon. **B33** (2002) 3019-3024

[97] Moch, S., J.A.M. Vermaseren, A. Vogt
Next-to-next-to-leading order QCD corrections to the photon's parton structure
Nucl. Phys. **B621** (2002) 413-458

[98] Thorne, R.S., H. Boettcher, A.M. Cooper-Sarkar, B. Reisert, V. Shekelyan, W.J. Stirling, D.R. Stump, A.Vogt
Questions on Uncertainties in Parton Distributions
J. Phys. **G28** (2002) 2717-2722

[99] Neerven, W. van, and A. Vogt
Parton densities and structure functions at next-to-next-to-leading order and beyond
J. Phys. **G28** (2002) 727

ZEUS

[100] Chekanov, S. *et al.*; C.H. Bokel, J.J. Engelen, S.J.L.A. Grijpink, E.N. Koffeman, P.M. Kooijman, E. Maddox,A. Pellegrino, S.E.S. Schagen, S. Stonjek, H. Tiecke, N. Tuning, J.J. Velthuis, L. Wiggers, E. de Wolf; ZEUS Collaboration
Measurement of high-Q^2 charged current cross sections in e-p deep inelastic scattering at HERA.
Phys. Lett. **B539** (2002) 197

[101] Chekanov, S. *et al.*; C.H. Bokel, J.J. Engelen, S.J.L.A. Grijpink, E.N. Koffeman, P.M. Kooijman, E. Maddox, S.E.S. Schagen, S. Stonjek, H. Tiecke, N. Tuning, J.J. Velthuis, L. Wiggers, E. de Wolf; ZEUS Collaboration
Leading Neutron production in e+p collisions at HERA
Nucl. Phys. **B637** (2002) 3

[102] Chekanov, S. *et al.*; C.H. Bokel, J.J. Engelen, S.J.L.A. Grijpink, E.N. Koffeman, P.M. Kooijman, E. Maddox, S.E.S. Schagen, S. Stonjek, H. Tiecke, N. Tuning, J.J. Velthuis, L. Wiggers, E. de Wolf; ZEUS Collaboration
Measurement of the Q^2 and energy dependence of diffractive interactions at HERA
Europ. Phys. Journal **C25** (2002) 169

[103] Chekanov, S. *et al.*; C.H. Bokel, J.J. Engelen, S.J.L.A. Grijpink, E.N. Koffeman, P.M. Kooijman, E. Maddox, S.E.S. Schagen, S. Stonjek, H. Tiecke, N. Tuning, J.J. Velthuis, L. Wiggers, E. de Wolf; ZEUS Collaboration
Exclusive photoproduction of J/ψ mesons at HERA
Europ. Phys. Journal **C24** (2002) 3,345

[104] Chekanov, S. *et al.*; C.H. Bokel, J.J. Engelen, S.J.L.A. Grijpink, E.N. Koffeman, P.M. Kooijman, E. Maddox, S.E.S. Schagen, H. Tiecke, N. Tuning, J.J. Velthuis, L. Wiggers, E. de Wolf; ZEUS Collaboration
Search for lepton-flavor violation in e+p collisions at HERA
Phys. Rev. **D65** (2002) 092004

[105] Chekanov, S. *et al.*; C.H. Bokel, J.J. Engelen, S.J.L.A. Grijpink, E.N. Koffeman, P.M. Kooijman, E. Maddox, S.E.S. Schagen, H. Tiecke, N. Tuning, J.J. Velthuis, L. Wiggers, E. de Wolf; ZEUS Collaboration
Dijet photoproduction at HERA and the structure of the photon
Europ. Phys. Journal **C23** (2002) 4,615

[106] Chekanov, S. *et al.*; C.H. Bokel, J.J. Engelen, S.J.L.A. Grijpink, E.N. Koffeman, P.M. Kooijman, E. Maddox, S.E.S. Schagen, H. Tiecke, N. Tuning, J.J. Velthuis, L. Wiggers, E. de Wolf; ZEUS Collaboration
High-mass dijet cross sections in photoproduction at HERA
Phys. Lett. **B531** (2002) 9

[107] Chekanov, S. *et al.*; C.H. Bokel, J.J. Engelen, S.J.L.A. Grijpink, E.N. Koffeman, P.M. Kooijman, E. Maddox, S.E.S. Schagen, H. Tiecke, N. Tuning, J.J. Velthuis, L. Wiggers, E. de Wolf; ZEUS Collaboration
Measurement of the photon-proton total cross section at a center-of-mass energy of 209 GeV at HERA
Nucl. Phys. **B627** (2002) 3

[108] Chekanov, S. *et al.*; C.H. Bokel, J.J. Engelen, S.J.L.A. Grijpink, E.N. Koffeman, P.M. Kooijman, E. Maddox, S.E.S. Schagen, H. Tiecke, N. Tuning, J.J. Velthuis, L. Wiggers, E. de Wolf; ZEUS Collaboration
Searches for excited fermions in ep collisions at HERA
Phys. Lett. **B549** (2002) 32

[109] Chekanov, S. *et al.*; C.H. Bokel, J.J. Engelen, S.J.L.A. Grijpink, E.N. Koffeman, P.M. Kooijman, E. Maddox, S.E.S. Schagen, H. Tiecke, N. Tuning, J.J. Velthuis, L. Wiggers, E. de Wolf; ZEUS Collaboration
Dijet production in neutral current deep inelastic scattering at HERA
Europ. Phys. Journal **C23** (2002) 1,13

[110] Chekanov, S. *et al.*; C.H. Bokel, J.J. Engelen, S.J.L.A. Grijpink, E.N. Koffeman, P.M. Kooijman,

E. Maddox, S.E.S. Schagen, H. Tiecke, N. Tuning, J.J. Velthuis, L. Wiggers, E. de Wolf; ZEUS Collaboration
Properties of hadronic final states in diffractive deep inelastic scattering at HERA
Phys. Rev. **D65** (2002) 052001

[111] Grijpink, S.J.L.A.
Measurements of the Charged Current Cross Sections with the ZEUS Detector
Acta Phys. Polonica **B33** (2002) 2891

[112] Schagen, S.
Measurement of charm production in deep inelastic scattering with the ZEUS detector
Proc. 9th Int. workshop on Deep Inelastic Scattering DIS2001, World Scientific (2002)

[113] Velthuis, J.J.
Irradiation tests of the ZEUS vertex detector front end chips, the HELIX128-3.0
Proc. 7th Int. Conf. on ICATPP-7 Villa Olmo, Como, Italy, Oct. 15-19, 2001, World Scientific (2002)

2 PhD Theses

[1] Dalen, J. van
Bose-Einstein Correlations in e^+e^- Events
Universiteit Nijmegen, January 2002

[2] Mangeol, D.J.
Correlations in the Charged-Particle Multiplicity Distribution
Universiteit Nijmegen, January 2002

[3] Buis, E.J.
Detecting R-parity violation in the Atlas inner detector
Universiteit van Amsterdam, April 2002

[4] Vulpen, I. van
Measurement of Z boson pair production and a search for the Higgs boson in e+e- collisions at LEP
Universiteit van Amsterdam, April 2002

[5] Bruinsma, M.
J/ψ in pA - Performance of the First Level Trigger of Hera-B and Nuclear Effects in J/ψ Production
Universiteit Utrecht, May 2002

[6] Boersma, D.
Polarization Observables in ^{3}He(e,e'n) and the neutron electric form factor
Universiteit Utrecht, June 2002

[7] Huiszoon, L.
D-branes and O-planes in string theory
Universiteit Nijmegen, June 2002

[8] Hulsbergen, W.
A Study of Track Reconstruction and Massive Di-electron Production in Hera-B
Universiteit van Amsterdam, July 2002

[9] Eijk, R. van der
Track reconstruction in the LHCb experiment
Universiteit van Amsterdam, September 2002

[10] Visser, J.
Deep inelastic scattering off hydrogen and deuterium
Rijksuniversiteit Groningen, September 2002

[11] Simani, M.C.
Flavor decomposition of the nucleon spin at HERMES
Vrije Universiteit Amsterdam, October 2002

[12] Woudstra, M.J.
Precision of the ATLAS muon spectrometer
Universiteit van Amsterdam, December 2002

3 Invited Talks

ALICE

[1] P.G. Kuijer
The ALICE experiment at the CERN LHC
ICHEP 2002 Amsterdam, July 27, 2002

[2] A.P. de Haas *et al.*
Aluminium microcable technology for the Alice silicon strip detector: a status report
8th Workshop on electronics for LHC experiments, Colmar, France, 9-13 Sept., 2002

[3] N.J.A.M. van Eijndhoven
Probing the Universe by means of Cosmic Rays
General colloquium, ASTRON, Dwingeloo, May 31, 2002

[4] N.J.A.M. van Eijndhoven
Relativistic Kinematics. Invited lectures on Particle Astrophysics
University of Cape Town, South Africa, August 2002

[5] N.J.A.M. van Eijndhoven
(Astro)Physics Aspects of Heavy-Ion Collisions
Invited lectures on Particle Astrophysics, University of Cape Town, South Africa, August 2002

[6] N.J.A.M. van Eijndhoven
Photons and Neutrinos : Messengers from Outer Space
Invited lectures on Particle Astrophysics, University of Cape Town, South Africa, August 2002

[7] N.J.A.M. van Eijndhoven
The Universe : Our Ultimate Laboratory
General physics colloquium, University of Cape Town, South Africa, August 2002

[8] P.G. Kuijer
The Quark-Gluon Plasma, an experimental view
Lecture at the Nuclear Physics department of Kiev university, Kiev Ukraine, May 2002

ANTARES

[9] J.J. Engelen
ANTARES: Een Detector voor Kosmische Neutrino's
Natuurkundige Voordrachten, Reeks 80, Koninklijke Maatschappij voor Natuurkunde (Diligentia), 2002

ATLAS

[10] M. Barisonzi; Boterenbrood, H ; Jansweijer, P ; Kieft, G ;Vermeulen, J ; König, A ; Wijnen, T ;
The MROD : the read out driver for the ATLAS MDT muon precision chambers
8th Workshop on Electronics for LHC Experiments, Colmar, France, September 9-13, 2002

B Physics

[11] N. van Bakel
Characterisation of a radiation hard front-end chip for LHCb at CERN
4th IWORID, Amsterdam, September 8-12, 2002

[12] M. Mevius
First results from HERA-B on charmonium and b quark production in pN collisions at $\sqrt{(s)}$=42.6 GeV
5th Int. Conf. on Hyperons, Charm and Beauty Hadrons, Vancouver, Canada, June 25-29, 2002

[13] Th. S. Bauer
Production of J/ψ, χ_c, and B-mesons at Hera-B
Charm Production: from Threshold via SPS to RHIC and LHC , Trento, Italy June 17-22, 2002

[14] M. Merk
Prospects of B Physics at LHC
Hadron Collider Physics 2002 Conference, Karlsruhe, October 2, 2002

[15] M. van Beuzekom, W. Vink and L.W. Wiggers
Pile-Up Veto L0 Trigger System for LHCb using large FPGA's
8th Workshop on Electronics for LHC Experiments, Colmar, September 2002

[16] T. Ketel *et al.*
Measuring the linear polarization of gammas in 20-GeV to 170-GeV range
16th Int. Conf. on Particles and Nuclei (PANIC 02), Osaka, Japan, September 30-October 4, 2002

[17] N. van Bakel, M. van Beuzekom, E. Jans, S. Klous, H. Verkooijen *et al.*
Performance of the Beetle Readout Chip for LHCb
8th Workshop on Electronics for LHCb Experiments Colmar, September 9-13, 2002

[18] T. Ketel
Beam tests with prototype vertex detectors for LHCb
Florence, March 15, 2002

[19] J.F.J van den Brand
Materie, antimaterie en Big Bang
Publiekslezing, Open Dag, Amsterdam, October 20, 2002

[20] G. Raven
CP violation: observing matter-antimatter asymmetries
Meeting of the Dutch Physical Society, Lunteren, October 2002

[21] H. Snoek
A front-end chip for the LHCb vertex locator: pulse shapes and signal over noise ratios
Meeting of the Dutch Physical Society, Lunteren, October 2002

[22] H. Wahlberg
Physics Results and Prospects from HERA-B
Meeting of the Dutch Physical Society, Lunteren, October 2002

[23] A. Sbrizzi
The HERA-B first level trigger
Meeting of the Dutch Physical Society, Lunteren, October 2002

[24] M. Zupan
The Pile-up Veto detector for LHCb
Meeting of the Dutch Physical Society, Lunteren, October 2002

[25] B. Hommels
Triggering with Outer Tracker stations in LHCb
Meeting of the Dutch Physical Society, Lunteren, October 2002

DATAGRID

[26] D. Groep
Security in the European Data Grid
TERENA Grid-AN BoF, March 2002

[27] D. Groep
Grid Computing: from a solid past to a bright future?
Oracle Nederland BV, August 2002

[28] J. Templon
Grids: How, Why, and What Next?
ESA Grid Workshop 2002, October 25, 2002, ESA ESTEC, Noordwijk, The Netherlands

[29] D. Groep
DutchGrid
NG4-NLHC6 meeting, Uppsala, November 2002

HERMES

[30] E. Garutti
HERMES results on nuclear effects in DIS
Workshop on Low x Physics, Antwerp, Belgium, Sept. 16-19, 2002

[31] G. van der Steenhoven
Polarized structure functions
Int. Conf. on the Structure of Baryons, Jefferson Lab., Newport News, Virginia, March 3-8, 2002

[32] G. van der Steenhoven
Concluding remarks on the QCD-N'02 workshop
European Workshop on the QCD Structure of the Nucleon (QCD-N'02), Ferrara, April 3-6, 2002

[33] G. van der Steenhoven
The (spin) structure of the nucleon
Int. Conf. on quark-nuclear physics, (QNP02), Juelich, June 9-14, 2002

[34] B. Zihlmann
Nuclear Effects in Deep Inelastic Scattering
Gordon Conf. on Photonuclear Reactions, Tilton, New Hampshire, August 18-23, 2002

[35] M. van Beuzekom
The HERMES Silicon project - the radiation protection system
9th European Symposium on Semi-Conductor Detectors, New Developments on Radiation Detectors, Schloss Elmau, June 23-27, 2002

[36] M. van Beuzekom
Recoil Detection at Future QCD Facilities
6th Int. Conf. on Position Sensitive Detectors, University of Leicester, Leicester, UK, September 9-13, 2002

[37] E. Garutti
Hadron Formation in Nuclei in Deep Inelastic Lepton Scattering
Int. Conf. on the Structure of Baryons, Jefferson Lab., Newport News, Virginia, March 3-8, 2002

[38] E. Garutti
Hadron Formation in Nuclei in DIS
Int. Workshop on Deep Inelastic Scattering (DIS2002), Cracow, Poland, April 30-May 4, 2002

[39] A.J. Reischl
Beam Loss Monitor: a protection system for the new silicon tracker in HERMES
Meeting of the the Dutch Physics Society, Lunteren, The Netherlands, October 25, 2002

[40] M.C. Simani
Recent results on the helicity structure of the nucleon from HERMES
Int. Workshop on Deep Inelastic Scattering (DIS2002), Cracow, Poland, April 30-May 4, 2002

[41] G. van der Steenhoven,
Nuclear effects in deep-inelastic scattering
University of Giessen, Germany, January 17, 2002

[42] V. Tvaskis
Nuclear Dependence of $R = \sigma_L/\sigma_T$ at low Q^2
Meeting of the the Dutch Physics Society, Lunteren, The Netherlands, October 25, 2002

LEP-DELPHI

[43] M. Blom
Single W measurement at DELPHI
Meeting of the American Physical Society, Albuquerque, New Mexico, April 2002

[44] P. Kluit
B_s mixing at LEP/SLD/CDF-1
Workshop on the CKM Unitarity Triangle, CERN, Geneva, February 2002

[45] I. van Vulpen
On-shell Z boson pair production at DELPHI
Lake Louise Winter Institute on Fundamental Interactions, Lake Louise, Canada, February 2002

[46] J. Timmermans
R&D for a Linear Collider TPC at NIKHEF
ECFA-DESY LC Workshop, Prague, November 2002

LEP-L3

[47] A.J.M. Muijs
Fermion Pair Production and New Physics Interpretations of LEP Precision Measurements
Lake Louise Winter Conference, Lake Louise, Canada, February 17–23, 2002

[48] M. Dierckxsens
Final state interactions, QCD effects in WW→4q events
Rencontres de Moriond, Les Arcs, France, March 9-16, 2002

[49] J. van Dalen
Update of the L3 BE results, using MCs based on new tuning
LEP WW Workshop, CERN, Geneva, Switzerland, April 19, 2002

[50] Š. Todorova-Nová
Bose-Einstein correlations in $e^+e^- \rightarrow$WW events at LEP
Xth Int. Workshop on Multiparticle Production, Crete, Greece, June 8-15, 2002

[51] Š. Todorova-Nová
Experimental evidence in favour of internal structure of the Lund string
Xth Int. Workshop on Multiparticle Production, Crete, Greece, June 8-15, 2002

[52] Š. Todorova-Nová
Bose-Einstein correlation at LEP and HERA
ICHEP 2002, Amsterdam, The Netherlands, July 25, 2002

[53] W.J. Metzger
Oscillating H_q, Intermittency Indices, and QCD
XXXII Int. Symposium on Multiparticle Dynamics, Alushta (the Crimea), Ukraine, September 11, 2002

[54] W.J. Metzger
Color Reconnection and Bose-Einstein Effects in W^+W^- Events from L3 at CERN
Colloquium, IOPP, Wuhan, China, October 4, 2002

[55] W.J. Metzger
Color Reconnection and Bose-Einstein Effects in W^+W^- Events from L3 at CERN
Colloquium, IHEP, Beijing, China, October 11, 2002

[56] H. Wilkens
Electron and Muon Densities from Extensive Air Showers Measured at L3+C
NIKHEF Annual Scientific Meeting, December 18, 2002

Transition Program (AmPS, CHORUS, Medipix)

[57] D. Vavrik
X-ray Dynamic Defectoscopy
14th European Conf. of Fracture, Cracow, Poland, September 9-13

[58] A. Fornaini
A multi-chip board for X-ray imaging in build-up technology
IWORID-2002 workshop, Amsterdam, September 9, 2002

[59] D. San Segundo Bello
Design of an interface board for the control and DAQ of the Medipix2 chip
IWORID-2002 workshop, Amsterdam, September 9, 2002

[60] E. Heijne
Semiconductor Detectors in the Low Countries
IWORID-2002 workshop, Amsterdam, September 8, 2002

[61] H.J. Bulten
Few-body systems studied with internal targets in the NIKHEF electron storage ring
Nuclear Physics Spring Meeting DPG, NNV, BNV/SBP, Muenster, March 11-15, 2002

[62] H.P. Blok *et al.*
The Pion Form-Factor
Exclusive Processes at High Momentum Transfer, Newport News, Virginia, May 15-18, 2002

[63] P. Barneo
Investigation of the 3He(e,e'pn) reaction
Nuclear Physics Spring Meeting DPG, NNV, BNV/SBP, Muenster, March 11-15, 2002

Theory

[64] A. Vogt
Mellin Moment Techniques for Parton Distribution Analyses
Workshop on Advanced Statistical Techniques in Particle Physics, Durham, March 2002

[65] F. Riccioni
Low-energy couplings for brane supersymmetry breaking
XIV Workshop Beyond the Standard Model, Bad Honnef, March 11, 2002

[66] F. Riccioni
Considerations about non-perturbative type-I strings
Rijksuniversiteit Groningen, November 11, 2002

[67] J. van der Heide
Pion Form Factor in Non-Perturbative QCD
DRSTP AiO School Theoretical Physics, Jonkerbosch (Nijmegen), January 2002

[68] J. van der Heide
Pion From Factor in Lattice QCD
NNV Meeting, Lunteren, October 2002

[69] J.W. van Holten
Inflation and Quintessence
Universiteit Nijmegen, January 18, 2002

[70] J.W. van Holten
Inflation and Quintessence
NIKHEF, February 8, 2002

[71] J.W. van Holten
Inflation and Quintessence
Universiteit Utrecht, May 15, 2002

[72] J.W. van Holten
Inflation and Quintessence
RWTH Aachen, November 28, 2002

[73] E. Laenen
The Standard Model and the Strong Force
Universiteit Nijmegen. February 2002

[74] E. Laenen
ICHEP Summary
University of Iceland, Reykjavik, December 2002

[75] A. Vogt
Higher-order QCD effects in parton densities and structure functions
Karlsruhe University, May 2002

[76] A. Vogt
DIS at three loops
NIKHEF Annual Scientific Meeting, December 2002

[77] J.H. Koch
Meson structure from lattice QCD
NIKHEF Annual Scientific Meeting, December 2002

[78] A.N. Schellekens
An unoriented trip to the edge of string theory
Ehrenfest Colloquium, Leiden, January 30, 2002

[79] A.N. Schellekens
String Theory – Van Leidsche Flesch tot Kleinse Fles
Symposium "De Leidsche Flesch", March 19, 2002

[80] A.N. Schellekens
Meromorphic c=24 conformal field theory
Wiskunde colloquium, Universiteit Nijmegen, April 2002

[81] A.N. Schellekens
The geometry of WZW orientifolds
Seminarium, Universidad Autonoma (Madrid), May 2002

[82] A.N. Schellekens
The geometry of WZW orientifolds
Seminarium, LPTHE, Jussieu (Parijs), June 2002

[83] L. Huiszoon
D-branes and O-planes in WZW models
Seminarium, KUL, Leuven, March 2002

[84] F. Riccioni
Low-energy analysis of non-supersymmetric strings
Rijksuniversiteit Groningen, January 18, 2002

[85] F. Riccioni
Considerations about non-perturbative type-I strings
Rijksuniversiteit Groningen, Nov. 11, 2002

[86] N. Marques de Sousa
The Bosonic String: introduction and developments
University of Coimbra, November 21, 2002

[87] N. Marques de Sousa
Introduction to the Bosonic String (3 lectures)
University of Porto, December 2-4, 2002

[88] N. Marques de Sousa
Principles of String Theory
University of Porto, November 29, 2002

[89] J.W. van Holten
Topical lectures on Supersymmetry at the LHC
NIKHEF, March 26-28, 2002

[90] E. Laenen
Topical lectures on QCD
NIKHEF, December 16-17, 2002

[91] E. Laenen
Lecture on Resummation in QCD
DRTSP AIO School Theoretical Physics, Jonkerbosch (Nijmegen), January 2002

[92] E. Laenen
Inzicht in de subatomaire quantumwereld
Oratie, Universiteit Utrecht, November 2002

ZEUS

[93] E. Tassi
ZEUS NLO QCD fits
10th Int. workshop on Deep Inelastic Scattering DIS2002, Cracow, April 3-May 4, 2002

[94] S.J.L.A. Grijpink
Measurements of the Charged Current Cross Sections with the ZEUS Detector
10th Int. workshop on Deep Inelastic Scattering DIS2002, Cracow, April 3-May 4, 2002

[95] J.J. Engelen,
QCD: HERA and more
A series of lectures given at the NATO Advanced Study Institute, St. Croix, Virgin Islands, June 2002

4 Seminars at NIKHEF

[1] January 11, 2002, Amsterdam
Dr. David Wark
Results from the Sudbury Neutrino Observatory

[2] January 17, 2002, Amsterdam
Dr. J. Bahcall
NIKHEF+CHEAF: Solar Neutrinos - An Overview

[3] January 25, 2002, Amsterdam
Prof. Dr. K. Jungmann
Low-energy searches for physics beyond the Standard Model using atoms and muons

[4] February 8, 2002, Amsterdam
J.W. van Holten
Inflation and quintessence

[5] February 15, 2002, Amsterdam
Simon Hands
Modelling Quark Superconductivity

[6] February 22, 2002, Amsterdam
H. Paar
Experimental Investigation into the Two-Photon Width of Charmonium

[7] March 1, 2002, Amsterdam
Dr. James Gillies
How the Web Was Born

[8] March 15, 2002, Amsterdam
Neil Turok
The Ekpyrotic Universe and its cyclic extension

[9] March 22, 2002, Amsterdam
Thorsten Ohl
Monte Carlo Event Generation for Future (and Present) Colliders

[10] April 5, 2002, Amsterdam
A. de Rujula
Gamma Ray Bursts

[11] April 16, 2002, Amsterdam
Einan Gardi
Soft and collinear radiation and factorization in perturbation theory and beyond.

[12] April 19, 2002, Amsterdam
Leif Lonnblad
The future of Event Generation

[13] April 26, 2002, Amsterdam
Fernando Quevedo
Phenomenological Aspects of D-branes

[14] May 3, 2002, Amsterdam
Charles Timmermans
The Nijmegen NAHSA and LOFAR projects

[15] May 17, 2002, Amsterdam
Francis Farley
The 45 years of muon g-2

[16] May 24, 2002, Amsterdam
Herman ten Kate
Large Scale Superconducting Magnets for Physics Research, LHC, ATLAS and ITER

[17] June 7, 2002, Amsterdam
Stefan Kluth
Soft and hard QCD tests with e^+e^- Annihilation data

[18] June 21, 2002, Amsterdam
E Tassi
Summary of DIS2002

[19] June 28, 2002, Amsterdam
R. Snellings
Heavy-ion physics at RHIC

[20] July 23, 2002, Amsterdam
Dr. J. Huston
A Potpourri of Physics

[21] September 6, 2002, Amsterdam
Hans Chang
FOM: Accenten voor 2002/2003

[22] September 17, 2002, Amsterdam
M. Nozar
The JLAB program - with emphasis on meson spectroscopy

[23] September 20, 2002, Amsterdam
G. Giudice
Extra Dimensions and Quantum Gravity at the LHC

[24] September 27, 2002, Amsterdam
D. Ryckbosch
Physics at Hermes: Present and Future

[25] October 4, 2002, Amsterdam
Renate Loll (Utrecht)
Space-time from nothing

[26] October 9, 2002, Amsterdam
N. Hari Dass
How to get sensible scalars

[27] October 10, 2002, Amsterdam
Lorenzo Magnea
String techniques for the computation of scattering amplitudes in field theory

[28] October 11, 2002, Amsterdam
Cinzia da Via
Advances in semiconductor detectors for particle tracking in extreme radiation environments

[29] October 18, 2002, Amsterdam
Dirk Peter van der Werf
Status of Athena and Low-Energy Anti-Proton Physics at CERN

[30] November 1, 2002, Amsterdam
Fons Rademakers
AliRoot – the ALICE simulation and reconstruction framework

[31] November 15, 2002, Amsterdam
Rene Laureijs
The Planck mission: scientific objectives and technical capabilities

[32] November 22, 2002, Amsterdam
H.V. Klapdor-Kleingrothaus
First evidence for neutrinoless double beta decay – and implications

[33] November 29, 2002, Amsterdam
Ignatios Antoniadis
Testing string theory in accelerators?

[34] December 6, 2002, Amsterdam
Prof. R.H. Sanders
Modified Newtonian dynamics as an alternative to dark matter.

[35] December 13, 2002, Amsterdam
Prof. Dr. Wim de Boer
Unification scale physics

5 NIKHEF Annual Scientific Meeting, December 18-19, 2002, Amsterdam

[1] W. Metzger
Status of Delphi and L3

[2] H. Wilkens
Electron and Muon Densities from Extensive Air Showers Measured at L3+C

[3] M. de Jong
Antares Status Report

[4] B. van Rens
First Test Results from Antares

[5] J. Koch
Meson Structure from Lattice QCD

[6] A. Vogt
Deep-inelastic Scattering at Three Loops

[7] P. Kooijman
Startup of HERA II

[8] E. Maddox
First ep-Collisions Analysed with Vertex Detector

[9] J. van den Brand
Status of LHCb

[10] J. van Tilburg
Tracking and Physics Studies

[11] M. van Beuzekom
LHCb Vertex Detector and Beetle Chip

[12] M. Ouchrif
HERA-B Results

[13] G. de Rijk (CERN)
The LHC Magnets Project

[14] F. Linde
The Making of Atlas and CMS

[15] G. van der Steenhoven
Status of Hermes

[16] B. Zihlmann
DIS on Nuclear Targets

[17] K. Bos
Grid Demonstration

[18] A. Naumann
Status D0

[19] F. Blekman
Top Physics

[20] N. Hessey
Status Atlas and Silicon Tracker

[21] M. Woudstra
The Atlas Muon Spectrometer

[22] R. Snellings
Results from STAR

[23] T. Peitzmann
Status of the Alice Project

[24] E. Schillings
Lambda Polarization in Heavy Ion Collisions

[25] J. Engelen
Reflections of the Director

F Resources and Personnel

1 Resources

In 2002 the NIKHEF income was 18.9 million Euro. The budget figures of the NIKHEF partners were: FOM-institute 12.4 M Euro, universities 4.2 M Euro of which 1.3 M Euro through the FOM working groups. In addition, third parties contributed 2.3 M Euro to the NIKHEF income. Expenses for the largest program, Atlas, consumed almost 30% of the total budget. Capital investments in 2002 (2.9 M Euro) were allocated for Antares, Atlas, Alice and LHCb.

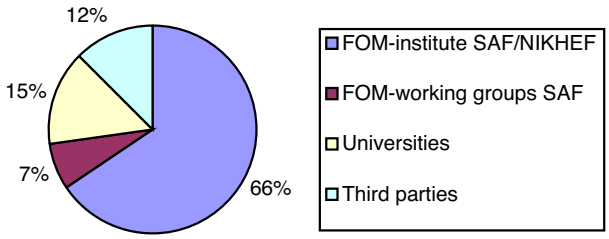

Figure 1.1: *Income 2002: 18.9 M Euro*

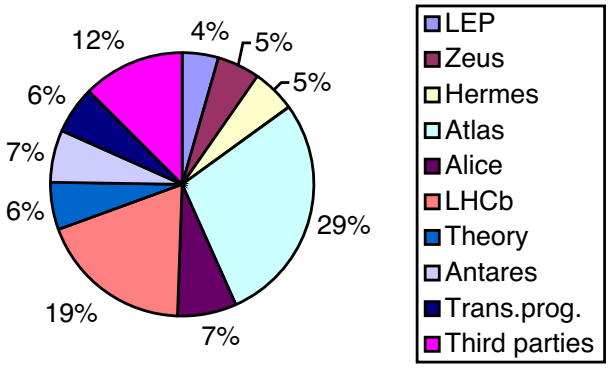

Figure 1.2: *Expenses 2002: 18.9 M Euro*

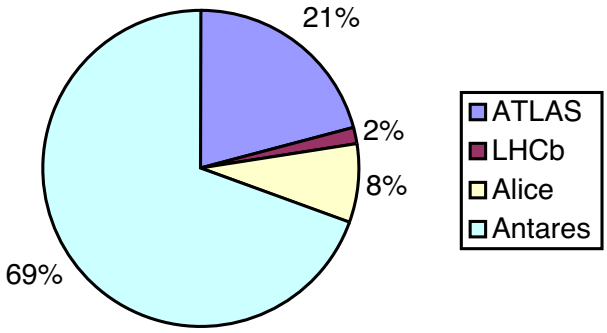

Figure 1.3: *Capital Investments 2002: 2.9 M Euro*

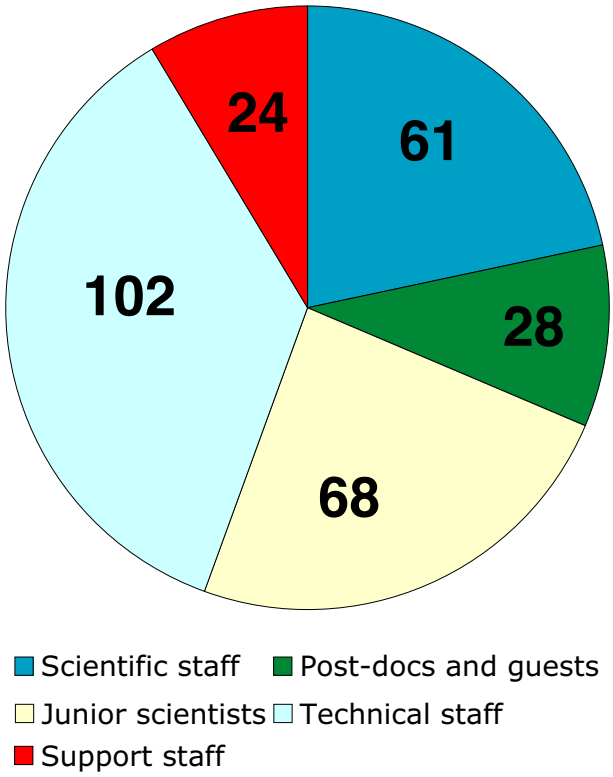

Figure 1.4: *NIKHEF personnel as of December 31, 2002.*

2 Membership of Councils and Committees during 2002

In 2002 NIKHEF staff members have acted as (anonymous) referees for the journals Classical and Quantum Gravity, European Physical Journal A, European Journal of Physics, IEEE Trans. Nucl. Science, Journ. High Energy Physics, J. Phys. G, Nature, Phys Letters B, Phys. Rev. C, Phys. Rev. D, Phys. Rev. Letters, Nucl. Phys. A, Nucl. Phys. B, Nucl. Instr. A and Rev. Mod. Physics. In total 102 papers were reviewed. In addition 23 proposals were reviewed for the funding agencies US National Science Foundation, South African Nat. Res. Foundation, Fonds voor Wet. Onderzoek Vlaanderen, FOM-VICI commissie, Deutsche Forschungs Gemeinschaft, Fonds National Suisse and EU ISTIC program.

NIKHEF Board

S. Groenewegen (VU, chair)
F.T.M. Nieuwstadt (FOM)
K.H. Chang (FOM)
P. van der Heijden (UvA)
S.E. Wendelaar Bonga (KUN)
J.G.F. Veldhuis (UU)
H.G. van Vuren (secretary, FOM)

Scientific Advisory Committee NIKHEF

G. Goggi (Pavia)
K. Pretzl (Bern)
G. Ross (Univ. Oxford)
M. Spiro (IN2P3)
J. Stachel (Univ. Heidelberg)
J. Dainton (Univ. Liverpool)

NIKHEF Works Council

P. de Jong (chairman)
M. Vreeswijk (2nd chairman)
R. Hart (1st secretary)
J. Hogenbirk (2nd secretary)
A. Boucher
J. Dokter
E. van Kerkhoff
R. Kluit
S. Schagen
H. Schuijlenburg
J. Velthuis

Wetenschappelijke Advies Raad NIKHEF

J.W. van Holten (chairman)
P. de Jong (observer from works council)
M. de Jong
F. Linde
K.J.F Gaemers
G. van der Steenhoven
S. de Jong
A.J. van Rijn
J.J. Engelen
R. Snellings
J.F.J. van den Brand
W. Hoogland

FOM Board

S.J. de Jong

Raad voor de Natuur- en Sterrenkunde

J.J. Engelen

Contactcommissie in CERN aangelegenheden

J.J. Engelen
R. Kamermans
F. Linde (secretary)
G. van Middelkoop
S.J. de Jong
further members are :
J. Bezemer
G. 't Hooft
W. Hoogland
J. Panman
G. de Rijk
H. van Vuuren
H. Weijma
B.Q.P.J. de Wit

Stichting voor de Hoge-energiefysica

J.J. Engelen (chairman)
A. van Rijn (treasurer)
R. Kleiss (secretary)
further members are:
J. Langelaar
K.J.F. Gaemers
W. Hoogland
B.Q.P.J. de Wit

Stichting beta-plus

J.J. Engelen (chairman)
further members are:
W. Wadman
H. Hooghiemstra
J. Walraven
R. Zsom

A. Smeulders
E. Sennema

NNV Sectie H

K.J.F. Gaemers
E. Koffeman

Restricted ECFA

J.J. Engelen

ECFA

J.J. Engelen
K.J.F. Gaemers
R. Kamermans
E.W. Kittel
G. van Middelkoop

Linear Collider Steering Group in Organisational Matters

J.J. Engelen

Extended Scientific Council DESY

J.J. Engelen

Astroparticle Physics European Coordination (ApPEC) Steering Committee

J.J. Engelen (dep. chairman)

INFN Comitato di Valutatione Interna

J.J. Engelen

OECD Global Science Forum's Consultative Group on High Energy Physics

J.J. Engelen

LHCC-CERN

H. Tiecke

SPSC-CERN

M. de Jong

NuPECC

G. van Middelkoop (until Dec. 2002)
G. van der Steenhoven (from Dec. 2002)

EPAC Organizing Committee and EPAC Scientific Committee

G. Luijckx

Beleidsadvies college KVI

G. Luijckx
P.J.G. Mulders

Wetenschappelijke Adviescommissie (WAC) KVI

G. van der Steenhoven

Physical Review Letters

G. van der Steenhoven (Divisional Associate Editor)

Nuclear Physics News International

G. van der Steenhoven (correspondent)

Scientific Committee Frascati Laboratory

G. van Middelkoop

Scientific Council JINR, Dubna

G. van Middelkoop

Scientific Advisory Committee, Physique Nucleaire, Orsay

P.K.A. de Witt Huberts

Scientific Advisory Committee DFG Hadronen Physik

J.H. Koch
P.K.A. de Witt Huberts

Program Advisory Committee, ELSA (Bonn)/MAMI (Mainz)

H.P. Blok

Program Advisory Committee, Jefferson Laboratory

H.P. Blok

NNV Board

E.W.A. Lingeman
J. Konijn
P.J.G. Mulders

Peer Review Committee of the Astro Particle Physics European Coordination

M. de Jong

Stichting Physica Board

G. van der Steenhoven (from April 2002)
J. Konijn

Stichting Conferenties en Zomerscholen over de Kernfysica

G. van der Steenhoven
J. Konijn
G. van Middelkoop
P.J.G. Mulders

ICHEP2002, local organizing committee

G. van Middelkoop (chairman)
G. van der Steenhoven (treasurer)
J.H. Koch
E. Laenen
P. de Jong
F. Linde
S. Bentvelsen
E. Koffeman

Int. Panel Antrag Sonderforschungsbereich Gravitationswellenastronomie DFG Transregio 6020

J.W. van Holten

High Energy Physics Computing Coordination Committee (HEPCCC)

A.J. van Rijn

Kuratorium Institut für Hochenergiephysik der Oesterr. Akademie der Wissenschaften

E.W. Kittel

FOM Springplankcommissie

J.F.J. van den Brand

Advisory Comittee of CERN Users (ACCU)

M. Merk

European Data Grid Project Architecture Task Force

J.A. Templon

Gebiedsbestuur Exacte Wetenschappen NWO

R. Kamermans

Standing Committee for Physical and Engineering Sciences of the European Science Foundation

R. Kamermans

Editorial Board Nuclear Physics A

P.J.G. Mulders

Laboratory correspondent CERN COURIER

P.J.G. Mulders

Other committees

CERN/LCG RTAG: J.A. Templon
CERN, Task Force 2: G. van Middelkoop
ECOS-exact, KNAW: G. van Middelkoop
HTASC: E. de Wolf
IWORID Scientific Committee: J.L. Visschers
IWORID-2002: J.L. Visschers (chairman local organizing committee)
IEEE-Nuclear Science Symposium Program Committee: J.L. Visschers
Medipix2: J.L. Visschers (deputy spokesperson)
IdePhix Consortium: J.L. Visschers (work-package manager for WP8)
WCW Board: A.J. van Rijn
Steering group Development Science park Amsterdam: A.J. van Rijn
CERN/LCG Grid Deployment Board: K. Bos
European DataGrid Project, Project Management Board: K. Bos
European DataGrid Project, Project Technical Board: K. Bos
HENP InterGrid Collaboration Board: K. Bos

3 Personnel as of December 31, 2002

1. Experimental Physicists

Akker, Drs. M. van den	KUN	L-3
Apeldoorn, Dr. G.W. van	UVA	B-Phys.
Baak, Drs. M.	VU	B-Phys.
Bakel, Drs. N.A. van	FOM	B-Phys.
Baldew, Drs. S.V.	UVA	L-3
Balm, Drs. P.W.	FOM	ATLAS
Barisonzi, Drs. M.	UT	ATLAS
Barneo González, Drs. P.J.	FOM	Other Projects
Bauer, Dr. T.S.	FOM-UU	B-Phys.
Bentvelsen, Dr. S.C.M.	FOM	ATLAS
Blekman, Drs.Mw. F.	FOM	ATLAS
Blok, Dr. H.P.	VU	HERMES.
Blom, Drs. H.M.	FOM	DELPHI
Bobbink, Dr. G.J.	FOM	L-3
Boer, Dr. F.W.N. de	GST	Other Projects
Bos, Dr. K.	FOM	ATLAS
Botje, Dr. M.A.J.	FOM	ALICE
Bouhali, Dr. O.	GST	HERMES
Bouwhuis, Drs. Mw. M.C.	FOM	ANTARES
Brand, Prof. Dr. J.F.J. van den	VU	Other Projects
Bruinsma, Ir. P.J.T.	GST	ANTARES
Bulten, Dr. H.J.	FOM-VU	B-Phys.
Buuren, Drs. L.D. van	GST	Other Projects
Cornelissen, Drs. T.G.	FOM	ATLAS
Crijns, Dipl.Phys.F.J.G.H.	FOM-KUN	ATLAS
Dalen, Drs. J. van	FOM-KUN	L-3
Dam, Dr. P.H.A. van	UVA	DELPHI
Dantzig, Dr. R. van	GST	Other Projects
Demey, Drs. M.	FOM	HERMES
Diddens, Prof.Dr. A.N.	GST	DELPHI
Dierckxsens, Drs. M.E.T.	FOM	L-3
Djordevic, Drs. M.	KUN	Other Projects
Duensing, Drs. Mw. S.	KUN	ATLAS
Duinker, Prof. Dr. P.	GST	L-3
Eijk, Prof. Dr. B. van	FOM	ATLAS
Eldik, Drs. J.E. van	GST	DELPHI
Eldik, Dipl. Phys. N. van	FOM	ATLAS
Engelbertink, Dr., G.A.P.	FOM	Other Projects
Engelen, Prof. Dr. J.J.	UVA	DIR
Eyndhoven, Dr. N. van	FOM-UU	Other Projects
Ferreira Montenegro, Drs. Mw. J.	FOM	DELPHI
Filthaut, Dr. F.	KUN	ATLAS
Fornaini, Drs. A.	FOM	ATLAS
Galea, Drs. Mw. C.F.	FOM	ATLAS
Garutti, Drs. Mw. E.	FOM	HERMES
Gorfine, Dr. G.	FOM	ATLAS
Graaf, Dr. Ir. H. van der	FOM	ATLAS
Grijpink, Drs. S.J.L.A.	FOM	ZEUS
Groep, Dr. D.L.	FOM	Other Projects
Hartjes, Dr. F.G.	FOM	ATLAS
Heesbeen, Drs. D.	GST	HERMES
Heijboer, Drs. A.J.	UVA	ANTARES
Hesselink, Dr. W.H.A.	VU	HERMES
Hessey, Dr. N.P.	FOM	ATLAS
Hierck, Drs. R.H.	FOM-VU	B-Phys.
Hommels, Ir. L.B.A.	FOM	B-Phys.
Hunen, Dr. J.J. van	FOM	B-Phys.
Jans, Dr. E.	FOM	AmPS-Phys.
Jong, Dr. M. de	FOM	ANTARES
Jong, Dr. P.J.	FOM	ATLAS
Jong, Prof. Dr. S.J.	KUN	ATLAS
Kamermans, Prof. Dr. R.	FOM-UU	ALICE
Ketel, Dr. T.J.	FOM-VU	B-Phys.
Kittel, Prof. Dr. E.W.	KUN	L-3
Klok, Drs. P.F.	FOM-KUN	ATLAS
Klous, Drs. S.	FOM-VU	B-Phys.
Kluit, Dr. P.M.	FOM	ATLAS
Koffeman, Dr. Ir. Mw. E.N.	FOM	ZEUS
König, Dr. A.C.	KUN	ATLAS
Konijn, Dr. Ir. J.	GST	Other Projects
Kooijman, Prof. Dr. P.M.	UVA	ZEUS
Kuijer, Dr. P.G.	FOM	ALICE
Laan, Dr. J.B. van der	FOM	Other Projects
Lapikás, Dr. L.	FOM	HERMES
Lavrijsen, Drs. W.T.L.P.	FOM-KUN	ATLAS
Laziev, Drs. A.E.	FOM-VU	HERMES
Leeuwen, Drs. M. van	FOM	ALICE
Linde, Prof. Dr. F.L.	UVA	ATLAS
Luijckx, Ir. G.	FOM	ATLAS
Maas, Dr. R.	FOM	Other Projects
Maddox, Drs. E.	UVA	ZEUS
Massaro, Dr. G.G.G.	FOM	ATLAS
Merk, Dr. M.H.M.	FOM	B-Phys.
Metzger, Dr. W.J.	KUN	L-3
Mevius, Drs. Mw. M.	FOM-UU	B-Phys.
Mexner, Drs. Mw. I.V.	FOM-BR	HERMES
Middelkoop, Prof. Dr. G. van	GST	Other Projects
Muijs, Dr. Mw. A.J.M.	FOM	ATLAS
Nat, Drs. P.B.	FOM	HERMES
Naumann, Drs. A.	FOM	ATLAS
Nooren, Dr. Ir. G.J.L.	FOM-UU	ALICE
Novak, Drs. T.	KUN	L-3
Ouchrif, Dr. M.	FOM	B-Phys.
Peeters, Ir. S.J.M.	FOM	ATLAS
Peitzmann, Prof. Dr. T.	UU	ALICE
Pellegrino, Dr. A.	FOM	B-Phys
Peters, Drs. O.	UVA	ATLAS
Phaf, Drs. L.K.	FOM	ATLAS
Pijll, Drs. E.C. van der	FOM-UU	Other Projects
Pohl, Prof. Dr. M.	KUN	Other Projects
Putte, Dr. Ir. M.J.J. van den	FOM	Other Projects
Raven, Dr. H.G.	VU	B-Phys.
Reischl, Drs. A.J.	FOM	HERMES
Rens, Drs. B.A.P. van	FOM	ANTARES
Rijke, Drs. P. de	FOM-UU	ALICE
San Segundo Bello, Drs. D.	FOM-HCM	Other Projects
Sbrizzi, Drs. A.	FOM	B-Phys.
Schagen, Drs. S.E.S.	FOM	ZEUS
Schillings, Drs. E.	FOM-UU	ALICE
Scholte, Ir. R.C.	UT	ATLAS
Schotanus, Dr. D. J.	KUN	L-3
Schrader, Ir. J.H.R.	FOM	Other Projects

Snellings, Dr. R.J.M.	FOM	ALICE
Sokolov, Drs. A.	UU	ALICE
Steenbakkers, Drs. M.F.M.	GST	Other Projects
Steenhoven, Prof. Dr. G. van der	FOM	HERMES
Stejger, Dr. J.J.M.	FOM	HERMES
Templon, Dr. J.A.	FOM	B-Phys
Tiecke, Dr. H.G.J.M.	FOM	ZEUS
Tilburg, Drs. J.A.N.	FOM	B-Phys.
Timmermans, Dr. J.J.M.	FOM	DELPHI
Tvaskis, Drs. V.	VU	HERMES
Uiterwijk, Ir. J.W.E.	GST	Other Projects
Velthuis, Ir. J.J.	FOM	ZEUS
Vermeulen, Dr. Ir. J.C.	UVA	ATLAS
Visschers, Dr. J.L.	FOM	Other Projects
Visser, Drs. E.	KUN	ATLAS
Vos, Drs. M.A.	UT	ATLAS
Vreeswijk, Dr. M.	FOM	ATLAS
Vries, Drs. G. de	UU	ANTARES
Vries, Dr. H. de	FOM	B-Phys.
Wahlberg, Drs. H.	UU	B-Phys.
Wang, Drs. Q.	KUN	L-3
Wiggers, Dr. L.W.	FOM	ZEUS
Wijngaarden, Drs. D.A.	KUN	ATLAS
Wilkens, Drs. H.G.S.	GST	L-3
Witt Huberts, Prof.Dr. P.K.A.	FOM	ANTARES
Wolf, Dr. Mw. E. de	UVA	ZEUS
Woudstra, Dr. Ir. M.J.	FOM	ATLAS
Zihlmann, Dr. B.	FOM-VU	HERMES
Zupan, Drs. M.	FOM	B-Phys.

2. Theoretical Physicists

Bachetta, Drs. A.	FOM-VU
Banfi, Dr. A.	FOM
Dijkstra, Drs. T.P.T.	FOM
Eynck, Dipl.Phys. T.O.	FOM
Fuster, Drs. Mw. A.	GST
Gaemers, Prof. Dr. K.J.F.	UVA
Gato–Rivera, Dr. Mw. B.	GST
Heide, Drs. J. van der	FOM
Henneman, Drs. A.	GST
Holten, Prof. Dr. J.W. van	FOM
Iersel, Drs. M. van	FOM-VU
Kleiss, Prof. Dr. R.H.P.	KUN
Koch, Prof.Dr. J.H.	FOM
Laenen, Dr. E.	FOM
Marques de Sousa, Drs. N.M.	GST
Mulders, Prof. Dr. P.J.G.	VU
Nyawelo, B.Sc. T.S.	FOM
Pijlman, Drs. F.	VU
Riccioni, Dr. F.	FOM
Schellekens, Prof. Dr. A.N.J.J.	FOM
Veltman, Prof. Dr. M.J.G.	GST
Vermaseren, Dr. J.A.M.	FOM
Vogt, Dr. A.	TMP
Warringa, Drs. H.	VU
Wit, Prof. Dr. B.Q.P.J. de	UU

3. Computer Technology Group

Akker, T.G.M. van den	FOM
Antony, A.T.	FOM
Blokzijl, Dr. R.	FOM
Boterenbrood, Ir. H.	FOM
Damen, Ing. A.C.M.	FOM
Eijk, Dr. Ir. R.M. van der	FOM
Geerts, M.L.	FOM
Harapan, Drs. D.	FOM
Hart, Ing. R.G.K.	FOM
Heubers, Ing. W.P.J.	FOM
Huyser, K.	FOM
Joosten, Dr. Mw. K.	GST
Kuipers, Drs. P.	FOM
Leeuwen, Drs. W.M. van	FOM
Oudolf, J.D.	TMP
Schimmel, Ing. A.	FOM
Steenbakkers, Ir. M.F.M.	FOM
Tierie, Mw. J.J.E.	FOM
Venekamp, Drs. G.M.	FOM
Wijk, R.F. van	FOM

4. Electronics Technology Group

Balke, D.	FOM-UU
Berkien, A.W.M.	FOM
Beuzekom, Ing. M.G.van	FOM
Boer, J. de	FOM
Boerkamp, A.L.J.	FOM
Born, E.A. van den	FOM
Evers, G.J.	FOM
Fransen, J.P.A.M.	FOM
Gotink, G.W.	FOM
Groen, P.J.M. de	FOM
Groenstege, Ing. H.L.	FOM
Gromov, Drs. V.	FOM
Haas, Ing. A.P. de	FOM
Harmsen, C.J.	FOM
Heine, Ing. E.	FOM
Heutenik, B.	FOM
Hogenbirk, Ing. J.J.	FOM
Jansen, L.W.A.	FOM
Jansweijer, Ing. P.P.M.	FOM
Kieft, Ing. G.N.M.	FOM
Kluit, Ing. R.	FOM
Kok, Ing. E.	FOM
Koopstra, J.	UVA
Kroes, Ir. F.B.	FOM
Kruijer, A.H.	FOM
Kuijt, Ing. J.J.	FOM
Mos, Ing. S.	FOM
Peek, Ing. H.Z.	FOM
Reen, A.T.H. van	FOM
Rewiersma, Ing. P.A.M.	FOM
Schipper, Ing. J.D.	FOM
Sluijk, Ing. T.G.B.W.	FOM
Stolte, J.	FOM
Timmer, P.F.	FOM
Verkooijen, Ing. J.C.	FOM

Vink, Ing. W.E.W.	FOM
Wieten, P.	FOM
Zevering, J.	FOM-VU
Zwart, Ing. A.N.M.	FOM
Zwart, F. de	FOM

5. Mechanical Engineering Group

Arink, R.P.J.	FOM
Band, H.A.	FOM
Boer Rookhuizen, H.	FOM
Boomgaard–Hilferink, Mw. J.G.	FOM
Boucher, A.	FOM
Buskop, Ir. J.J.F.	FOM
Doets, M.	FOM
Duisters, D.H.	TMP
Kaan, Ir. A.P.	FOM
Korporaal, A.	FOM
Kraan, Ing. M.J.	FOM
Lassing, P.	FOM
Lefévere, Y.	FOM
Liem, Ing. A.M.H.	FOM
Munneke, Ing. B.	FOM
Riet, Ing. M.	FOM
Schuijlenburg, Ing. H.W.A.	FOM
Snippe, Ir. Q.H.C.	FOM
Thobe, P.H.	FOM
Verlaat, Ing. B.A.	FOM
Werneke, Ing. P.J.M.	FOM

6. Mechanical Workshop

Apel, A.W.	FOM
Arends, Mw. W.	FOM
Berbee, Ing. E.M.	FOM
Beumer, H.	FOM
Boer, R.P. de	FOM
Bron, M.	FOM
Brouwer, G.R.	FOM
Buis, R.	FOM
Burg, R.H. van der	TMP
Ceelie, L.	UVA
Hagedorn, J.	TMP
Homma, J.	FOM
Jaspers, M.J.F.	UVA
John, D.	FOM
Kok, J.W.	FOM
Kuilman, W.C.	FOM
Langedijk, J.S.	FOM
Leguyt, R.	FOM
Mul, F.A.	FOM-VU
Oskamp, C.J.	FOM
Overbeek, M.G. van	FOM
Petten, O.R. van	FOM
Rem, Ing. N.	FOM
Rietmeijer, A.A.	FOM
Roeland, E.	FOM
Rövekamp, J.C.D.F.	UVA
Stoffelen, N.	FOM
Tump, I.	TMP
Veen, J. van	FOM

7. Management and Administration

Berg, A. van den	FOM
Buitenhuis, W.E.J.	FOM
Bulten, F.	FOM
Cossee, Mw. N.	FOM
Doest, Mw. C.J.	FOM
Dokter, J.H.G.	FOM
Echtelt, Ing. H.J.B. van	FOM
Egdom, T. van	FOM
Geerinck, Ir. J.	TMP
Greven–v.Beusekom, Mw. E.C.L.	FOM
Heuvel, Mw. G.A. van den	FOM
Hooff, F.B. van	TMP
Kerkhoff, Mw. E.H.M. van	FOM
Kesgin–Boonstra, Drs. Mw. M.J.	FOM
Langelaar, Dr. J.	UVA
Langenhorst, A.	FOM
Lemaire–Vonk, Mw. M.C.	FOM
Louwrier, Dr. P.W.F.	TMP
Mors, A.G.S.	UVA
Pancar, M.	FOM
Post, Mw. E.C.	FOM
Rijksen, C.	FOM
Rijn, Drs. A.J. van	FOM
Spelt, Ing. J.B.	FOM
Vervoort, Ing. M.B.H.J.	FOM
Visser, J.	FOM
Vries, W. de	FOM
Willigen, E. van	FOM
Witlox, Ing. W.M.	TMP
Woortmann, E.P.	FOM

8. Apprentices in 2002

Abou El Khair, M.M.	Computer Technology
Adamakis, I.	ANTARES
Alazhar, M.	Computer Technology
Amoraal, J.M.	B-Phys.
Bobeldijk, A.	Mechanical Engineering
Boer, Y.R. de	ATLAS
Bozkus, B	Mechanical Workshop
Bruijn, R.	ANTARES
Cuperus, M.	Electronics Technology
Dalhuizen, J.M.	ATLAS
Dirks, B.P.F.	ATLAS
Elbers, M.C.	HERMES
Esajas, E.	Mechanical Workshop
Faquir, M.	THEORY
Goossen, R	Electronics Technology
Hadri, A.	ATLAS
Hagebeuk, J.C.	Mechanical Engineering
Hegeman, J.G.	ATLAS
Hoekstra, T.	Electronics Technology
Horvath, F.L.	Electronics Technology
Huijse, L.	THEORY
Jansen, F.M.	ATLAS
Jimenez–Delgado, P.	B-Phys.

Kemmers, P.	L-3
Kocabas, K.	Electronics Technology
Koeroo, O.A.	Computer Technology
Kop, A.	Mechanical Workshop
Koutsman, A.J.	ZEUS
Krujtzer, G.L.	ATLAS
Laldjsing, S.	Mechanical Workshop
Li, H.	Other Projects
Lim, G.M.A.	ATLAS
Limper, M.	ATLAS
Nat, P.B. van der	HERMES
Nijenhuis, N.	ANTARES
Plas, B.A. van der	ZEUS
Rantwijk, J. van	Computer Technology
Reus, D.	Electronics Technology
Scholten, M.	Mechanical Engineering
Schouten, S.S.	Electronics Technology
Snoek, H.L.	B-Phys.
The, J.	Computer Technology
Timmer, R.L.A.	ATLAS

9. They left us

Blouw, Dr. J.	HERMES
Bobeldijk, A.	Mechanical Engineering
Boersma, Dr. D.J.	Other Projects
Bokel, Drs. C.H.	ZEUS
Bozkus, B	Mechanical Workshop
Bruijn, R.	ANTARES
Bruinsma, Dr. M.	B-Phys.
Bruyn, E.J.	Mechanical Workshop
Buis, Dr. E.J.	ATLAS
Cârloganu, Dr. Mw. F.C.	ANTARES
Cherzor, Drs. Mw. P.	HERMES
Dalen, Dr. J.A. van	L-3
Dulmen, Mw. A.C.M. van	Management and Administration
Eijk, Dr. Ir. R.M. van der	B-Phys.
Ganesh, A.J.	Mechanical Workshop
Gouz, Dr. I.	B-Phys.
Gulik, Drs. R.C.W. van	L-3
Hemmer, Mw. M.W.	Management and Administration
Hollenberg, P.A.M.	Mechanical Workshop
Horazdovski, Dr. ZT	Other Projects
Hover, Ing. E.P.	Mechanical Engineering
Huiszoon, Dr. L.R.	THEORY
Hulsbergen, Dr. W.D.	B-Phys.
Jacobs, J.	Mechanical Workshop
Jiang, X	Electronics Technology
Koene, Dr. B.K.S.	B-Phys.
Kohout, Dr. Z.	Other Projects
Kop, A.	Mechanical Workshop
La Rooij–Cooper, Mw. T.J.	Other Projects
Malyshev, P.	Other Projects
Manach, Dr. E.	ATLAS
Mangeol, Dr. D.	L-3
Mettivier, Dr. G.	THEORY
Metz, Dr. A.	THEORY
Montesi, Dr. M.C.	THEORY
Needham, Dr. M.D.	B-Phys.
Nozar, Dr. Mw. M.	Other Projects
Pomarede, Dr. D.	ATLAS
Populе, Dr. J.	ATLAS
Profijt, R.S.	Mechanical Workshop
Roux, Drs. B.	L-3
Sanders, Dr. M.	L-3
Simani, Dr. Mw. M.C.	HERMES
Spada, Dr. Mw. F.R.	Other Projects
Steenbakkers, Ir. M.F.M.	Other Projects
Stonjek, Dipl. Phys. S.	ZEUS
Stuurop, B.	Management and Administration
Tassi, Dr. E.	ZEUS
Tilborg, R.J.	Mechanical Workshop
Tomasek, Dr. M.	ATLAS
Vankov, P.H.	B-Phys.
Vavrik, Dr. D.	Other Projects
Ven, Dr. P.A.G. van de	Other Projects
Verschuijl, J.R.	Mechanical Engineering
Visser, Dr. J.	HERMES
Vulpen, Dr. I.B. van	L-3
Zalmijn, R.W.	Mechanical Workshop
Zegers, Ing. A.J.M.	Mechanical Engineering
Zhou, Dr. M.	THEORY
Zonderman, N.	Mechanical Workshop

FOM, and the universities UVA, VU, KUN and UU are partners in NIKHEF (See colofon). UL and UT denote the universites of Leiden and Twente. TMP stands for temporary employee, GST for guest. Other abbreviations refer to the experiments, projects and departments.